ENERGY EFFICIENT CONNECTION PROVISIONING IN IP OVER WDM NETWORKS

WU GAOFENG

NATIONAL UNIVERSITY OF SINGAPORE

2014

ENERGY EFFICIENT CONNECTION PROVISIONING IN IP OVER WDM NETWORKS

WU GAOFENG

(*B. Eng. South China Normal University, M. Sc. Sun Yat-sen University*)

A THESIS SUBMITTED

FOR THE DEGREE OF DOCTOR OF PHILOSOPHY

DEPARTMENT OF ELECTRICAL AND COMPUTER ENGINEERING

NATIONAL UNIVERSITY OF SINGAPORE

2014

Declaration

I hereby declare that this thesis is my original work and it has been written by me in its entirety. I have duly acknowledged all the sources of information which have been used in the thesis.

This thesis has also not been submitted for any degree in any university previously.

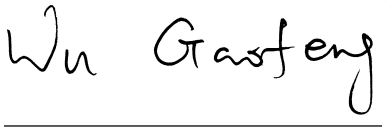

Wu Gaofeng

12 September 2014

Acknowledgement

First and foremost, I am grateful to my supervisor Associate Professor Mohan Gurusamy for his considerable guidance and patience during my enduring journey of PhD study. Without his help, this thesis would have not been possible. I will always cherish our numerous technical conversations which get me to know the essence of professional and high-quality research, and several non-technical conversations which provide me with insights into balancing all aspects of my life.

I am indebted to the National University of Singapore for the award of a research scholarship.

I would like to thank the professors for serving as my PhD qualification exams and PhD dissertation committee members.

I am grateful to Associate Professor Li Xiying as her constant guidance while I was pursuing my master's degree refined my research and interpersonal skills.

I am also thankful to a number of previous members of Optical Networks Lab, Dr. Qiu Jian, Dr. Liu Yong, Dr. Qin Zheng, Dr. He Rong, Dr. Shan Dongmei, Dr. Ratnam Krishanthmohan, Nguyen Hong Ha, and David Koh, for their support and encouragement.

I would like to thank fellow current and previous members of Communications and Networks Lab, Wang Yu, Liu Liang, Wu Tong, Amna Jamal, Yu Yi, Xu Zhuoran, Dinil Mon Divakaran, Xu Jie, Wu Mingwei, Mahmood Ahmed, Liu Jun, Han Xiao, Zeng Yong, Bi Suzhi, Yuan Haifeng, Jiao Xiaopeng, Anshoo Tandon,

Luo Shixin, Song Tianyu, Jia Chenlong, Zhou Xun, Guo Zheng, Wang Qian, Zheng Huanhuan, Zhou Jingjing, Guo Yinghao, Kang Heng, Hu Qikai, Aissan Dalvandi, Farshad Rassaei, Hu Yang, Chen Can, Zhang Shuowen, Huang Cheng, Zeng Zeng, Chen Fan, and Yang Gang for creating a friendly and stimulating environment. I would like to specially thank Jiang Xiaofang and Du Guojun for their continuous support and companionship. My thanks also go to many other friends in my life for making me who I am.

Last but not least, I thank my family for their unconditional love and support.

Contents

Summary

Over the last decade, green networking has attracted a great deal of attention from researchers and engineers in academia and industry due to the huge amount of power consumed by the Information and Communication Technology (ICT) sector and the corresponding CO_2 emission which is a major cause of global warming. Optical networks have been widely deployed due to their capability of providing huge bandwidth, low bit error rate, and high security. Moreover, optical networking is generally more power efficient than its electronic counterpart. In this thesis, we investigate the problem of energy efficient connection provisioning in IP over Wavelength-Division-Multiplexing (WDM) optical networks which consist of an IP layer and an optical layer.

We first study the problem of power efficient provisioning of static and dynamic connection requests considering traffic splitting and the impact of different power profiles. For static connection requests, we formulate Integer Linear Programming (ILP) models for affine power profile and Integer Quadratic Programming (IQP) models for convex power profile to optimize network-wide power consumption with or without traffic splitting. For dynamic connection requests, we construct an auxiliary graph and assign the weight of each link according to its power consumption; thereby a shortest-path routing algorithm can be used.

Next, we investigate the problem of achieving a tradeoff between power efficiency and blocking performance when provisioning connection requests. We propose an

algorithm named Balanced Power efficient Integrated Routing (B-PIR), which strives to strike a balance between power efficiency and blocking performance by preventing critical resources from being exhausted too fast. We use the idea of link criticality which is defined as the number of times that a link belongs to the minimum cut sets of s-d pairs in the network.

Third, we explore the problem of energy efficient provisioning of bandwidth-varying scheduled connection requests. The key issue is to decide the routing, time and bandwidth allocation schemes for a set of scheduled connection requests (of which continuous and fixed-bandwidth data transmission are not mandatory) such that their energy consumption is minimized while meeting their data transmission deadlines, which has not been studied before to the best of our knowledge. We first present an ILP formulation for scheduling and allocating resources to bandwidth-varying scheduled connection requests, such that the total energy consumption is minimized. We further extend the ILP formulation and propose a computationally simple and efficient heuristic algorithm that provisions one connection request at a time such that the incremental energy consumption of the network due to the admission of the connection request is minimized.

Finally, we research on the problem of power efficient provisioning of dynamic connection requests with reliability constraints. We propose a k-shortest path based routing algorithm that tries to find a minimum power consumption path for a connection request while satisfying the reliability requirements.

We demonstrate the effectiveness of our proposed energy efficient schemes through numerical results obtained from solving integer programming models or simulation results acquired based on various network topologies and scenarios.

List of Tables

List of Figures

List of Acronyms

ALR	Adaptive Link Rate
ATM	Asynchronous Transfer Mode
BER	Bit Error Rate
B-PIR	Balanced Power efficient Integrated Routing
CMOS	Complementary Metal Oxide Semiconductor
DFS	Dynamic Frequency Scaling
DSL	Digital Subscriber Line
DVS	Dynamic Voltage Scaling
EDFA	Erbium-doped fiber amplifier
EEE	Energy Efficient Ethernet
FEC	Forward Error Correction
HIR	Hop-efficient Integrated Routing
ICT	Information and Communication Technology
IETF	Internet Engineering Task Force
ILP	Integer Linear Programming
IP	Internet Protocol
IQP	Integer Quadratic Programming
ISP	Internet Service Provider
LAN	Local Area Network
LP	Linear Programming

LPI	Low Power Idle
LSP	Label Switched Path
MHIRR	Minimum physical Hops Integrated Routing with Reliability constraints
MILP	Mixed Integer Linear Programming
MPLS	Multi-Protocol Label Switching
OXC	Optical Cross-Connect
PEIRR	Power Efficient Integrated Routing with Reliability constraints
PIR	Power efficient Integrated Routing
PIRTS	Power efficient Integrated Routing with Traffic Splitting
PON	Passive Optical Networking
QoS	Quality of Service
RWA	Routing and Wavelength Assignment
SDH	Synchronous Digital Hierarchy
SONET	Synchronous Optical Networking
TCP	Transmission Control Protocol
VNI	Visual Networking Index
WDM	Wavelength Division Multiplexing

Chapter 1

Introduction

Over the last ten years, green networking has attracted a great deal of attention from researchers in academia and industry due to the huge amount of power consumed by the Information and Communication Technology (ICT) sector and the corresponding CO_2 emission which is a major cause of global warming [2, 3]. The number of end users of the Internet has been increasing rapidly at a rate of about 3% per annum [4], with Asia as the most important engine for maintaining the high-speed growth rate. There were 2.8 billion (1.3 billion from Asia, and 1.5 billion from rest of world) Internet users as in December 2013 [4], accounting for about 40% of the world population. The bandwidth requirements of current Internet users are also growing, partially because of the emerging bandwidth-intensive applications such as video-on-demand, video conferencing, and remote medical monitoring. The Cisco Visual Networking Index™(Cisco VNI™) forecast predicts that the annual global Internet Protocol (IP) traffic will surpass the zettabyte [1] threshold (1.3 zettabytes) by the end of 2016 [5]. In fact, the annual global IP traffic has increased eightfold over the past 5 years, and is projected to increase threefold over the next 5 years [5, 6]. The rapid growth of the number of end users and their surging bandwidth requirements have

[1] 1 zettabyte (ZB) = 10^9 TB = 10^{21} bytes

driven the Internet Service Providers (ISPs) to deploy more powerful and also more power-hungry routers and switches. In fact, it is estimated that the Internet accounts for about 0.4% of the total power consumption in broadband-enabled countries, and this figure is forecast to be approaching 1% in future [7]. As a result, the expansion of the Internet may be hindered by the tremendous power consumption instead of the bandwidth limitation [8]. To sustain the growth of the Internet and control the environmental impact, it is necessary to design power efficient network equipment together with power-aware network protocols. As the access solutions shift from traditional energy-consuming technologies to Passive Optical Networking (PON), the major fraction of energy consumption of the Internet is moving from access to backbone networks [9–11]. The wide deployment of optical backbone networks and their ever-increasing energy consumption necessitate the efforts to improve their energy efficiency.

1.1 Problem and Objectives

The energy consumption of the current network is far from being energy proportional to the network load. This thesis mainly considers energy efficient connection provisioning in IP over WDM networks, focusing on four issues. We first study the problem of using traffic splitting mechanism to improve energy efficiency of connection provisioning. We noticed the impact of power profiles on whether a connection is worth splitting or not, thus we investigate how to use traffic splitting to gain power savings considering the characteristics of different power profiles. We then study the problem of achieving a tradeoff between power efficiency and blocking performance when provisioning connection requests. Improving power efficiency should not compromise other metrics such as network stability and blocking performance too much. We mitigate the implications of improving power efficiency on blocking performance

by preventing critical resources from being exhausted too fast. We next explore the problem of energy efficient provisioning of bandwidth-varying scheduled connection requests. We noticed that continuous and fixed-bandwidth data transmission are not mandatory for some applications such as data backup and thus can be relaxed to allow shorter data transmission time which leads to less fixed energy overhead on transmitters and receivers. Finally, we study the problem of connection provisioning with joint considerations of power efficiency and reliability constraints. We propose an algorithm that can power efficiently provision connections while meeting their reliability requirements. More details on the four issues are listed as follows.

1.1.1 Power Efficient Traffic Splitting

Traffic splitting is to split the traffic of a connection request onto multiple paths. It is an effective traffic engineering mechanism to improve performance in terms of blocking probability or congestion in networks such as Multi-Protocol Label Switching (MPLS) networks [12]. The traffic of a connection request in optical backbone networks is the aggregation of multiple small traffic flows with varying source and destination nodes, therefore making it possible for traffic splitting. With the help of multi-path Transmission Control Protocol (TCP) [13], even splitting within a traffic flow is also achievable. A power profile is defined as the dependence of the power consumption of a network component as a function of its traffic load. Recently there has been interest in studying the energy efficiency problem with different power profiles [1]. It would be ideal for the power consumption of a network component to be proportional to the amount of traffic being processed. However, this is not the case for most of current network equipment [8]. With technology advances, it is expected that equipment with proportional power profiles will be developed in future. We notice that the power needed to route an amount of traffic might be reduced

if the traffic is split and distributed over multiple paths, under some power profiles and bandwidth requirements. Therefore, it is worthwhile to investigate how to gain power savings by jointly considering traffic splitting and power profile.

1.1.2 Balanced Power Efficient Integrated Routing

Most current works focus on and only focus on energy[2] efficiency. Recently, there is an argument that it might not be practical to just consider energy efficiency while ignoring the implications on capital expenditure, blocking performance, network stability, and network robustness, etc [14, 15]. Some energy-saving methods require more optical switch ports, which increases the capital expenditure. Power-only algorithms would not balance the network load, therefore the blocking performance might not be desirable. These schemes might compromise network stability because the network might find it hard to reconverge if network components are switched on and off frequently. What is more, many energy efficient approaches try to gain energy savings by decreasing network redundancy which was practically designed to improve network robustness. It is desirable to study the tradeoff between power efficiency and other metrics such as blocking performance.

1.1.3 Energy Efficient Provisioning of Bandwidth-varying Scheduled Connection Requests

Scheduled connection requests typically specify a data transmission start time and the deadline for data transmission to be completed [16]. Scheduled traffic models [3] generally benefit the network because *a priori* knowledge of transmission start

[2]Energy is the product of power and time. But in this thesis we use energy and power interchangeably on the premise of not causing ambiguity.

[3]A traffic model specifies the pattern of a type of connection requests.

time and end time can be used to improve the admission control and resource provisioning so as to increase network utilization and/or maximize profits, and are beneficial to users as well because the network can provide better quality of service and/or charge less if users are willing to avoid network peak periods [16]. Scheduled traffic models were initially proposed for non-optical networks [17, 18]. This concept was later introduced to optical networks in [19]. Although there are some common solution techniques for scheduled traffic model in electrical and optical domains, there are also some unique challenges for optical networks (such as traffic grooming, wavelength continuity constraint, and survivability) which make it worthwhile to study scheduled traffic models in optical networks separately from that in non-optical networks [16]. Scheduled traffic models have extensive applications in current optical backbone networks, which stimulates the attempt to devise energy efficient provisioning strategies. Most of existing works assume that the bandwidth of a connection request is constant. However, there are applications (such as data backup, and data transfer in large scientific experiments) in which both continuous and fixed-bandwidth data transmission are unnecessary. This leads to bandwidth-varying scheduled traffic model, which adds another degree of flexibility and can be exploited to improve network energy efficiency. Therefore, it is interesting and useful to study energy efficient provisioning of bandwidth-varying scheduled connection requests.

1.1.4 Power Efficient Integrated Routing with Reliability Constraints

Due to the large quantity and the criticality of data carried in optical networks, link failures may cause significant loss. A cable cut is estimated to occur at the rate of 4.39 cuts/year/1000 sheath miles [20], which can be translated to one cable cut

every day for a typical optical backbone network. Therefore, it is better to take fiber link reliability into account when routing connections [21]. A most reliable path may not be a most power efficient path and vice versa. A routing algorithm based only on reliability will treat existing lightpaths and newly-created lightpaths equally so long as they have the same reliability metric. It may employ excessive electrical switching components in order to find a reliable route, which is costly from the perspective of power efficiency. Thus, it is important to combine power efficiency and reliability together to achieve better performance.

1.2 Thesis Contributions

The main contributions of this thesis are summarized as follows.

- We studied the problem of power efficient provisioning of static and dynamic connection requests considering traffic splitting and the impact of different power profiles. We demonstrated that the concept of traffic splitting can be adopted to improve energy efficiency of networks. We decompose the power consumption of an IP over WDM network into five components and study two power profiles (affine and convex) of the components. We deal with both static and dynamic traffic models. For the static traffic model, we formulate integer programming models to minimize the total power consumption of the network, they are Integer Linear Programming (ILP) for affine power profile and Integer Quadratic Programming (IQP) for convex power profile, respectively. For the dynamic traffic model, we propose power efficient integrated routing algorithms which are based on a specifically-designed auxiliary graph that assigns weights for links according to the power consumption, thereby capturing the power consumption flow of each path. We conducted performance study to show that traffic-splitting-enabled networks outperform non-traffic-splitting

networks with respect to power consumption and blocking probability.

- We investigated the problem of achieving a tradeoff between power efficiency and blocking performance when provisioning connection requests. Much work in the literature focuses on improving network energy efficiency only, while neglecting the impact on other metrics. We hold the view that improving network energy efficiency should not affect other metrics significantly. Therefore we proposed an algorithm named Balanced Power efficient Integrated Routing (B-PIR), which strives to strike a balance between power efficiency and blocking performance by preventing critical resources from being exhausted too fast. We use the idea of link criticality, which is defined as the number of times that a link belongs to the minimum cut sets of *s-d* pairs in the network, to achieve the goal. The rationale for the definition of link criticality is that if a link belongs to the minimum cut set of an *s-d* pair then reducing its residual bandwidth capacity will lead to decreasing of the maximum flow value between that *s-d* pair. Therefore the higher the number of times a link belongs to the minimum cut sets of *s-d* pairs in the network, the more critical the link is. Simulation results show that our proposed B-PIR significantly reduces the blocking probability compared to Power efficient Integrated Routing (PIR) (which aims at reducing power consumption only and is widely studied in the literature) at the cost of relatively little degradation of power efficiency.

- We explored the problem of energy efficient provisioning of bandwidth-varying scheduled connection requests. Bandwidth-varying scheduled traffic model has many applications, yet few work has been carried out to improve its energy efficiency. We first present an ILP formulation for scheduling and allocating resources to bandwidth-varying scheduled connection requests, such that the total energy consumption is minimized. Next, we extend the ILP formulation

and propose a computationally simple and efficient heuristic algorithm that provisions one connection request at a time such that the incremental energy consumption of the network due to the admission of the connection request is minimized. Performance study demonstrates the effectiveness of our proposed ILP formulation and heuristic algorithm for bandwidth-varying scheduled traffic model in saving energy compared to that for fixed-window scheduled traffic model.

- We studied the problem of power efficient provisioning of dynamic connection requests with reliability constraints. It is of paramount importance to ensure the reliability of optical networks considering the huge amount of data being processed and the fact that almost all indudstries rely on reliable optical networks to function well. Therefore it is worthy of jointly considering power efficiency and reliability when provisioning connection requests. We presented a Power Efficient Integrated Routing algorithm for dynamic connection requests with Reliability constraints (PEIRR). An auxiliary graph is constructed by assigning the power consumption value as the weight of a link so as to capture the power consumption of a route. The algorithm tries to find a minimum power consumption path for a connection while satisfying the reliability requirements. Simulation results show the effectiveness of the proposed algorithm PEIRR in terms of power efficiency, blocking probability, and the average number of physical/virtual hops per connection goes through, compared to the Minimum physical Hops Integrated Routing with Reliability constraints (MHIRR) algorithm in the literature.

1.3 Thesis Outline

The remainder of this thesis is organized as follows.

Chapter 2 provides the background information necessary to understand our research and presents a review of related work.

Chapter 3 studies power efficient integrated routing with traffic splitting under different power profiles and traffic models. We formulate integer programming models for static connection requests with convex and affine power profiles, respectively. We propose a power efficient integrated routing algorithm based on a specifically-designed auxiliary graph for dynamic connection requests. We conduct performance study to show the superiority traffic-splitting-enabled networks with respect to non-traffic-splitting networks in terms of power consumption and blocking probability.

Chapter 4 proposes an algorithm named Balanced Power efficient Integrated Routing (B-PIR) which achieves a tradeoff between power efficiency and blocking performance by preventing critical resources from being exhausted too fast. The description of the auxiliary graph for B-PIR is provided. We present simulation results to show that B-PIR significantly reduces blocking probability at the cost of relatively little degradation of power efficiency.

Chapter 5 investigates energy efficient provisioning of bandwidth-varying scheduled connection requests. Continuous and fixed-bandwidth data transmission are not mandatory for bandwidth-varying scheduled connection requests, paving the way for shorter data transmission time and thus less fixed energy overhead is needed for transmitters and receivers. ILP formulation and heuristic algorithm are presented, of which the effectiveness in improving energy efficiency is demonstrated through numerical and simulation results.

Chapter 6 develops a power efficient integrated routing algorithm under dynamic traffic model considering reliability constraints. The algorithm basically searches for the first k most power efficient paths and then tries to find the first path that meets reliability constraints. The proposed algorithm is evaluated together with a benchmark algorithm in terms of various metrics.

Chapter 7 concludes the thesis and discusses future research directions.

Chapter 2

Background and Related Work

In this chapter, we will begin by giving a description of the Internet and classifying it into three categories based on function and size: access, metro, and core networks. Then we will explore the basics of IP over WDM networks. We will next look at the common power profiles used in the literature. We will then review the research work in the literature on energy efficiency in the Internet, covering the related work of our contributions in this thesis.

2.1 The Internet

The Internet is a global system of interconnected computer networks [1] that use the standard Internet protocol suite—TCP/IP—to link several billion devices worldwide [22]. The Internet which provides fast and extensive information has transformed our lives fundamentally. Typical networks of an ISP or telco can be categorized into a three-level hierarchy based on function and size: access, metro, and core/backbone [23]. An access network is a network that physically connects an end system [2] to its ISP or telco [24, 25]. An access network typically covers a range

[1] The term computer network sounds dated as there are many nontraditional devices connected.

[2] An end system (host) can be a laptop, a smartphone, a server, etc.

of several kilometers. There are several types of access networks including Digital Subscriber Line (DSL), coaxial cable Internet access, PON, Ethernet, and WiFi. A metro network covers a larger geographical area than an access network, ranging from several blocks to entire city, with link lengths of few tens to few hundreds of kilometers [25]. It provides Internet connectivity for access networks within a metropolitan area and connects them to core networks. The common technologies used in metro networks are Synchronous Optical Networking (SONET)/Synchronous Digital Hierarchy (SDH) and Metro Ethernet [26]. A core/backbone network geographically spans nation- or even continent-wide distances, with link lengths of few hundreds to few thousands of kilometers [27]. A backbone network is the highest level of aggregation in an ISP or telco's network, and is composed of high-end switches and routers interconnected by high-bandwidth links. The common technologies used are SONET/SDH and Wavelength Division Multiplexing (WDM).

2.2 IP over WDM Networks

The explosive growing number of Internet users and the emerging of bandwidth-intensive applications such as video-on-demand and video conferencing have driven the need for optical networking. Optical networks have advantages such as huge bandwidth (about 50 Tb/s), low bit error rate (BER, fractions of bits that are received in error, typically 10^{-12}, compared to 10^{-6} in copper cable), and high security [28]. Moreover, optical networking is generally more power efficient than its electronic counterpart, which is desirable as the energy consumption of the Internet is playing a more and more significant role in the total energy consumption of the world.

Optics as a way to transmit information can be dated back to ancient China, in which soldiers stationed along the Great Wall would alert each other of the im-

pending enemy invasion by signaling from tower to tower [29]. By doing so they were able to transmit a message as far away as several hundred kilometers in just a few hours [29]. However, this way is not energy efficient at all because they burnt so much firewood just for transmitting one bit of information, which is whether there is enemy attack or not. In 1960's, Dr. Charles Kuen Kao and his co-workers did their pioneering work in the realization of fiber optics as a telecommunications medium [30], which is the curtain-raiser for optical communication and networking.

It is very difficult to exploit the full bandwidth available in an optical fiber by using only one high-capacity wavelength channel [3] due to optical-electronic bandwidth mismatch or "electronic bottleneck"[4]. However, with WDM, multiple wavelength channels can be multiplexed onto an optical fiber, greatly increasing the data volume of an optical fiber while considering electrical bottleneck.

This thesis mainly considers IP over WDM networks, which is an attractive architecture for optical backbone networks. IP over WDM networks are more advantageous compared to IP over Asynchronous Transfer Mode (ATM) over SONET over WDM networks in that they have higher transmission efficiency, lower management complexity, higher service provisioning flexibility, etc. As shown in Fig. 2.1, a typical IP over WDM network consists of an IP layer and an optical layer. The optical layer uses an architecture named *wavelength routed WDM network*. A wavelength routed WDM network consists of reconfigurable *optical cross-connects (OXCs)* interconnected by fiber links in an arbitrary topology. An OXC switches optical signals from an input port to an output port. A wavelength of a fiber link is termed as a *wavelength channel*. Multiple wavelength channels are multiplexed onto a single fiber link by a *multiplexer*. To enable optical signals to travel long distances, amplifiers are deployed at a specific distance intervals along fiber links. The optical

[3] A wavelength transmitted in a fiber is called a wavelength channel.

[4] So far, electronic speed is a few Gb/s.

layer provides lightpaths which serve as data transmission channels for IP routers in the IP layer. A *lightpath* is an all-optical circuit-switched end-to-end communication path between a pair of network nodes (the source node and the destination node of the lightpath), that is routed through multiple intermediate nodes [31] and established by allocating the same wavelength throughout the fiber links of the path [28]. All the fiber links along the path must use the same wavelength if there is no wavelength converters at intermediate nodes. This is also known as *wavelength continuity constraint*. Electrical Processing (and buffering) is needed at the source and the destination nodes of a lightpath, other than that no electrical processing and buffering within a lightpath is needed. A lightpath is uniquely identified by a wavelength and a physical path [32]. Two lightpaths with sharing fiber link(s) cannot be assigned the same wavelength. On the other side, two lightpaths can use the same wavelength if they use disjoint sets of fiber links. This property is known as wavelength reuse. An algorithm used for selecting routes and wavelengths to establish lightpaths is called a Routing and Wavelength Assignment (RWA) algorithm. RWA is a fundamental problem in a wavelength routed WDM network, and wavelength assignment is a unique feature that separates a wavelength routed WDM network from a non-optical network. The common wavelength assignment algorithms are most-used, least-used, fixed-order, and random-order [28]. In this thesis by default we use the fixed-order algorithm which searches for the first available wavelength on a path according to the indices of wavelengths. We do not explicitly mention wavelength assignment problem in the following chapters, and thus "routing" has the same meaning as "RWA".

In the IP layer, an IP router aggregates low-speed traffic flows through the agregation ports as shown in Fig. 2.1 and transfers them through lightpaths provided by the optical layer. A fiber link is a physical link (hop). An IP router treats a lightpath as a virtual link (hop) which is just like a link (hop) in non-optical

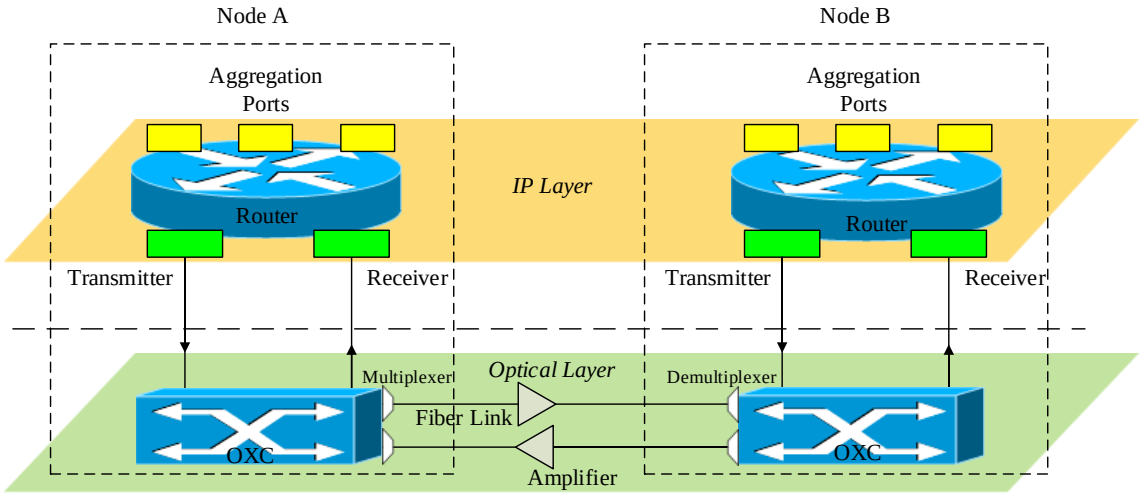

Figure 2.1: Architecture of an IP over WDM network

networks. All the lightpaths of provide by the optical layer form a virtual topology which is the topology that can be seen by IP routers. An IP router is connected to an OXC through transmitters and receivers, which are parts of transponders. A transmitter converts data coming from a router into a WDM-compatible optical signal, while a receiver receives a WDM-compatible optical signal and converts it back to electrical data that can be processed by routers. A network node consists of an IP router and an OXC.

The bandwidth requirements of low-speed traffic flows aggregated by an IP router might be lower than the bandwidth capacity of a lightpath, leading to bandwidth waste. *Traffic grooming*, which multiplexes multiple low-speed traffic flows onto a single lightpath in order to fill the gap between the huge single wavelength bandwidth and the relatively small traffic demands [28], improves bandwidth utilization and reduces the number of transmitters and receivers needed. Traffic grooming is well known to be NP-complete [33], meaning it cannot be solved in polynomial time in any known way [34]. *Optical bypass* enables a lightpath to traverse multiple fiber links without being electrically processed by the intermediate nodes, and therefore the burden on the underlying electronics at the intermediate nodes would be sig-

nificantly alleviated. Optical bypass is made possible by the intelligent switching capability of an OXC. Note that traffic grooming empowers a lightpath to be shared by several traffic flows with sublambda bandwidth requirements while optical bypass capacitates a lightpath to span a series of fiber links.

We assume all IP routers are MPLS enabled. MPLS is an framwork specified by the Internet Engineering Task Force (IETF) to address the problems of traffic engineering, Quality of Service (QoS) management, and service provisioning of IP networks. MPLS provides connection-oriented services to IP networks by setting up a series of Label Switched Paths (LSPs) before data transmission. It directs data from one network node to the next node based on short path labels rather than long network addresses, thereby avoiding complex lookups in a routing table [35]. An LSP is routed on lightpaths provided by the optical layer. We use the terms "LSP", "connection", and "connection request" interchangeably in this thesis.

An IP over WDM network may select one among the two connection request routing models: *overlay* model and *integrated* (peer) model [36]. In overlay model, IP layer and optical layer are controlled separately, each with its own control plane. Here a connection request is first routed on existing lightpaths. Only when existing lightpaths are not able to accommodate the connection request then new lightpaths will be established, leading to inefficient routes. Whereas in integrated model, IP layer and optical layer are controlled by a unique plane; a connection request may use existing lightpaths, create new lightpaths, or partially use existing lightpaths and partially create new lightpaths, for the purpose of improving bandwidth utilization, minimizing power consumption, etc. In the rest of this thesis, integrated routing model is adopted unless otherwise specified.

Survivability (or fault tolerance) is the ability of a network to withstand and recover from failures [37]. Survivability is an important issue in communication networks, especially in optical backbone networks, since a huge amount of traffic is

carried in those networks. A single failure can disrupt millions of users and may result in millions of dollars of revenue lost. Therefore, it is desirable for networks to continue providing services in case of failures. Failure recovery procedures can be classified according to different criteria such as the layer(s) at which recovery operates, the level of recovery resources usage, the scope of a recovery procedure, etc [38]. In Chapter 6, we partially achieve survivability by proposing an algorithm with link failure probability awareness. By partially we mean on the one hand the algorithm proposed in Chapter 6 satisfies the reliability requirements of an accepted connection request; on the other hand, the algorithm does not have the capability of automatically recovering from link failures.

2.2.1 Traffic Models

A traffic model is used to describe the pattern of a set of connection requests. There are many traffic models available in the literature for connection requests in optical networks. The well-known models are:

- *static*, wherein connection requests are known *a proiri* and are assumed to hold for a long time. A traffic matrix is usually used to specify the bandwidth requirements of source-destination pairs.

- *incremental*, wherein connection requests arrive sequentially and are considered to hold for a long time.

- *dynamic*, wherein connection requests arrive and leave randomly, with the arrival intervals and holding times (or durations) typically following some statistical distribution.

Recently in [39], *fixed-window scheduled* traffic model was proposed, wherein the setup and teardown times, denoted as t_{setup} and t_{teardown} respectively, of a connection

request are known when the connection request is known to (or arrives at) the network at time t_{know}. Here, we have $t_{\text{teardown}} > t_{\text{setup}}$, $t_{\text{setup}} > t_{\text{know}}$. Note that $t_{\text{know}} = 0$ means the connection request is known to the network in advance, and $t_{\text{know}} > 0$ means the network does not know the connection request in advance and will know it only when it arrives at the network at time t_{know}. A more general case to fixed-window scheduled traffic model is *sliding scheduled* traffic model [40], wherein the constraint of having fixed setup and teardown times for a connection request is relaxed such that the setup and teardown times can slide within a larger time window W_{out}, although the holding time of the connection request remains fixed. The actual setup and teardown times of a connection request is determined by the network based on some resource allocation scheme for the sake of, say, minimizing resource usage. Sliding scheduled traffic model is reduced to fixed-window scheduled traffic model if W_{out} is equal to the holding time for all connection requests. A more general case to sliding scheduled traffic model is *segmented sliding scheduled* traffic model [41], wherein a connection request need not keep transferring data continuously once started. In other words, it can halt and resume data transmission in other time-disjoint segments so long as the data transmission is complete within W_{out}. Segmented sliding scheduled traffic model is reduced to sliding scheduled traffic model if the number of segments is 1 for all connection requests.

All the aforementioned traffic models assume that the bandwidth of a connection request is constant throughout its existence. In Chapter 5, we consider a *bandwidth-varying scheduled* traffic model which is a more general case to segmented sliding scheduled traffic model. The difference between bandwidth-varying traffic model and segmented sliding scheduled traffic model lies in that the former assumes the bandwidth of a connection request can vary with time, so long as the data volume of the connection request can be complete within W_{out}. There are applications (such as bank data backup, and data transfer in large scientific experiments)

in which both continuous and fixed-bandwidth data transmission is unnecessary. Bandwidth-varying scheduled traffic model adds another degree of flexibility to the existing segmented sliding scheduled traffic model, which can be exploited to improve network energy efficiency.

Scheduled traffic models (be it fixed-window, sliding, segmented sliding, or bandwidth-varying) can borrow features from the static and the dynamic traffic models and therefore can be further divided into two categories: static scheduled traffic model and dynamic scheduled traffic model. Static scheduled traffic model requires $t_{\text{know}} = 0$ for all the connection requests, meaning the connection requests are known to the network in advance; whereas dynamic scheduled traffic model assumes $t_{\text{know}} > 0$ for all the connection requests, meaning the connection requests arrive at the network randomly.

Scheduled traffic models have useful applications in current optical backbone networks. One application scenario is that companies need to backup their databases periodically [42]. These backup tasks usually happen at night when the network is less busy and the price of bandwidth is discounted. Continuous data transmission is not mandatory. The only requirement of the customer may be to finish transferring the backup data during a specified time window, say, between 0 A.M. and 5 A.M. Another application scenario is that large scientific experiments generate huge amounts of data (on the order of terabytes or even higher) which need to be transferred to different data centers in specified time periods for processing and analyzing.

2.3 Power Profiles

A power profile is defined as the dependence of the power consumption of a network component as a function of its traffic load. Recently there has been interest in

studying the energy efficiency problem with different power profiles [1]. It would be ideal for the power consumption of a network component to be proportional to the amount of traffic being processed. However, this is not the case for most of current network equipment [8]. With technology advances, it is expected that equipment with proportional power profiles will be developed in future. There are four common power profiles in the literature as shown in Fig. 2.2:

- *Affine*: Under this profile the power consumption increases linearly with the traffic load. It can be formulated as

$$p(t) = \alpha P + (1 - \alpha)Pt \tag{2.1}$$

  where P is the maximum power consumption value of a network component; α is the fixed overhead proportion of a network component, meaning αP amount of power has to be consumed so long as the network component is switched on, $\alpha \in (0, 1]$; t is the normalized traffic going through the network component, $p(t)$ is the power consumption of a network component when the traffic load is t.

- *Convex*: This profile corresponds to network equipment utilizing energy reduction techniques like Dynamic Voltage Scaling (DVS) and Dynamic Frequency Scaling (DFS) [43]. Ethernet interface cards applying DVS and DFS have been shown to follow this profile [1, 43]. It can be modeled as

$$p(t) = \alpha P + (1 - \alpha)Pt^2 \tag{2.2}$$

  where $P, \alpha, t, p(t)$ have the same meanings as in (2.1).

- *On-Off*: So long as the network component is turned on, 100% power is consumed regardless of the traffic load. This is not power-friendly but is the case for a large proportion of existing equipment [8]. It can be modeled as

$$p(t) = P \tag{2.3}$$

where $P, t, p(t)$ have the same meanings as in (2.1).

- *Concave*: This profile is possible for Network Interface Cards (NICs) that implement IEEE 802.3az Energy Efficient Ethernet (EEE) standard [44]. In this standard, Low Power Idle (LPI) mode is adopted to reduce the energy consumption of a link when no packets is being sent [45]. This power profile can be modeled as

$$p(t) = \alpha P + (1 - \alpha) P \sqrt{t} \tag{2.4}$$

where $P, \alpha, t, p(t)$ have the same meanings as in (2.1).

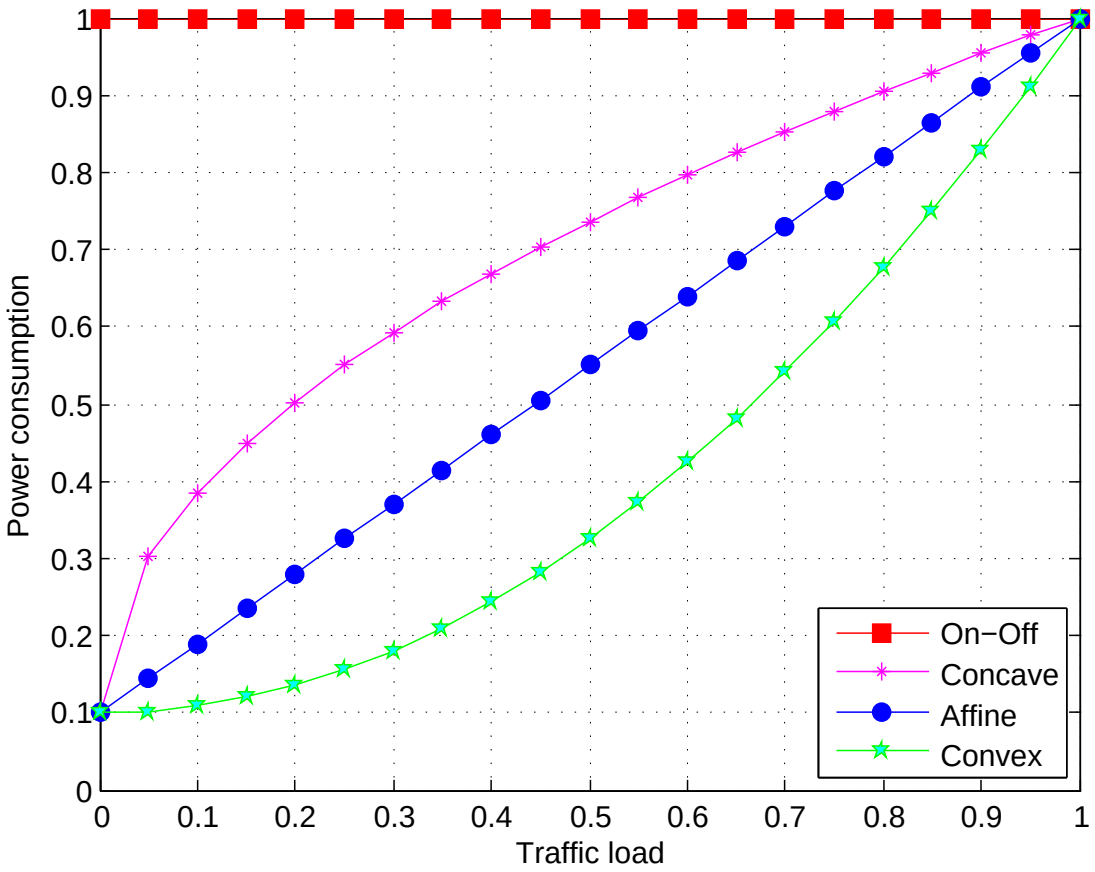

Figure 2.2: Different power profiles (adapted from [1])

2.4 Energy Efficiency in the Internet

Energy efficiency in wireless networks has been studied for many years due to the inherently limited power supply of mobile networking devices. A comprehensive summary of research efforts in the literature addressing energy efficient and low-power design within all layers of the wireless network protocol stack is presented in [46]. As to energy efficiency in wired networks, it has long been ignored since people have been more concerned with improving network performance, reducing capital investments, etc. The Internet is estimated to currently consume about 0.4% of the total electricity consumption in broadband-enabled countries, and this figure could approach 1% as access rates increase [7]. This enormous amount of energy consumption together with its corresponding impact on the climate change has drawn much attention from academia and industry. Therefore, energy efficient Internet, or green Internet, has become a hot research topic in recent years. Solely relying on low power silicon technologies such as Complementary Metal Oxide Semiconductor (CMOS) may not be enough to curb the ever-increasing trend of power consumption. To achieve this aim, comprehensive strategies combing power efficient architectures and protocols may be necessary.

Gupta and Singh [3] point out the energy inefficiency of the Internet and suggest putting network components to sleep for saving energy. Several promising strategies are suggested from the component level to the network level. They further explore this idea in [47–49] by detecting the periods when the links remain idle or under-utilized. In [8], the authors advocate power-aware network design and routing in wired networks. Power-aware network design problem considers how to deploy chassis/line cards such that provisioning requirements are satisfied while power consumption is minimized. Power-aware routing tackles how traffic flows might be altered in order to put line cards and/or chassis to sleep during low utilization pe-

riods. They use Mixed Integer Linear Programming (MILP) to investigate power consumption, performance, and robustness in static network design and dynamic routing. Case study and simulation results indicate the potential for significant power savings.

2.4.1 Energy Efficient Ethernet

Ethernet is the dominant wired access network technology for campus and enterprise users; therefore improving the current Ethernet to achieve EEE is of great importance. In view of this, IEEE has come up with an IEEE 802.3az EEE standard. The authors in [50] investigate Adaptive Link Rate (ALR) as a means of reducing the energy consumption of a typical Ethernet link by adaptively varying the link data rate in response to utilization. They use output buffer queue length thresholds and fine-grain utilization monitoring as effective policies to determine when to change the link data rate. Besides ALR, [51] also proposes the idea of protocol proxying, which turns off high performance devices during low activity periods and moves offered services to low power and performance components. [45] extends the work of IEEE 802.3az EEE by proposing packet coalescing which can significantly improve energy efficiency while keeping absolute packet delays to tolerable bound.

2.4.2 Energy Efficient Traffic Grooming

Traffic grooming aggregates multiple sublambda traffic flows onto a single wavelength so as to fill the gap between the enormous single wavelength bandwidth and the relatively small traffic demands [28]. The objective of traditional traffic grooming is to reduce network cost or accommodate as much traffic as possible with given network resources [33, 52–57]. In [58], the authors revisit traffic grooming problem from the perspective of improving power efficiency. They propose two ways to for-

mulate the power consumption of the network, i.e., a flow based formulation and an interface based formulation. The former one assumes the power consumption of a network component as a linear function of network load, while the latter one neglects the impact of traffic load on power consumption. In [59], based on some approximations, the problem of minimizing power consumption of the network is transformed into the problem of minimizing the number of lightpaths established. In [60] [61], the power consumption of a route is decomposed into different operations and an auxiliary graph which captures the flow of operations and their corresponding power is adopted for finding the most power efficient route. The authors in [62, 63] analyze the modular node architecture and propose a different auxiliary graph which captures the flow of a connection request as well as the power consumption of the entire network. They further extend the work noting that there may be a gradual shift towards green networks [64]. However, there is still much space for improving energy efficiency of traffic grooming towards the ultimate goal of achieving full energy proportionality with network load. In Chapter 3, we study the impact of traffic splitting on energy efficiency, using both traffic grooming and optical bypass techniques. We consider both affine and convex power profiles for the network power components. We deal with both static and dynamic traffic models.

2.4.3 Energy Efficiency Considering Other Metrics

Most research efforts in the literature focus on energy efficiency only. Recently, there is an argument that it might not be practical to just consider energy efficiency while ignoring the implications on capital expenditure, blocking performance, network stability, and network robustness, etc [14, 15]. Some energy-saving methods require more optical switch ports, which increases the capital expenditure. Power-only algorithms would not balance the network load, therefore the blocking performance

might not be desirable. These schemes might compromise network stability because the network might find it hard to reconverge if network components are switched on and off frequently. What is more, many energy efficient approaches try to gain energy savings by decreasing network redundancy which was practically designed to improve network robustness. Hou *et al.* [14] devote to achieving joint power efficiency and OXC ports savings. Wiatr *et al.* [15] hold the view that a powered-on fiber link might be run out of bandwidth too fast (and thus leads to the degradation of the blocking performance) if on-off model is adopted. Therefore, they adjust the weight of a fiber link ranging from zero (pure power minimization approach) to its actual power consumption (pure hop-count minimization approach). In Chapter 4, we propose an algorithm to strike a balance between power efficiency and blocking performance by preventing critical resources from being exhausted too fast. We use the idea of link criticality which is defined as the number of times that a link belongs to the minimum cut sets of *s*-*d* pairs in the network. The reason for the definition of link criticality is that if a link belongs to the minimum cut set of an *s*-*d* pair then reducing its residual bandwidth capacity will lead to decreasing of the maximum flow value between that *s*-*d* pair. Therefore the higher the number of times a link belongs to the minimum cut sets of *s*-*d* pairs in the network, the more critical the link is.

2.4.4 Energy Efficiency with Scheduled Connections

Scheduled connection request provisioning have been previously studied in [39–42] for better network resource (transmitters, receivers, wavelengths in fiber links, etc.) utilization only. Few works have studied scheduled connection request provisioning from the viewpoint of energy efficiency. In [65, 66], the authors study provisioning fixed-window scheduled connection requests with the objective of minimizing en-

ergy consumption. They investigate both static and dynamic fixed-window scheduled traffic models. In [67], energy efficient provisioning of sliding scheduled traffic demands was studied. In Chapter 5, we focus on the problem of energy efficient provisioning of bandwidth-varying scheduled connection requests, which has not been studied before to the best of our knowledge. We present an ILP formulation and a heuristic based on the ILP formulation for minimizing energy consumption by exploiting a feature of bandwidth-varying scheduled connection requests, i.e., continuous and fixed-bandwidth data transmission are not mandatory.

2.4.5 Energy Efficiency Considering Survivability

Survivability (or fault tolerance) is a necessity in practical networks as aforementioned. Earlier research efforts study survivability mainly from the perspective of improving resource utilization [21, 38, 68–71]. In [68], backup multiplexing is proposed to improve blocking performance when routing dynamic dependable connections. To further improve channel utilization, primary backup multiplexing is developed in [69]. Since different customers may differ in their needs of levels of fault tolerance, differentiated reliability is a suitable scheme [21, 38]. In [70], segmented protection wherein a protection path may be composed of several segments is studied. In [71], partial spatial-protection wherein only a subset of the links of a primary path is protected is proposed. Recently, joint consideration of energy efficiency and survivability has become a research interest. In [72], the problem of energy efficiently planning a WDM network with dedicated 1:1 path protection and devices supporting sleep mode is tackled. In [73], it focuses on energy efficient survivable network design with shared backup protection. It proposes an ILP formulation for the sake of minimizing both capacity and energy consumption. So far, no research effort on energy efficient routing of survivable sublambda connections has been found. In

Chapter 6, we present a power efficient integrated routing algorithm for dynamic sublambda connections with reliability constraints. The algorithm tries to find a minimum power consumption path for a connection while satisfying the reliability requirement. The algorithm achieves partial survivability by being aware of link failure probability.

2.5 Summary

In this chapter we walked through the basics of the Internet, including its definition, hierarchy, and common networking technologies. We gave a overview of a typical IP over WDM network, which consists of an IP layer and an optical layer. We explained the concepts like lightpath, RWA, traffic grooming, and optical bypass, which lay the foundation for appreciating the following chapters of this thesis. We described the two routing models: overlay and integrated, pointing out the advantages of the latter over the former. We also emphasized the importance of providing survivability to optical networks since there are enormous amount of data being handled by them. We explored several traffic models in the literature and specified some application scenarios for scheduled traffic models. We then examined the common power profiles to formulate the dependence of the power consumption of a network component with its traffic load. We then moved on to provide a survey of energy efficiency in the Internet. We covered some pioneering work on improving energy efficiency of the wired part of the Internet. We mentioned some techniques for EEE. We then explored the related work on energy efficiency in IP over WDM networks, which is the main focus of this thesis. We reviewed the research efforts in the literature which are closely related to the contributions of this thesis. Specifically, we reviewed energy efficient traffic grooming, the tradeoff between energy efficiency and other metrics, energy efficient provisioning of scheduled connection requests, and energy

efficiency with respect to survivability.

Chapter 3

Power Efficient Integrated Routing with Traffic Splitting

3.1 Introduction

This chapter investigates the problem of power efficient integrated routing with traffic splitting in IP over WDM networks. We consider two power profiles: affine and convex, which are desirable for the point of view of energy efficiency. We study both the static traffic model and the dynamic traffic model, the former is usually used in the network planning phase while the latter is a common model when the network is in operation. For static traffic model, we formulate ILP and IQP models to minimize the power consumption of the network. With respect to the dynamic traffic model, we propose power efficient routing algorithms which are based on an auxiliary graph. We conduct performance study to show that traffic-splitting-enabled networks outperform their non-traffic-splitting counterparts with respect to power consumption and blocking probability. We also explore the impact of fixed overhead proportion α on the power savings gained by traffic splitting.

3.2 Power Consumption Analysis

With the network architecture shown in Fig. 2.1, we can analyze the power consumption for different traffic flows. A lightpath can traverse one or more fiber links. For the latter case, the lightpath optically bypasses the intermediate nodes. We hereby illustrate the power consumption for two types of traffic flows: f_1 and f_2, as shown in Fig. 3.1. Traffic flow f_1 uses only one lightpath, meaning it bypasses the router of node 2; while traffic flow f_2 traverses two lightpaths in sequence, meaning it goes through the router of node 2. We assume the bandwidth requirement of traffic flow f_1 and traffic flow f_2 is the same and less than or equal to the full wavelength bandwidth.

Traffic flow f_1 is first electrically switched (E) to an output port of the IP router of node 1, and then transmitted (T) by the transmitter attached to the output port. Through this transmission process, traffic flow f_1 is converted to an optical signal. The optical signal is then destined to node 3. Along the route, the optical signal is optically switched (O) by the OXCs of node 1, node 2, and node 3 (without being electrically processed by IP routers); as well as amplified (A) by the amplifiers deployed along the fiber links. When the optical signal reaches node 3, it is received (R) by a receiver which is attached to an input port of the IP router of node 3. Through this reception process, the optical signal is converted back to an electrical signal. Finally, this electrical signal is electrically switched (E) by the IP router of node 3. Traffic flow f_2 goes through almost the same procedure as that of traffic flow f_1, except that it goes through one additional R, E, T, and O when it passes the intermediate node 2.

We denote P_e, P_t, P_o, P_a and P_r as the power consumption of components E, T, O, A and R, respectively. Note that P_e, P_t, P_o, P_a and P_r are dependent on the amount of traffic going through the components, they follow one of the two power

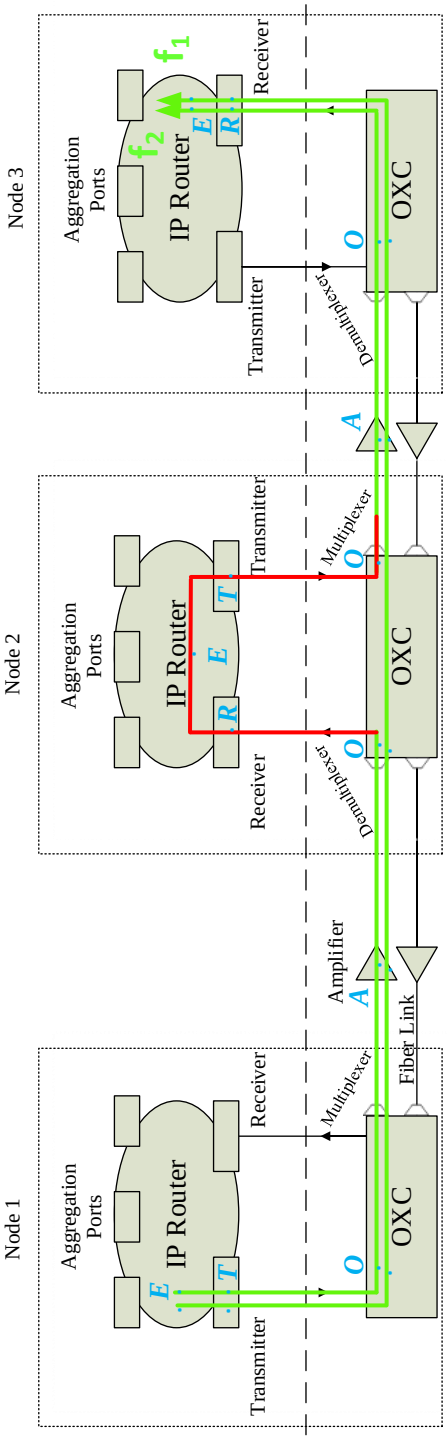

Figure 3.1: An illustration of the power consumption analysis of traffic flow f_1 and traffic flow f_2 (A blue dot is marked where power consumption takes place)

profiles (affine and convex power profiles) as aforementioned (Fig. 2.2). Also note that the set of components may vary with different network equipment vendors. Therefore the set of components listed here is for illustration only. For amplifiers (e.g., Erbium Doped Fiber Amplifiers (EDFAs)) of which the power consumption is independent on traffic volume, the power cost should be removed when calculating the power consumption of a traffic flow. Now we can evaluate the power consumption of traffic flow f_1 and traffic flow f_2 as follows:

$$\begin{aligned} P_{f_1} = {} & P_e + P_t + P_o \\ & + P_a + P_o \\ & + P_o + P_r + P_e \end{aligned} \tag{3.1}$$

$$\begin{aligned} P_{f_2} = {} & P_e + P_t + P_o \\ & + P_a + P_o \\ & + P_r + P_e + P_t + P_o \\ & + P_o + P_r + P_e \end{aligned} \tag{3.2}$$

where P_{f_1} is the power consumption of traffic flow f_1. In (3.1), the first row on the right-hand side is the power consumption of traffic flow f_1 at the source node 1; the second row represents the power consumption of amplifiers and intermediate OXCs along the route of traffic flow f_1; the third row represents the power consumption of traffic flow f_1 at the destination node 3. P_{f_2} is the power consumption of traffic flow f_2. In (3.2), the first row on the right-hand side is the power consumption of traffic flow f_2 at the source node 1; the second row stands for the power consumption of amplifiers and intermediate OXCs along the route of traffic flow f_2; the third row represents the power consumption of the additional R, E, T, and O at intermediate node 2; the fourth row represents the power consumption of traffic flow f_2 at the destination node 3.

The number of power components used by traffic flow f_2 is greater than that used by traffic flow f_1, but that does not necessarily mean $P_{f_2} > P_{f_1}$. For example, if the two lightpaths traversed by traffic flow f_2 are already set up in advance and the lightpath gone through by traffic flow f_1 needs to be newly created, then the extra power consumed due to the larger number of power components for traffic flow f_2 might be offset by the fixed power overhead saved by multiplexing on existing two lightpaths. It is assumed that transmitters and receivers can be turned on and switched off in a negligible transient time and do not incur additional energy of signaling. Transmitters and receivers can be switched off (put into sleep mode) to save power if there is no traffic being processed. But for routers, OXCs, and amplifiers, they are always turned on so as to maintain network presence [74].

3.2.1 Will Traffic Splitting Save Power?

We show that splitting traffic properly would lead to power savings. We use Fig. 3.2 as an example for illustration. Suppose there are three existing lightpaths (labeled as Lightpath 1, Lightpath 2 and Lightpath 3 in the figure) between node 1 and node 2, all with the same residual bandwidth of 0.9. The power consumptions of these three lightpaths follow the same power profile denoted as $p_1(t), p_2(t)$, and $p_3(t)$ respectively. A connection request is specified as a triple $< s, d, \beta >$, where s is the source node; d is the destination node; β is the required bandwidth of the connection request. Now suppose there is an arrival $< 1, 2, 0.8 >$. If it is routed on Lightpath 1 only (marked in red in the figure), then the additional power consumption for provisioning this connection request is $P_{0.8}$. But if it is split evenly into two connection requests and routed on Lightpath 2 and Lightpath 3 respectively (marked in green in the figure), then the additional power needed to provisioning this connection request is $P_{2\times 0.4}$. Now the question is whether it is possible for traffic

splitting to lead to power savings? That is to say, to make $P_{0.8} > P_{2\times0.4}$ hold. We hereby consider the two power profiles separately as follows.

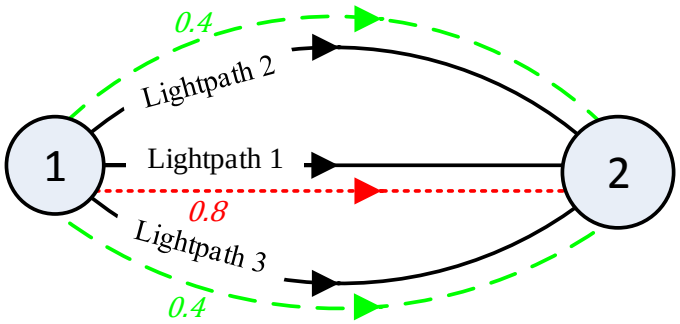

Figure 3.2: An example for traffic splitting

- *Convex*: We can assume $p_1(t) = p_2(t) = p_3(t) = 0.1 + 0.9t^2$, meaning the three lightpaths are identical with respect to power consumption characteristics. We have $P_{0.8} = [0.1 + 0.9 \times (0.8 + 0.1)^2] - [0.1 + 0.9 \times 0.1^2] = 0.72$; we also have $P_{2\times0.4} = 2 \times \{[0.1 + 0.9 \times (0.4 + 0.1)^2] - [0.1 + 0.9 \times 0.1^2]\} = 0.432$, therefore we have $P_{2\times0.4} = P_{0.8} \times 60\%$, meaning traffic splitting gains 40% power savings in this case.

- *Affine* : There will not be any power savings by traffic splitting if we assume $p_1(t) = p_2(t) = p_3(t) = 0.1 + 0.9t$ for this power profile. But if Lightpath 1 is more power-consuming than Lightpath 2 and Lightpath 3; and neither Lightpath 2 nor Lightpath 3 has enough bandwidth to accommodate the connection request, then traffic splitting again leads to power savings. We let $p_1(t) = 2 \times (0.1 + 0.9t)$, $p_2(t) = p_3(t) = 0.1 + 0.9t$, and the residual bandwidths of Lightpath 1, Lightpath 2 and Lightpath 3 are 0.9, 0.5 and 0.5, respectively. We have $P_{0.8} = 2 \times \{[0.1 + 0.9 \times (0.8 + 0.1)] - [0.1 + 0.9 \times 0.1]\} = 1.44$; we also

have $P_{2\times0.4} = 2\times\{[0.1+0.9\times(0.4+0.5)]-[0.1+0.9\times0.5]\} = 0.72$, therefore we have $P_{2\times0.4} = P_{0.8}\times50\%$, meaning traffic splitting gains 50% power savings in this case.

In our work, we adopt both traffic splitting and sleep mode for gaining power savings. Whenever a lightpath is idle (meaning there is no traffic going through it), it will be released and its transmitter and receiver will be shut down (put into sleep mode). A more general case when adopting sleep mode is to put a network component with low traffic volume, e.g., 10% of its full capacity, into sleep mode and divert its traffic to other paths [75, 76]. We note that traffic splitting might compromise the effectiveness of adopting sleep mode to gain power savings. If traffic splitting is disabled, network load might be concentrated on smaller number of lightpaths, allowing more lightpaths to be put into sleep mode. Therefore, there is a tradeoff between these two power-saving mechanisms, on which further investigation to achieve better power savings is beyond the scope of this work.

3.3 Power Minimization with the Static Traffic Model

In this section we study the power minimization with the static traffic model. In the static traffic model, all the connection requests are known in advance, therefore the problem of minimizing the power consumption of an IP over WDM network with the static traffic model turns out to be a mathematical optimization problem. We first define the problem, then we present the ILP formulation for affine power profile. We next introduce the IQP formulation for convex power profile. Numerical results are shown to demonstrate that traffic splitting helps in saving power.

3.3.1 Problem Definition

We define the problem of minimizing the power consumption in an IP over WDM network for dynamic routing of connection requests as follows:

We are given a network graph $\boldsymbol{G} = (\boldsymbol{V}, \boldsymbol{F})$ representing the physical topology of an IP over WDM network, where $\boldsymbol{V}$ is the set of network nodes and $\boldsymbol{F}$ is the set of fiber links. The power consumption value of each component is also given as an input. We are given a set of connection requests in advance. A connection request is specified as a triple $< s, d, \beta >$, where s is the source node of the connection request; d is the destination node of the connection request; β is the required bandwidth of the connection request. The goal is to find the routing and bandwidth allocation schemes for the set of connection requests considering traffic splitting such that their energy consumption is minimized.

3.3.2 ILP for Affine Power Profile

We are given the following *inputs* to the problem:

1. $\boldsymbol{G} = (\boldsymbol{V}, \boldsymbol{F})$, which represents the network topology. $\boldsymbol{V}$ is the set of network nodes and $\boldsymbol{F}$ is the set of fiber links. An entry $F_{m,n}$ of $\boldsymbol{F}$ is a Boolean variable that represents whether the fiber link from node m to node n exists or not. Each fiber link can support W wavelengths and the bandwidth capacity of each wavelength is C, which is in multiple of the minimal granularity. The number of nodes in $\boldsymbol{V}$ is denoted as $N = |\boldsymbol{V}|$.

2. $\boldsymbol{\lambda}$, which is the connection requests matrix. $\boldsymbol{\lambda}$ is a two-dimensional matrix of $N \times N$. An entry $\lambda^{s,d}$ in $\boldsymbol{\lambda}$ denotes a connection request from node s to node d with the bandwidth requirement of $\lambda^{s,d}$. The bandwidth requirement of a connection request may be at sublambda granularity, meaning it can be a

fraction of a wavelength bandwidth. We call this type of connection requests as sublambda connection requests.

3. $\boldsymbol{Q}$, which is the set of subconnection indexes for a connection request. We have $\boldsymbol{Q} = \{0, 1, \cdots, |\boldsymbol{Q}| - 1\}$, where $|\boldsymbol{Q}|$ is the maximum allowable number of subconnections for a connection request. If traffic splitting is prohibited, we have $|\boldsymbol{Q}| = 1$; else we have $|\boldsymbol{Q}| > 1$. We hereby consider only splitting at the source or destination node of a connection request.

4. P_E, P_O, P_T, P_R, and P_A, which are the power consumption for processing a full wavelength bandwidth amount of traffic, in terms of electrical switching, optical switching, transmitting, receiving, and amplifying, respectively. We denote α as the fixed overhead proportion of a power consumption component, as same in (2.1) and (2.2).

5. $\boldsymbol{\phi_T}, \boldsymbol{\phi_R}$, which represent the numbers of transmitters and receivers, respectively of network nodes. An entry ϕ_T^i of $\boldsymbol{\phi_T}$ denotes the number of transmitters of node i. Similarly, an entry ϕ_R^i of $\boldsymbol{\phi_R}$ denotes the number of receivers of node i.

6. $\boldsymbol{\eta}$, which is a two-dimensional matrix of $N \times N$ with each entry $\eta^{m,n}$ representing the number of amplifiers on physical link (m, n).

7. W, which is the number of wavelengths on a physical link.

We apply the following general *indexing* rules to the formulation:

1. m, n: index the nodes in the optical layer.

2. i, j: index the nodes in the IP layer.

3. s, d: index the source and the destination nodes of a connection request.

4. q: index the subconnections of a connection request.

5. k: index the transmitters.

6. l: index the receivers.

7. ω: index the wavelengths on physical links (fiber links).

8. a connection request is denoted as $< s, d, \beta >$, where s is the source node, d is the destination node, β is the required bandwidth of the connection request.

9. a lightpath is indexed as $< i, j, k, l, \omega >$, where i is the source node, j is the destination node, k is the index of the transmitter used by the lightpath, l is the index of the receiver used by the lightpath, and ω is the wavelength of the lightpath. Note that a lightpath cannot be denoted just as $< i, j, \omega >$ because there may be more than one lightpath sourced at node i, destined to node j, and allocated with wavelength ω, so long as they follow link-disjoint routes.

The following *variables* are defined:

1. ε_E^i: the amount of traffic being electrically switched by node i; we have $\varepsilon_E^i \geq 0$.

2. ε_O^i: the amount of traffic being optically switched by node i; we have $\varepsilon_O^i \geq 0$.

3. $\delta_{i,k}$: 1 if the kth transmitter of node i is turned on, 0 otherwise.

4. $\delta_{i,l}$: 1 if the lth receiver of node i is turned on, 0 otherwise.

5. $\varepsilon_{i,k}$: the amount of traffic going through the kth transmitter of node i; we have $0 \leq \varepsilon_{i,k} \leq C$.

6. $\varepsilon_{i,l}$: the amount of traffic going through the lth receiver of node i; we have $0 \leq \varepsilon_{i,l} \leq C$.

7. $\varepsilon_{m,n,\omega}$: the amount of traffic going through physical link (m,n) using wavelength ω; we have $0 \leq \varepsilon_{m,n,\omega} \leq C$.

8. $\lambda^{s,d,q}$: the amount of traffic allocated to subconnection $< s,d,q >$; we have $\lambda^{s,d,q} \geq 0$.

9. $\mu^{s,d,q}_{i,j,k,l,\omega}$: 1 if subconnection $< s,d,q >$ is routed through lightpath $< i,j,k,l,\omega >$, 0 otherwise.

10. $\nu^{s,d,q}_{i,j,k,l,\omega}$: the amount of traffic from subconnection $< s,d,q >$ that traverses lightpath $< i,j,k,l,\omega >$; we have $0 \leq \nu^{s,d,q}_{i,j,k,l,\omega} \leq C$.

11. $\rho^{i,j,k,l,\omega}_{m,n}$: 1 if lightpath $< i,j,k,l,\omega >$ goes through physical link (m,n), 0 otherwise.

12. $\theta^{i,j,k,l,\omega}_{m,n}$: the amount of traffic from lightpath $< i,j,k,l,\omega >$ that traverses physical link (m,n); we have $0 \leq \theta^{i,j,k,l,\omega}_{m,n} \leq C$.

13. $\rho^{i,j,k,l,\omega}$: 1 if lightpath $< i,j,k,l,\omega >$ exists, 0 otherwise.

14. $\theta^{i,j,k,l,\omega}$: the amount of traffic traverses lightpath $< i,j,k,l,\omega >$; we have $0 \leq \theta^{i,j,k,l,\omega} \leq C$.

The ILP model for affine power profile is defined as follows:

Objective: Minimize

$$\underbrace{\sum_{i\in\boldsymbol{V}} \frac{\varepsilon^i_E}{C}(1-\alpha)P_E}_{\text{Electrical Switching Power}} + \underbrace{\sum_{i\in\boldsymbol{V}} \frac{\varepsilon^i_O}{C}(1-\alpha)P_O}_{\text{Optical Switching Power}} + \underbrace{\sum_{i\in\boldsymbol{V}}\sum_{k=0}^{\phi^i_T} P_T\left[\delta_{i,k}\alpha + (1-\alpha)\frac{\varepsilon_{i,k}}{C}\right]}_{\text{Transmitters Power}}$$
$$+ \underbrace{\sum_{i\in\boldsymbol{V}}\sum_{l=0}^{\phi^i_R} P_R\left[\delta_{i,l}\alpha + (1-\alpha)\frac{\varepsilon_{i,l}}{C}\right]}_{\text{Receivers Power}} + \underbrace{\sum_{m\in\boldsymbol{V}}\sum_{n\in\boldsymbol{V}:n\neq m}\sum_{\omega=0}^{W-1}\frac{\varepsilon_{m,n,\omega}}{C}P_A(1-\alpha)\eta_{m,n}}_{\text{Amplifiers Power}} \tag{3.3}$$

Subject to:

1. *Power Components Equalities*

$$\sum_{j\in\boldsymbol{V}:j\neq i}\sum_{k=0}^{\phi_T^i}\sum_{l=0}^{\phi_R^j}\sum_{\omega=0}^{W-1}\theta^{i,j,k,l,\omega} \quad + \sum_{j\in\boldsymbol{V}:j\neq i}\sum_{k=0}^{\phi_T^j}\sum_{l=0}^{\phi_R^i}\sum_{\omega=0}^{W-1}\theta^{j,i,k,l,\omega} = \varepsilon_E^i \quad \forall i \in \boldsymbol{V}. \tag{3.4}$$

Constraint (3.4) says that the amount of traffic being electrically switched by node i is composed of two parts:

- The traffic amount of the lightpaths with node i as the source node.
- The traffic amount of the lightpaths with node i as the destination node.

$$\begin{aligned}\sum_{j\in\boldsymbol{V}:j\neq i}\sum_{k=0}^{\phi_T^i}\sum_{l=0}^{\phi_R^j}\sum_{\omega=0}^{W-1}\theta^{i,j,k,l,\omega} \quad &+ \sum_{j\in\boldsymbol{V}:j\neq i}\sum_{k=0}^{\phi_T^j}\sum_{l=0}^{\phi_R^i}\sum_{\omega=0}^{W-1}\theta^{j,i,k,l,\omega} \\ + \sum_{s\in\boldsymbol{V}:s\neq i}\sum_{j\in\boldsymbol{V}:j\neq s,i}\sum_{n\in\boldsymbol{V}:n\neq i}\sum_{k=0}^{\phi_T^s}\sum_{l=0}^{\phi_R^j}\sum_{\omega=0}^{W-1}\theta_{i,n}^{s,j,k,l,\omega} &= \varepsilon_O^i \quad \forall i \in \boldsymbol{V}.\end{aligned} \tag{3.5}$$

Constraint (3.5) says that the amount of traffic being optically switched by node i is composed of three parts:

- The traffic amount of the lightpaths with node i as the source node.
- The traffic amount of the lightpaths with node i as the destination node.
- The traffic amount of the lightpaths with node i as the intermediate node.

$$\sum_{j\in\boldsymbol{V}:j\neq i}\sum_{l=0}^{\phi_R^j}\sum_{\omega=0}^{W-1}\theta^{i,j,k,l,\omega} = \varepsilon_{i,k} \quad \forall i \in \boldsymbol{V}, k \in [0, \phi_T^i]. \tag{3.6}$$

Constraint (3.6) says that the amount of traffic going through the kth transmitter of node i is equal to the traffic amount of the lightpath using that transmitter.

$$\sum_{j\in\boldsymbol{V}:j\neq i}\sum_{k=0}^{\phi_T^j}\sum_{\omega=0}^{W-1}\theta^{j,i,k,l,\omega} = \varepsilon_{i,l} \quad \forall i \in \boldsymbol{V}, l \in [0, \phi_R^i]. \tag{3.7}$$

Constraint (3.7) says that the amount of traffic going through the lth receiver of node i equals the traffic amount of the lightpath using that receiver.

$$\sum_{j\in\boldsymbol{V}:j\neq i}\sum_{l=0}^{\phi_R^j}\sum_{\omega=0}^{W-1}\rho^{i,j,k,l,\omega}=\delta_{i,k}\quad\forall i\in\boldsymbol{V},k\in[0,\phi_T^i]. \tag{3.8}$$

$$\sum_{j\in\boldsymbol{V}:j\neq i}\sum_{k=0}^{\phi_T^j}\sum_{\omega=0}^{W-1}\rho^{j,i,k,l,\omega}=\delta_{i,l}\quad\forall i\in\boldsymbol{V},l\in[0,\phi_R^i]. \tag{3.9}$$

Constraint (3.8) and (3.9) say that a transmitter/receiver is turned on if there is a lightpath using it.

$$\sum_{i\in\boldsymbol{V}}\sum_{j\in\boldsymbol{V}:j\neq i}\sum_{k=0}^{\phi_T^i}\sum_{l=0}^{\phi_R^j}\theta_{m,n}^{i,j,k,l,\omega}=\varepsilon_{m,n,\omega}\quad\forall m,n\in\boldsymbol{V}:m\neq n,\omega\in[0,W-1]. \tag{3.10}$$

Constraint (3.10) says that the amount of traffic going through physical link (m,n) using wavelength ω is equal to the traffic amount of the lightpath using the wavelength ω of physical link (m,n).

2. *Flow conservation constraints in the IP layer*

$$\begin{aligned}&\sum_{j\in\boldsymbol{V}:j\neq i}\sum_{k=0}^{\phi_T^i}\sum_{l=0}^{\phi_R^j}\sum_{\omega=0}^{W-1}\nu_{i,j,k,l,\omega}^{s,d,q}-\sum_{j\in\boldsymbol{V}:j\neq i}\sum_{k=0}^{\phi_T^j}\sum_{l=0}^{\phi_R^i}\sum_{\omega=0}^{W-1}\nu_{j,i,k,l,\omega}^{s,d,q}\\&=\begin{cases}\lambda^{s,d,q}, & \text{if } i=s\\ -\lambda^{s,d,q}, & \text{if } i=d\\ 0, & \text{otherwise}\end{cases}\quad\forall s,d,i\in\boldsymbol{V}:s\neq d;\forall q\in\boldsymbol{Q}.\end{aligned} \tag{3.11}$$

Constraint (3.11) represents the flow conservation constraints in the IP layer. It ensures that in all nodes, excluding the source and the destination nodes, the total amount of incoming traffic equals the total amount of outgoing traffic.

3. *Virtual link capacity constraints*

$$\begin{aligned} &\sum_{s\in\boldsymbol{V}}\sum_{d\in\boldsymbol{V}:d\neq s}\sum_{q\in\boldsymbol{Q}}\nu_{i,j,k,l,\omega}^{s,d,q}=\theta^{i,j,k,l,\omega} \\ &\forall i,j\in\boldsymbol{V}:i\neq j; \\ &\forall k\in[0,\phi_T^i],l\in[0,\phi_R^j],\omega\in[0,W-1]. \end{aligned} \tag{3.12}$$

Constraint (3.12) says that the traffic amount of a lightpath equals the sum of the traffic amount of each connection request using that lightpath.

$$\begin{aligned} &\theta^{i,j,k,l,\omega}\leq C \\ &\forall i,j\in\boldsymbol{V}:i\neq j; \\ &\forall k\in[0,\phi_T^i],l\in[0,\phi_R^j],\omega\in[0,W-1]. \end{aligned} \tag{3.13}$$

Constraint (3.13) ensures that the traffic amount of a lightpath does not exceed its capacity.

4. *Subconnection bandwidth constraints*

$$\sum_{q\in\boldsymbol{Q}}\lambda^{s,d,q}=\lambda^{s,d}\quad\forall s,d\in\boldsymbol{V}:s\neq d. \tag{3.14}$$

Constraint (3.14) says that the sum of the traffic amount of the subconnections should be equal to that of the original connection request.

5. *Flow conservation constraints in the optical layer*

$$\sum_{n\in\boldsymbol{V}:n\neq m}\theta_{m,n}^{i,j,k,l,\omega}-\sum_{n\in\boldsymbol{V}:n\neq m}\theta_{n,m}^{i,j,k,l,\omega}=\begin{cases}\theta^{i,j,k,l,\omega}, & \text{if } m=i\\ -\theta^{i,j,k,l,\omega}, & \text{if } m=j\\ 0, & \text{otherwise}\end{cases} \tag{3.15}$$

$$\forall m,i,j\in\boldsymbol{V}:i\neq j;\forall k\in[0,\phi_T^i],l\in[0,\phi_R^j],\omega\in[0,W-1].$$

Constraint (3.15) represents the flow conservation constraints in the optical layer. It ensures that in all nodes, excluding the source and the destination

nodes, the total amount of incoming traffic equals the total amount of outgoing traffic.

6. *Wavelength constraints*

$$\sum_{i\in\boldsymbol{V}}\sum_{j\in\boldsymbol{V}:j\neq i}\sum_{k=0}^{\phi_T^i}\sum_{l=0}^{\phi_R^j}\sum_{\omega=0}^{W-1}\rho_{m,n}^{i,j,k,l,\omega}\leq F_{m,n} \qquad (3.16)$$
$$\forall m,n\in\boldsymbol{V}:m\neq n;\forall\omega\in[0,W-1].$$

Constraint (3.16) says that a wavelength on a fiber link can be used by at most one lightpath traversing this fiber link, provided that the fiber link exists.

7. *Physical link capacity constraints*

$$\sum_{i\in\boldsymbol{V}}\sum_{j\in\boldsymbol{V}:j\neq i}\sum_{k=0}^{\phi_T^i}\sum_{l=0}^{\phi_R^j}\sum_{\omega=0}^{W-1}\theta_{m,n}^{i,j,k,l,\omega}\leq WCF_{m,n} \qquad (3.17)$$
$$\forall m,n\in\boldsymbol{V}:m\neq n.$$

Constraint (3.17) says that the total amount of traffic going through a fiber link should not exceed its capacity.

8. *Variable value constraints*

$$\mu_{i,j,k,l,\omega}^{s,d,q}\leq\nu_{i,j,k,l,\omega}^{s,d,q}\leq C\mu_{i,j,k,l,\omega}^{s,d,q}$$
$$\forall s,d,i,j\in\boldsymbol{V}:s\neq d,i\neq j;\forall q\in\boldsymbol{Q}; \qquad (3.18a)$$
$$\forall k\in[0,\phi_T^i],l\in[0,\phi_R^j],\omega\in[0,W-1].$$

$$0\leq\lambda^{s,d,q}-\nu_{i,j,k,l,\omega}^{s,d,q}\leq C(1-\mu_{i,j,k,l,\omega}^{s,d,q})$$
$$\forall s,d,i,j\in\boldsymbol{V}:s\neq d,i\neq j;\forall q\in\boldsymbol{Q}; \qquad (3.18b)$$
$$\forall k\in[0,\phi_T^i],l\in[0,\phi_R^j],\omega\in[0,W-1].$$

Constraints (3.18a) and (3.18b) ensure that if $\mu_{i,j,k,l,\omega}^{s,d,q}=0$, we have $\nu_{i,j,k,l,\omega}^{s,d,q}=0$; if $\mu_{i,j,k,l,\omega}^{s,d,q}=1$, we have $\nu_{i,j,k,l,\omega}^{s,d,q}=\lambda^{s,d,q}>0$.

$$\rho_{m,n}^{i,j,k,l,\omega} \leq \theta_{m,n}^{i,j,k,l,\omega} \leq C\rho_{m,n}^{i,j,k,l,\omega}$$
$$\forall i,j,m,n \in \boldsymbol{V} : i \neq j, m \neq n; \tag{3.19a}$$
$$\forall k \in [0,\phi_T^i], l \in [0,\phi_R^j], \omega \in [0,W-1].$$

$$0 \leq \theta^{i,j,k,l,\omega} - \theta_{m,n}^{i,j,k,l,\omega} \leq C(1-\rho_{m,n}^{i,j,k,l,\omega})$$
$$\forall i,j,m,n \in \boldsymbol{V} : i \neq j, m \neq n; \tag{3.19b}$$
$$\forall k \in [0,\phi_T^i], l \in [0,\phi_R^j], \omega \in [0,W-1].$$

Constraints (3.19a) and (3.19b) ensure that if $\rho_{m,n}^{i,j,k,l,\omega} = 0$, we have $\theta_{m,n}^{i,j,k,l,\omega} = 0$; if $\rho_{m,n}^{i,j,k,l,\omega} = 1$, we have $\theta_{m,n}^{i,j,k,l,\omega} = \theta^{i,j,k,l,\omega} > 0$.

$$\rho^{i,j,k,l,\omega} \leq \theta^{i,j,k,l,\omega} \leq C\rho^{i,j,k,l,\omega}$$
$$\forall i,j \in \boldsymbol{V} : i \neq j; \forall k \in [0,\phi_T^i]; \tag{3.20}$$
$$\forall l \in [0,\phi_R^j], \omega \in [0,W-1].$$

Constraints (3.20) ensures that if $\theta^{i,j,k,l,\omega} = 0$, we have $\rho^{i,j,k,l,\omega} = 0$; if $\theta^{i,j,k,l,\omega} > 0$, we have $\rho^{i,j,k,l,\omega} = 1$.

$$\delta_{i,k} \leq \varepsilon_{i,k} \leq C\delta_{i,k} \quad \forall i \in \boldsymbol{V}, k \in [0,\phi_T^i]. \tag{3.21}$$

Constraints (3.21) ensures that if $\varepsilon_{i,k} = 0$, we have $\delta_{i,k} = 0$; if $\varepsilon_{i,k} > 0$, we have $\delta_{i,k} = 1$.

$$\delta_{i,l} \leq \varepsilon_{i,l} \leq C\delta_{i,l} \quad \forall i \in \boldsymbol{V}, l \in [0,\phi_R^i]. \tag{3.22}$$

Constraints (3.22) ensures that if $\varepsilon_{i,l} = 0$, we have $\delta_{i,l} = 0$; if $\varepsilon_{i,l} > 0$, we have $\delta_{i,l} = 1$.

3.3.3 IQP for Convex Power Profile

The IQP formulation for convex power profile is the same as the ILP formulation for affine power profile except that the objective function should be modified as:

$$\begin{aligned}
&\sum_{i\in\boldsymbol{V}}(1-\alpha)P_E\cdot\left\{\sum_{j\in\boldsymbol{V}:j\neq i}\sum_{k=0}^{\phi_T^i}\sum_{l=0}^{\phi_R^j}\sum_{\omega=0}^{W-1}\left(\frac{\theta^{i,j,k,l,\omega}}{C}\right)^2+\sum_{j\in\boldsymbol{V}:j\neq i}\sum_{k=0}^{\phi_T^j}\sum_{l=0}^{\phi_R^i}\sum_{\omega=0}^{W-1}\left(\frac{\theta^{j,i,k,l,\omega}}{C}\right)^2\right\}\\
&+\sum_{i\in\boldsymbol{V}}(1-\alpha)P_O\cdot\left\{\sum_{j\in\boldsymbol{V}:j\neq i}\sum_{k=0}^{\phi_T^i}\sum_{l=0}^{\phi_R^j}\sum_{\omega=0}^{W-1}\left(\frac{\theta^{i,j,k,l,\omega}}{C}\right)^2+\sum_{j\in\boldsymbol{V}:j\neq i}\sum_{k=0}^{\phi_T^j}\sum_{l=0}^{\phi_R^i}\sum_{\omega=0}^{W-1}\left(\frac{\theta^{j,i,k,l,\omega}}{C}\right)^2\right.\\
&\left.+\sum_{s\in\boldsymbol{V}:s\neq i}\sum_{j\in\boldsymbol{V}:j\neq s,i}\sum_{n\in\boldsymbol{V}:n\neq i}\sum_{k=0}^{\phi_T^s}\sum_{l=0}^{\phi_R^j}\sum_{\omega=0}^{W-1}\left(\frac{\theta_{i,n}^{s,j,k,l,\omega}}{C}\right)^2\right\}\\
&+\sum_{i\in\boldsymbol{V}}\sum_{k=0}^{\phi_T^i}P_T\left[\delta_{i,k}\alpha+(1-\alpha)\left(\frac{\varepsilon_{i,k}}{C}\right)^2\right]+\sum_{i\in\boldsymbol{V}}\sum_{l=0}^{\phi_R^i}P_R\left[\delta_{i,l}\alpha+(1-\alpha)\left(\frac{\varepsilon_{i,l}}{C}\right)^2\right]\\
&+\sum_{m\in\boldsymbol{V}}\sum_{n\in\boldsymbol{V}:n\neq m}\sum_{\omega=0}^{W-1}\left(\frac{\varepsilon_{m,n,\omega}}{C}\right)^2P_A(1-\alpha)\eta_{m,n}
\end{aligned}\tag{3.23}$$

3.3.4 Numerical Results

It is well known that traffic grooming problem is NP-complete [33]. In terms of computational complexity, the aforementioned formulations have a total of $O(N^4\cdot\max\{\boldsymbol{\phi_T}\}\cdot\max\{\boldsymbol{\phi_R}\}\cdot W\cdot|\boldsymbol{Q}|)$ variables and constraints. There are a huge number of variables and constraints if N is very large, making the problem more complex to get optimal results at a reasonable time for real (large) networks and heavy loads. We use a 14-node 24-link NSFNET as shown in Fig. 3.3(a) as our test network. All OXCs are without wavelength conversion capability, but a connection request using more than one lightpath does not necessarily use the same wavelength as wavelength conversion is done at routers' side using optical-electrical-optical (O-E-O) conversion. A link that connects two OXCs is comprised of a bidirectional fiber link with 3 wavelengths for each direction. Amplifiers are deployed along fiber links

one for every 80 km. The bandwidth capacity of a wavelength is normalized to 1. Based on [61], [77] and [78], we calculate the power consumption (in unit) per wavelength of each component as listed in Table 3.1. Note that the power value of T is composed of two parts: the power consumed to convert an electrical signal to an optical signal at a router port, and the power needed to convert the optical signal to a WDM-compatible signal. Similarly, the power value of R is also composed of two parts: the power needed to convert the WDM-compatible signal back to the optical signal, and the power consumed to convert the optical signal to an electrical signal at a router port (which is assumed to consume 1 unit of power for 1 unit of traffic). Also we let α the fixed overhead proportion of a network component to be 10%. We randomly generate a set of connection requests and add them to the network sequentially. These connection requests are denoted as $c_1, c_2, \cdots, c_n$. We use CPLEX to solve the optimization problems. The optimization results for the ILP model (affine power profile) and for the IQP model (convex power profile) comparing the non-traffic-splitting case ($|\boldsymbol{Q}| = 1$) with the traffic splitting case ($|\boldsymbol{Q}| = 2$) are listed in Table 3.2 and Table 3.3, respectively. We can see that traffic splitting always leads to power savings for both affine and convex power profiles.

Table 3.1: Power consumption values

Component	Power (per wavelength)	Component	Power (per wavelength)
E	P_E =18.4	O	P_O =9.2
T	P_T =11.3	R	P_R =1.5
A	P_A =0.07		

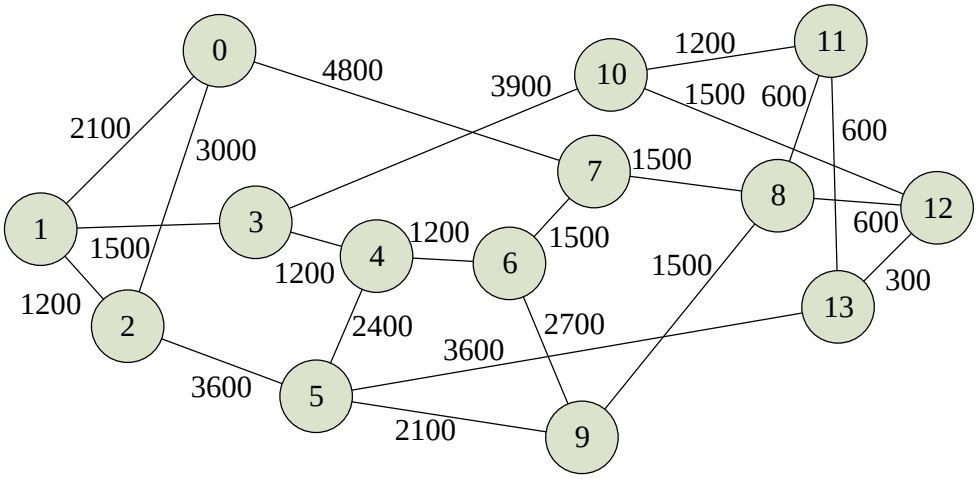

(a) NSFNET

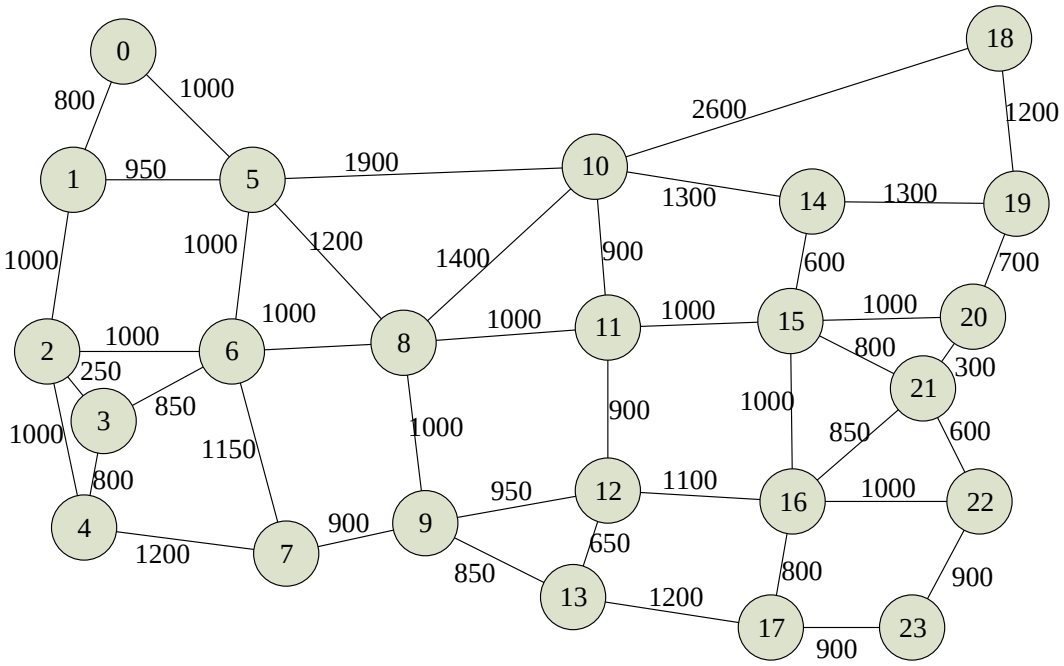

(b) USNET

Figure 3.3: Test networks with fiber link lengths (in km) marked on each link

Table 3.2: Optimization results (affine profile): $|\boldsymbol{Q}| = 1$ vs. $|\boldsymbol{Q}| = 2$

Connection requests	Total power consumption ($\|Q\| = 1$)	Total power consumption ($\|Q\| = 2$)
$c_1 - c_{30}$	1091.06	1088.72
$c_1 - c_{50}$	1923.59	1881.17
$c_1 - c_{70}$	2883.13	2773.00

Table 3.3: Optimization results (convex profile): $|\boldsymbol{Q}| = 1$ vs. $|\boldsymbol{Q}| = 2$

Connection requests	Total power consumption ($\|Q\| = 1$)	Total power consumption ($\|Q\| = 2$)
$c_1 - c_5$	124.29	79.75
$c_1 - c_{10}$	231.53	145.40
$c_1 - c_{15}$	352.28	209.47

3.4 Power Efficient Integrated Routing Algorithms for the Dynamic Traffic

The static traffic model is usually used in the network planning phase, wherein network planners design the network based on traffic predictions. However, the dynamic traffic model should be adopted when the network is in operation because connection requests arrive at and leave the network dynamically. In this section, we investigate power efficient integrated routing with the dynamic traffic model.

3.4.1 Problem Definition

We define the problem of minimizing the power consumption in an IP over WDM network for dynamic routing of connection requests as follows:

We are given a network graph $\boldsymbol{G} = (\boldsymbol{V}, \boldsymbol{F})$ representing the physical topology of an IP over WDM network, where $\boldsymbol{V}$ is the set of network nodes and $\boldsymbol{F}$ is the set of fiber links. The power consumption value of each component is also given as an input. Connection requests arrive to the network one by one in a random manner. A connection request is specified as a triple $< s, d, \beta >$, where s is the source node of the connection request; d is the destination node of the connection request; β is the required bandwidth of the connection request. The goal is to find the most power efficient route for a connection considering traffic splitting.

3.4.2 Auxiliary Graph

We construct an auxiliary graph to model the power consumption of each hop of a route and facilitate the application of the shortest-path algorithm. By assigning edge weights according to the power consumption, the shortest path in the auxiliary graph is equivalent to the most power efficient path. An auxiliary graph for a four-

node network is shown in Fig. 3.4, where there are two wavelengths for each fiber link and one fiber link for every physical hop between OXCs. Also, there is only one transmitter and one receiver for router a and router d, and two transmitters and two receivers for router b and router c. There are five types of edges in the auxiliary graph. They are:

- *supernode edge*, which is the link between a supernode and a transmitter (or receiver). The weight of a supernode edge is zero.
- *transmission edge*, which is the link from a transmitter to an OXC, and whose weight is the power consumption of transmission (denoted as T in the graph).
- *receiver edge*, which is the link from an OXC to a receiver and is assigned $O + R + E$ as its weight.
- *fiber edge*, which is the fiber link between a pair of OXCs and its weight is the sum of the power consumption of O and all the A's along the link. This weight varies with different fiber links since they may have different numbers of amplifiers. In Fig. 3.4, we use n_1, n_2, n_3, n_4 to represent the number of amplifiers along the fiber link of OXC A-OXC B, OXC B-OXC C, OXC C-OXC D, OXC D-OXC A, respectively.
- *lightpath*, if a new lightpath is created, then all the edges traversed by the lightpath shall be removed from the auxiliary graph, and a direct edge from the transmitter used by the lightpath to the receiver of the lightpath shall be set up. The weight of this edge is the sum of the weights of all the edges traversed by the lightpath.

We analyze the power consumption of lightpaths and connection requests as follows. Suppose a lightpath (denoted as LP1) is created on the route $\mathrm{b}_{\mathrm{t}_1} \rightarrow \mathrm{B}_1 \rightarrow \mathrm{C}_1 \rightarrow \mathrm{D}_1 \rightarrow \mathrm{D}_{\mathrm{r}_1}$. The power cost of LP1 for the first connection request (suppose

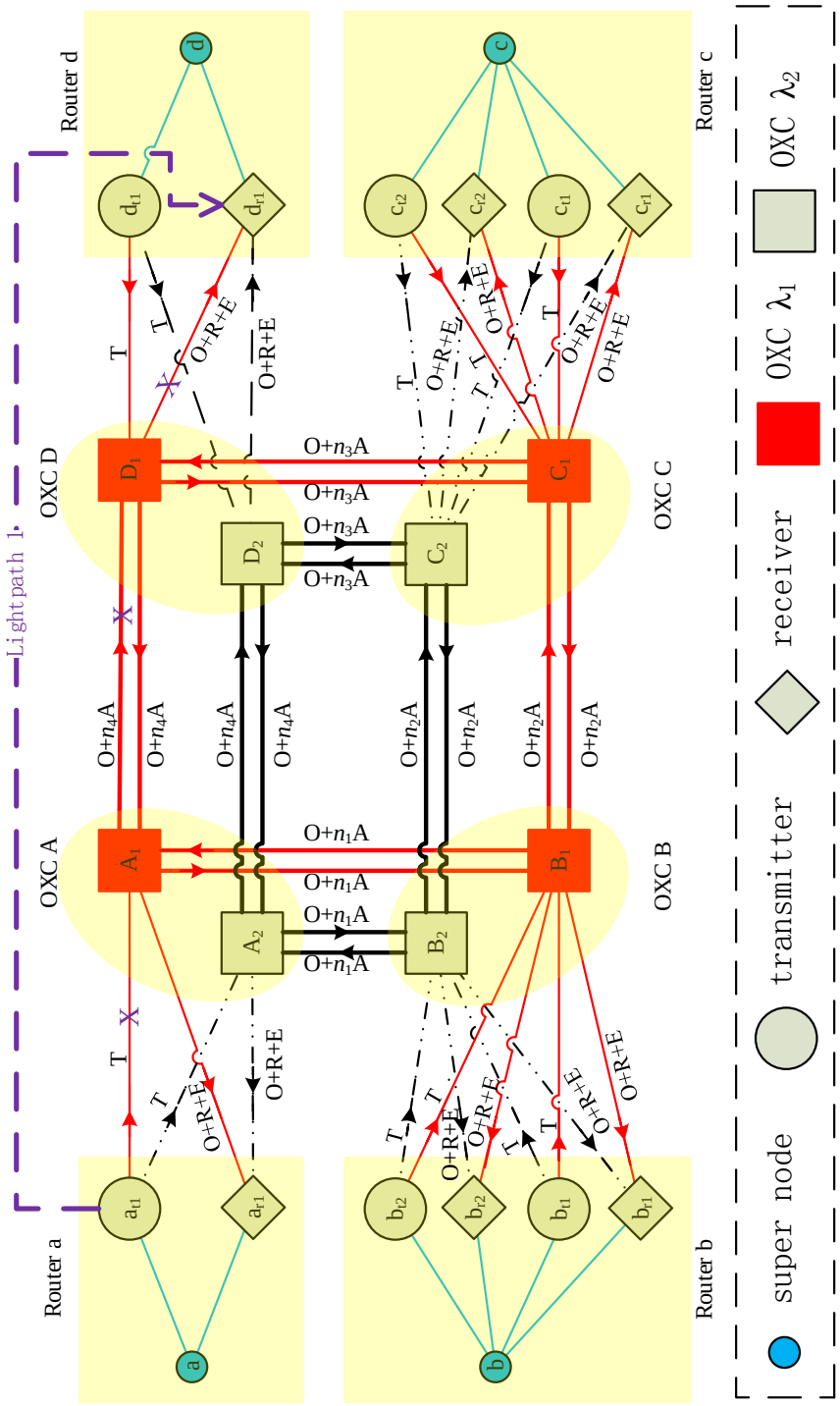

Figure 3.4: Auxiliary graph of a four-node network

its bandwidth requirement is β_1) that uses it is $(T+R)\alpha+[T+(O+n_2A)+(O+n_3A)+(O+R+E)](1-\alpha)\beta_1$ for affine power profile and $(T+R)\alpha+[T+(O+n_2A)+(O+n_3A)+(O+R+E)](1-\alpha){\beta_1}^2$ for convex power profile, where α is the fixed overhead proportion of a network component as defined in Section 3.1. The power cost of LP1 for the second connection request (suppose the bandwidth requirement is β_2) that uses it is $[T+(O+n_2A)+(O+n_3A)+(O+R+E)](1-\alpha)\beta_2$ for affine power profile and $[T+(O+n_2A)+(O+n_3A)+(O+R+E)](1-\alpha)[(\beta_2+\beta_1)^2-{\beta_1}^2]$ for convex power profile. The difference between the two scenarios lies in the fact that the first connection asks for creating LP1, therefore it should pay for the fixed overhead term of the power cost needed to switch on a transmitter and a receiver (i.e., the fixed overhead term of T and R). But for the following connection requests, they just use the already created LP1, so no fixed overhead term is needed.

Suppose a connection request with bandwidth requirement of β_3 creates and uses only LP1, then the power consumption of this connection request is $E(1-\alpha)\beta_3+P_{\text{LP1}}\beta_3$ for affine power profile and $E(1-\alpha){\beta_3}^2+P_{\text{LP1}}{\beta_3}^2$ for convex power profile, where P_{LP1} is the wavelength bandwidth power cost of LP1. Note that $E(1-\alpha)\beta_3$ (for affine power profile) is added besides the power cost ($P_{\text{LP1}}\beta_3$ for affine power profile here) recorded in the auxiliary graph when calculating the total power consumption of the connection request. This is because a connection request should be electrically switched by the IP router of the source node before it is transmitted. One may think this E can be appended to the weight of the transmission edge (meaning the weight of the transmission edge is set as $T+E$ instead of T) so as to be captured directly by the auxiliary graph. The reason why we do not do so is because the receiver edge is assigned $O+R+E$ as its weight, which already includes an E component. So we choose to append the electrical switching power consumed by the IP router of the source node of a connection request after we have obtained the power consumption value for that connection request as per what is recorded

in the auxiliary graph, in order to avoid unnecessary E's being wrongly included when calculating the total power consumption of a connection request, which occurs when the connection request traverses intermediate routers between two consecutive lightpaths. For example, suppose router b is traversed by a connection request as an intermediate router. The connection request enters router b through link $\mathrm{B}_1 \rightarrow \mathrm{b}_{\mathrm{r}_1}$ and leaves router b through link $\mathrm{b}_{\mathrm{t}_1} \rightarrow \mathrm{B}_2$, incurring $(O+R+E)+(T)$ amount of power which is desirable. But if we modify the weight of the transmission edge as $T+E$ instead of T, then the power incurred is $(O+R+E)+(E+T)$, which wrongly includes a duplicated E.

3.4.3 Algorithm Description

Based on the auxiliary graph constructed above, we develop an algorithm called Power efficient Integrated Routing with Traffic Splitting (PIRTS) as described in Algorithm 1. For a new connection request c, PIRTS searches for the most power efficient path p. It will then try splitting c into two subconnection requests c_1 and c_2 each with halved bandwidth of c. If c cannot be split in that proportion and p is not available, the connection request will be rejected. But if c can be split like that then PIRTS will choose the bandwidth proportion of each subconnection request such that the sum of the power consumption of the two subconnection requests is minimum and lower than that of routing on p only. If this is achievable, it means that traffic splitting helps in saving power and therefore is adopted; otherwise traffic splitting is discarded and the connection request will be routed on p only. Finally the auxiliary graph is updated to reflect the addition of new lightpaths, the marking of used network resources (such as transmitters, receivers, wavelength channels, etc.), and the latest residual bandwidth of existing lightpaths.

To verify the effectiveness of PIRTS, an algorithm called Power efficient Inte-

Algorithm 1 PIRTS

Input: A connection request c

Output: The provisioning scheme for c

Run Dijkstra's algorithm in an auxiliary graph $\boldsymbol{G}$ to find the most power efficient path p for c
Split c into two subconnection requests c_1 and c_2 each with halved bandwidth of c
Route in $\boldsymbol{G}$ to find two disjoint paths p_1 and p_2
if there do not exist such p_1 and p_2 **then**
    if there does not exist such p **then**
        Reject c
    else
        Discard traffic splitting
        Route c on path p only
        Record the provisioning information of c
    end if
else
    Determine the bandwidth proportions for c_1 and c_2 such that the sum of the power consumption of c_1 and c_2 is minimum and lower than that of routing on p only
    if there exist such bandwidth proportions **then**
        Adopt traffic splitting
        Route c on path p_1 and p_2
        Record the provisioning information of c
    else
        Discard traffic splitting
        Route c on path p only
        Record the provisioning information of c
    end if
end if
Update $\boldsymbol{G}$

grated Routing (PIR) is also implemented. PIR uses the same auxiliary graph as PIRTS. The difference between PIRTS and PIR lies in that the latter does not consider traffic splitting. If a most power efficient path for a connection request is available, then the connection request is provisioned successfully, otherwise it will be rejected by PIR.

3.4.4 Complexity Analysis

The physical topology of an IP over WDM network is represented by a network graph $\boldsymbol{G} = (\boldsymbol{V}, \boldsymbol{F})$, where $\boldsymbol{V}$ is the set of network nodes and $\boldsymbol{F}$ is the set of fiber links, as mentioned in Section. 3.4.1. For each network node in the physical topology, its corresponding nodes in the auxiliary graph comprise of a supernode, T_n transmitters, R_n receivers, and W OXC wavelength nodes, where T_n is the number of transmitters of the network node, R_n is the number of receivers of the network node, W is the number of wavelengths per fiber link. Therefore, the total number of nodes in the auxiliary graph is $(1 + T_n + R_n + W) \cdot |\boldsymbol{V}|$, and is denoted as V_n. We notice that network nodes may have different number of transmitters and receivers, but we hereby assume that all network nodes have the same number of transmitters and receivers so as to have an approximated estimation of the computational complexity of our algorithm. There are $(T_n + R_n) \cdot |\boldsymbol{V}|$ supernode edges, $T_n \cdot W$ transmission edges, $R_n \cdot W$ receiver edges, and $|\boldsymbol{F}| \cdot W$ fiber edges, which leads to a total number of $(T_n + R_n) \cdot |\boldsymbol{V}| + (T_n + R_n + |\boldsymbol{F}|) \cdot W$ edges in the auxiliary graph, and is denoted as E_n. The time is mainly consumed by running Dijkstra's algorithm in the auxiliary graph, of which the worst-case complexity is $O({V_n}^2)$. We hence conclude that the worst-case complexity of the proposed PIRTS routing algorithm is $O({V_n}^2)$. Similarly, we can conclude that the worst-case complexity of the PIR routing algorithm is also $O({V_n}^2)$.

3.5 Performance Study for the Dynamic Traffic

In this section, we study the performance of the proposed traffic-splitting based PIRTS algorithm and compare it with non-traffic-splitting based PIR algorithm in terms of various metrics. The 14-node 22-link NSFNET shown in Fig. 3.3(a) and 24-node 43-link USNET shown in Fig. 3.3(b) are employed for the simulations. The simulation settings are similar to the one depicted in Section 3.3.4. Here, a link that connects two OXCs is comprised of a bidirectional fiber link with 16 wavelengths for each direction. The connection requests are generated following Poisson process with arrival rate λ_c. The holding times of the connection requests follow negative exponential distribution with the mean μ_c set as 1 unit of time. The network load (in Erlangs) is equal to $\lambda_c\mu_c$. The source-destination node pairs of the connection requests are chosen uniformly among all the node pairs. The bandwidth of a connection request is generated randomly following uniform distribution within $[0.01, 1]$. Note that the minimum bandwidth interval is 0.01, meaning the bandwidth of a connection request should be an integral multiple of 0.01.

3.5.1 Power Consumption versus Network Load

Fig.s 3.5 and 3.6 show the power efficiency for both affine and convex power profiles under various network loads in NSFNET and USNET, respectively. We evaluate the power efficiency as the average power consumption per connection request staying in the network. We observe in both figures that PIRTS always requires less power than PIR for both power profiles, which demonstrates the effectiveness of traffic splitting in gaining power savings. We also notice that when the network load is relatively low, the average power consumption per connection request in the network decreases as the network load increases; however, when the network load is higher than a certain point, the average power consumption per connection request in the network begins

to increase with the raise of the network load. This is because when the traffic load is relatively low, incoming connection requests have more and more chance to use traffic grooming as traffic load increases, i.e., multiplexing on existing lightpaths to avoid creating new lightpaths, thus without paying for the fixed overhead incurred. However, when the traffic load is high, a connection request may have to detour along a long route in order to be accepted by the network, leading to the increase of the average power consumption per connection request staying in the network. It can be seen that the average power consumption per connection request staying in the network for the convex power profile is always less than that for the affine power profile, be it PIRTS or PIR. The reason is that for one component, it always consumes less power if convex power profile is adopted, as shown in Fig. 2.2. But it is worth noting that when the traffic load of a power component is very close to full load, the power consumption gap between convex and affine power profiles is very small. In the extreme case, when the traffic load is full, the gap diminishes.

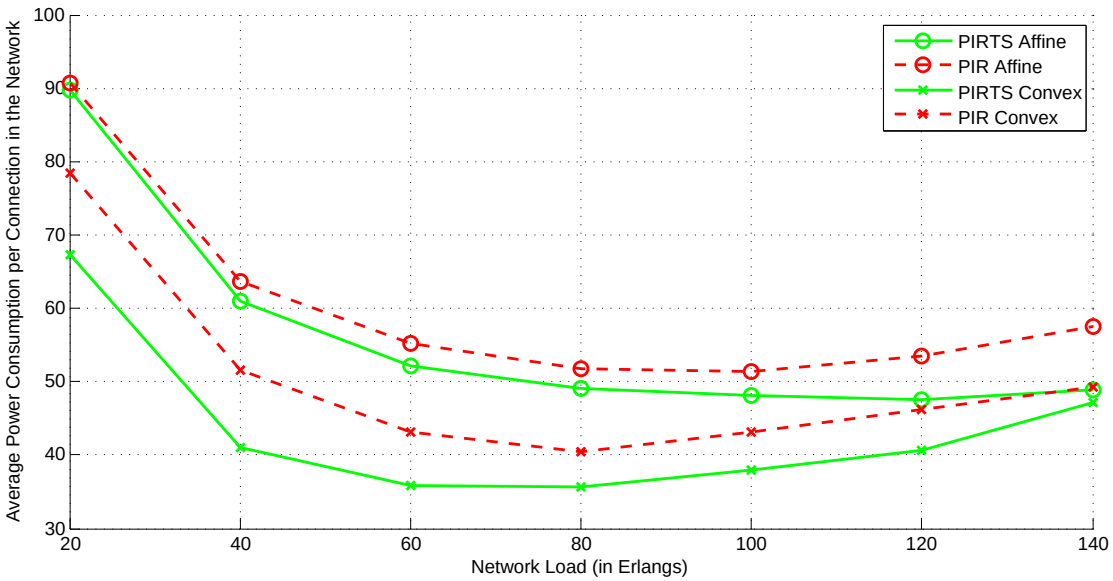

Figure 3.5: Average power consumption per connection request staying in NSFNET for different power profiles

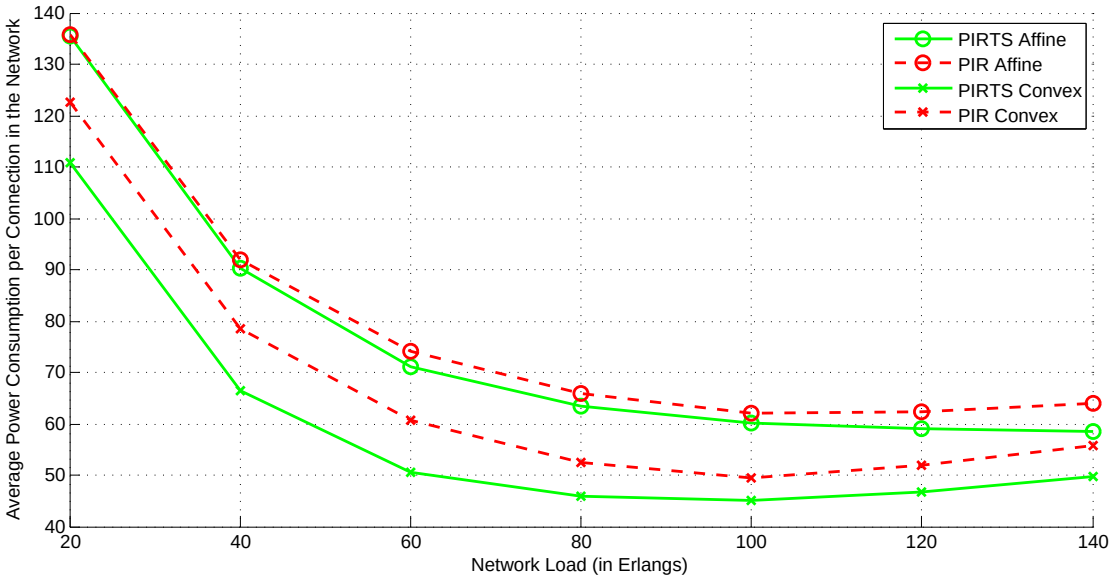

Figure 3.6: Average power consumption per connection request staying in USNET for different power profiles

3.5.2 Blocking Probability versus Network Load

We plot the blocking probability of PIRTS and PIR for both affine and convex power profiles in NSFNET and USNET, as shown in Fig.s 3.7(a), 3.7(b), 3.8(a), and 3.8(b). The blocking probability is defined as the probability that a connection request cannot be accepted. We observe in both network topologies that the blocking probability of PIRTS is always lower than that of PIR for both power profiles. The reason is that when a connection request is split into subconnection requests with smaller bandwidth requirements, the chances that the subconnection requests get accepted by the network are higher. We also observe that for PIR, the blocking probability for convex power profile is generally higher than that for affine power profile. That is because routing algorithms with convex power profile tend to keep the traffic load of lightpaths low in order to take advantage of the slowly-increasing power consumption curve for low traffic loads. Therefore, it may create more new lightpaths for connection requests, making it relatively harder for connection requests arriving

later to find suitable routes. For PIRTS, there is no much difference between the blocking probability curve for convex power profile and that for affine power profile, as traffic splitting has already reduced the blocking probability significantly.

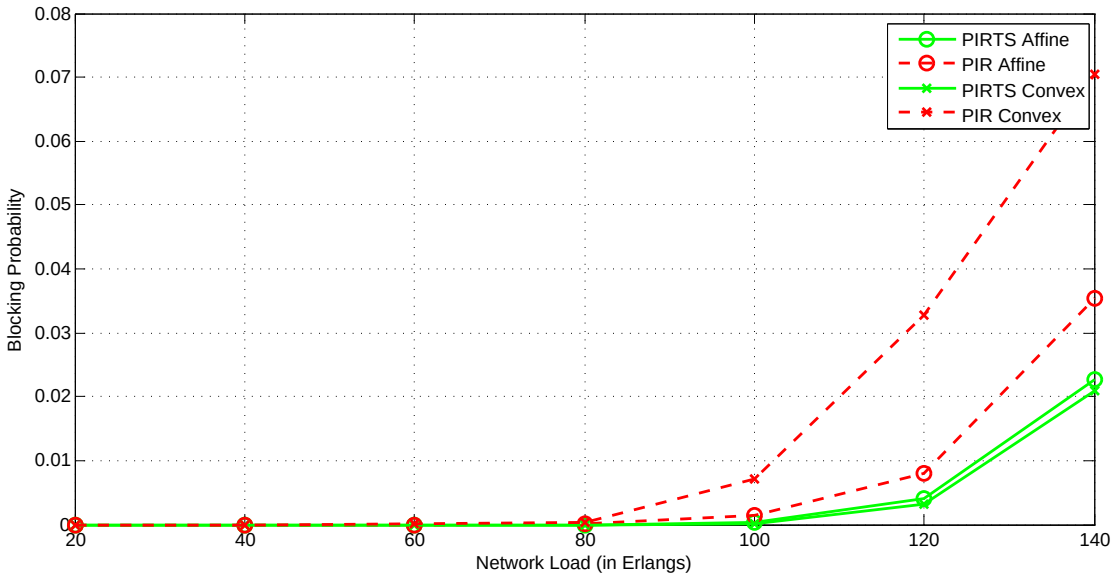

(a) Linear scale plot

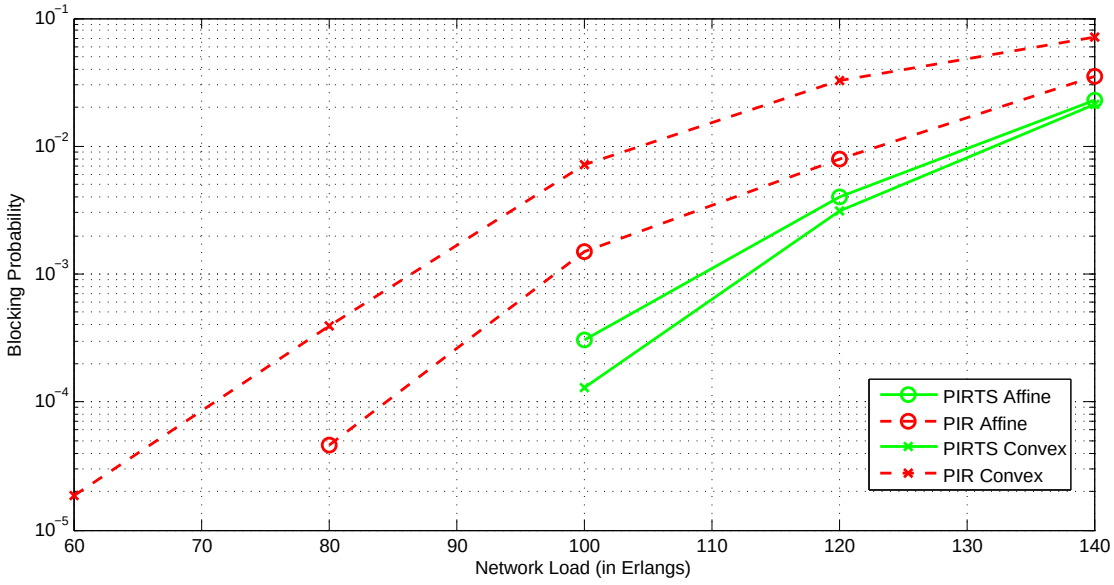

(b) Logarithmic scale plot for y-axis

Figure 3.7: Blocking probability in NSFNET for different power profiles

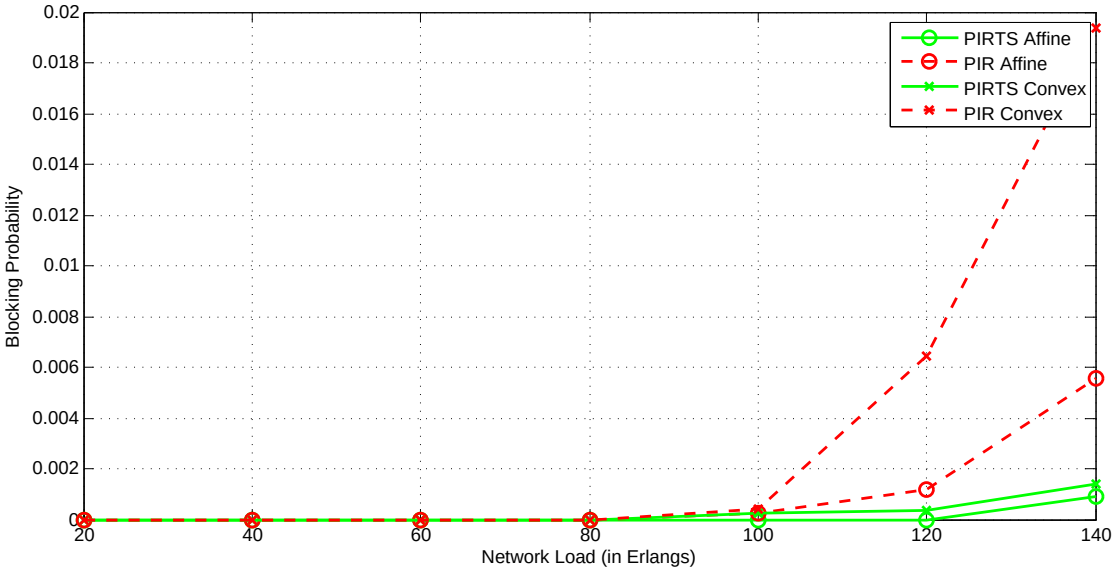

(a) Linear scale plot

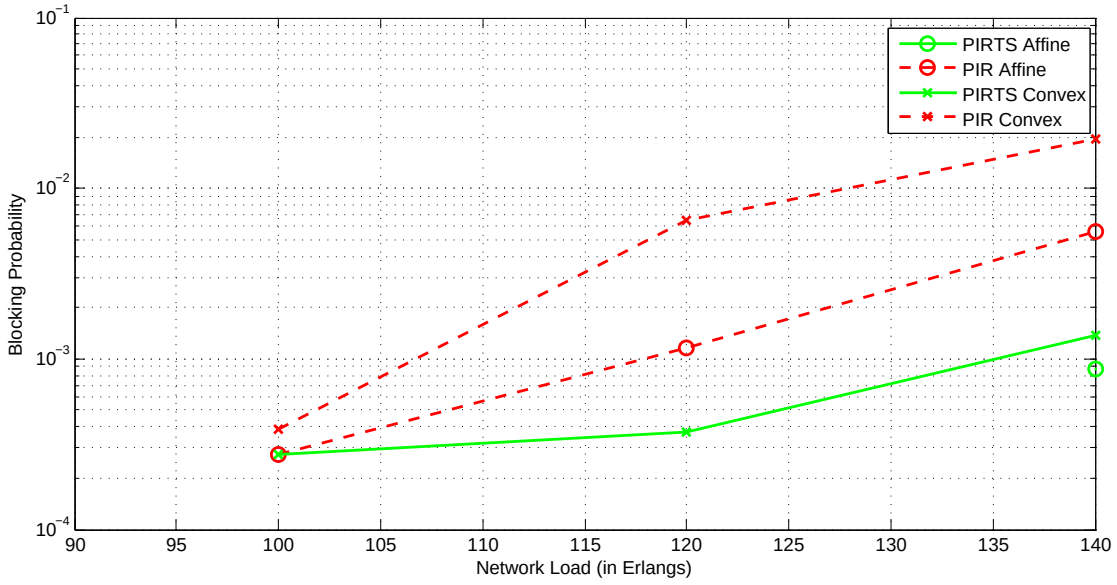

(b) Logarithmic scale plot for y-axis

Figure 3.8: Blocking probability in USNET for different power profiles

3.5.3 The Impact of the Fixed Overhead Proportion α

We study the impact of the fixed overhead proportion α on the power savings gained by PIRTS compared to PIR, as shown in Fig. 3.9. We plot the average power savings per connection request staying in the network of PIRTS with respect to PIR under all the network loads ranging from 20 to 140, for both power profiles in NSFNET. We notice from both power profiles that as the fixed overhead proportion increases from 0 to 100%, the power savings per connection request gained by PIRTS compared to PIR decreases from more than 10% (with maximum value of around 27%) to about 1% only. This is obvious because the increase of the fixed overhead proportion in the network will reduce the traffic-dependent power proportion, thereby cutting down the space for saving power by traffic splitting. It is interesting to see that even when the fixed overhead proportion is 100%, PIRTS is still more power efficient than PIR. This shows that PIRTS is more capable of packing connection requests on existing lightpaths, therefore fewer new lightpaths are needed compared to PIR. Note that when the fixed overhead proportion is 100%, the power consumption of a lightpath is constant regardless of the amount of traffic going through it. In this case, it is better to create as few lightpaths as possible in order to save power.

3.6 Summary

This chapter studied power efficient integrated routing with traffic splitting in IP over WDM networks considering both convex and affine power profiles. We studied both the static and the dynamic traffic models. For the static traffic, we formulate ILP and IQP models to optimize the power consumption of the network with or without traffic splitting. Through numerical results, we demonstrated the effectiveness of traffic splitting in saving power. For the dynamic traffic, we construct an auxiliary graph and assign the weight of each link according to its power con-

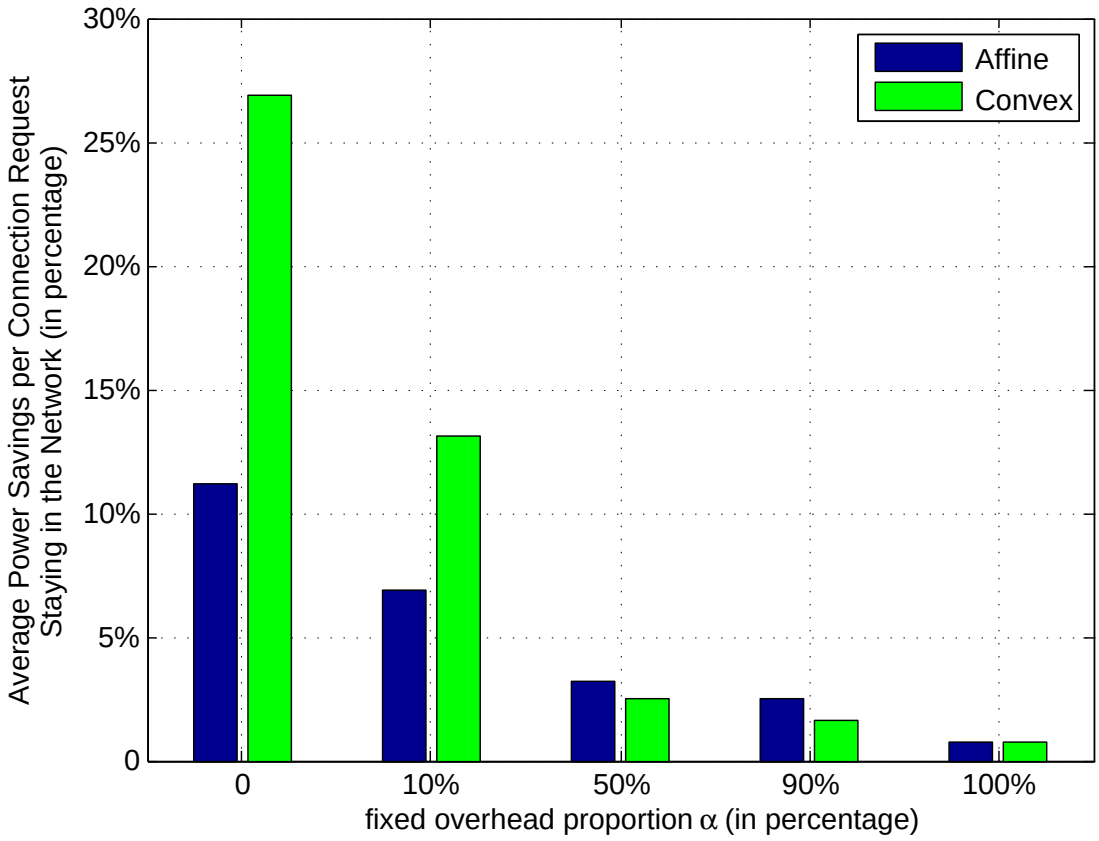

Figure 3.9: The impact of the fixed overhead proportion α on the power savings gained by traffic splitting

sumption, thereby a shortest-path routing algorithm can be used. The simulation results show that traffic splitting leads to better power efficiency and lower blocking probability compared to the one without traffic splitting, even in the scenario where the network elements are traffic-independent. Convex power profile leads to lower average power consumption per connection staying in the network with respect to affine power profile for the same routing algorithm. However, the latter outperforms the former in terms of blocking probability when traffic splitting is not allowed. We note that traffic splitting improves power efficiency at the cost that it will incur extra processing overhead together with more complex algorithms and it might not be good to split a connection request into too many subconnections.

Chapter 4

A Tradeoff Between Power Efficiency and Blocking Performance

4.1 Introduction

In this chapter, we propose an algorithm named Balanced Power efficient Integrated Routing (B-PIR), which strives to strike a balance between power efficiency and blocking performance by adopting the idea of link criticality. The adoption of the concept of link criticality is to prevent critical resources from being exhausted too fast. We present an auxiliary graph that takes both power and link criticality into consideration when assigning link weights. We conduct extensive simulations to show that B-PIR significantly reduces the blocking probability compared to PIR (which aims at reducing power consumption only) at the cost of relatively little degradation of power efficiency.

4.2 Maximum Flow and Minimum Cut

The maximum flow of a source-destination (s-d) pair is used to benchmark the available capacity between the s-d pair [36, 79]. If the maximum flow value of an s-d pair is 0 then it is impossible to provision any connection requests with the same s-d pair, meaning these connection requests will be rejected. According to the duality theorem for linear programming [79], the maximum flow value of an s-d pair is equal to the capacity of its minimum cut. The criticality (or importance) of a link is defined as in [36] according to the number of times a link belongs to the minimum cut sets of s-d pairs in the network. Since there might be more than one minimum cut for an s-d pair, we define the minimum cut set of an s-d pair as the collection of all the minimum cuts of the s-d pair. The rationale for the definition of link criticality is that (1) if a link belongs to the minimum cut set of an s-d pair then the reduction of its residual bandwidth capacity will lead to the decreasing of the maximum flow value between that s-d pair; (2) the higher the number of times a link belongs to the minimum cuts of s-d pairs in the network, the more s-d pairs the link will have an impact on. Therefore, it is of higher priority to protect the link from being exhausted too fast, meaning the link criticality is higher.

4.3 Balanced Power Efficient Integrated Routing

4.3.1 Problem Definition

We define the problem of minimizing the balanced power consumption (by balanced power consumption we mean the power consumption is weighted by link criticality) in an IP over WDM network for dynamic routing of connection requests as follows:

We are given a network graph $\boldsymbol{G} = (\boldsymbol{V}, \boldsymbol{F})$ representing the physical topology of an IP over WDM network, where $\boldsymbol{V}$ is the set of network nodes and $\boldsymbol{F}$ is the set

of fiber links. Connection requests arrive to the network one by one in a random manner. A connection request is specified as a triple $< s, d, \beta >$, where s, d, β are the source node, the destination node, and the required bandwidth of the connection request, respectively. The goal is to find the most balanced power efficient route for a connection request. Note that we call it the most balanced power efficient route because the power cost of a link is weighted by link criticality.

4.3.2 Auxiliary Graph Considering Both Power and Criticality

The auxiliary graph shown in Fig. 3.4 considers power only. We hereby devise an auxiliary graph that takes both power and criticality into consideration by adjusting the weights of fiber edges and existing lightpaths as follows (We call the adjusted weights as balanced weights):

- *fiber edge*: suppose the power cost of the fiber edge for current connection request is v, and the criticality of the fiber edge is χ, then the balanced weight of the fiber edge is $v \cdot f(\chi)$. We select $f(\chi)$ as a monotonically increasing function of χ and $f(\chi) \geq 1$. Therefore $v \cdot f(\chi) \geq v$. We assign the balanced weight of a fiber edge using this scheme so that for two links with the same power cost, the one with higher criticality will be assigned a higher weight, decreasing the chance of it being selected as a part of a route. This power cost v is the same as the corresponding fiber edge weight determined by the previous auxiliary graph (considering power only). The criticality of a fiber edge is equal to the number of times that it belongs to the minimum cut sets of source-destination (s-d) pairs in the network. The rationale is that if a link belongs to the minimum cut set(s) of an s-d pair then the decrease of its residual bandwidth capacity will lead to the reduction of the maximum

flow value between that s-d pair which benchmarks the traffic volume that can be routed through the s-d pair. In fact, if the maximum flow between a given s-d pair is zero then no traffic can go through that s-d pair. Therefore, it is reasonable to ensure that the higher the number of times a fiber edge belongs to the minimum cut sets of s-d pairs in the network, the more critical (important) the fiber edge is.

- *lightpath*: the balanced weight of a lightpath is similar to that of a fiber edge, except that the criticality of a lightpath is defined as proportional to the maximum fiber edge criticality among all the fiber edges traversed by the lightpath.

4.3.3 Algorithm Description

Based on the auxiliary graphs constructed above, we develop an algorithm called Balanced Power efficient Integrated Routing (B-PIR) as described in Algorithm 2. B-PIR creates an auxiliary graph (considering power only) $\boldsymbol{G}$ and an auxiliary graph (considering both power and criticality) $\boldsymbol{G'}$. For a new connection request $< s, d, \beta >$, we update the link weights of $\boldsymbol{G}$ and $\boldsymbol{G'}$ according to the bandwidth β. Thereafter we run a shortest-path routing algorithm (such as Dijkstra's algorithm) on the auxiliary graph $\boldsymbol{G'}$ to compute the most balanced power efficient path p for $< s, d, \beta >$. If there does not exist such a path then $< s, d, \beta >$ will be rejected; otherwise we record the provisioning information (route, number of new lightpaths created, and number of existing lightpaths multiplexed, etc.) of $< s, d, \beta >$ and calculate the power consumption of $< s, d, \beta >$ based on the auxiliary graph $\boldsymbol{G}$. Finally, the auxiliary graphs $\boldsymbol{G}$ and $\boldsymbol{G'}$ are updated to reflect the addition of new lightpaths, the marking of used network resources (such as transmitters, receivers, and wavelength channels.), and the latest residual bandwidth of existing lightpaths.

For comparison, we also implement two other algorithms, namely PIR and Hop-efficient Integrated Routing (HIR). PIR (presented in Section 3.4.3, similar to [61]) and HIR (which is a traditional routing algorithm and is power-unaware) are same to B-PIR in terms of network architecture and power consumption model assumed, the only difference lies in the link weight assignment schemes. PIR assigns link weight based on its power cost only (meaning if the power cost of a link for a connection request is v, then the weight of the link is also v), while HIR sets the weight of a fiber edge to 1, that of a lightpath to its number of physical hops, and that of other types of edges to 0.

Algorithm 2 B-PIR

Input: a connection request $< s, d, \beta >$

Output: The provisioning scheme for $< s, d, \beta >$

1: Update the auxiliary graph (considering power only) $\boldsymbol{G}$ based on the value of β
2: Update the auxiliary graph (considering both power and criticality) $\boldsymbol{G'}$ based on the value of β
3: Run Dijkstra's algorithm in $\boldsymbol{G'}$ to find the most balanced power efficient path p
4: **if** there does not exist such p **then**
5: Reject $< s, d, \beta >$
6: **else**
7: Record the provisioning information of $< s, d, \beta >$
8: Calculate the power consumption of $< s, d, \beta >$ based on $\boldsymbol{G}$
9: **end if**
10: Update $\boldsymbol{G}$ and $\boldsymbol{G'}$

4.3.4 Complexity Analysis

Similar to Section 3.4.4, the computational complexity of B-PIR is dominant by running Dijkstra's algorithm in the auxiliary graph, of which the worst-case complexity is $O({V_n}^2)$, where V_n is the total number of nodes in the auxiliary graph. We hence conclude that the worst-case complexity of the proposed B-PIR routing algorithm is $O({V_n}^2)$.

4.4 Performance Study

4.4.1 Simulation Settings and Metrics

We use the 14-node 22-link NSFNET as shown in Fig. 3.3(a) for the siumations. A bi-directional link that connects two OXCs is comprised of two fibers in opposite directions with a certain number of wavelengths for each direction. Amplifiers are deployed along fiber links one for every 80 km. The capacity of each wavelength is 10 Gbps and is normalized to 1. We calculate the power consumption (in unit) per wavelength of each component as listed in Table 3.1 before. We assume these components all follow affine power profile which is defined in Section 2.3, and we set the fixed overhead proportion α of a component to be 10% by default. It is assumed that transmitters and receivers can be turned on and switched off in a negligible transient time and do not incur additional energy of signaling. It is also assumed that there are sufficient transmitters and receivers for each routers. Connection requests are generated with source-destination node pairs chosen uniformly among all the node pairs. The bandwidth of a connection request is generated randomly following uniform distribution within $(0.01, 1]$. Note that the minimum bandwidth interval is 0.01, meaning the bandwidth of a connection request should be an integral multiple of 0.01. The connection request arrivals follow a Poisson process and the holding time is exponentially distributed with unit mean.

We compare the performance of B-PIR, PIR, and HIR in terms of average power consumption per connection request staying in the network, blocking probability, average number of virtual hops per connection request staying in the network, and average number of physical hops per connection request staying in the network. We consider number of virtual hops and number of physical hops metrics so as to better understand the behavior of different algorithms regarding to power consumption and blocking probability.

4.4.2 Simulation Results for 16 wavelengths

In this section we set the number of wavelengths per fiber link to be 16. We compare the performance of B-PIR, PIR, and HIR by plotting the figures of average power consumption per connection request staying in the network, blocking probability, average number of virtual hops per connection request staying in the network, and average number of physical hops per connection request staying in the network.

Power Consumption Vs. Network Load

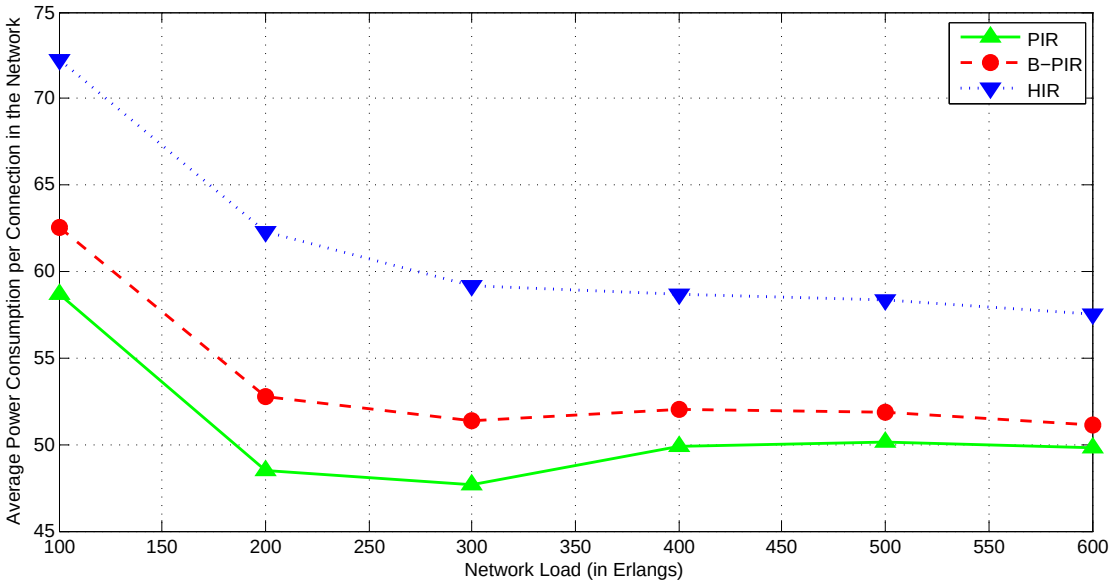

Figure 4.1: Average power consumption per connection request staying in the network (16 wavelengths)

Fig. 4.1 shows the power efficiency of B-PIR, PIR, and HIR under various network loads. We evaluate the power efficiency as the average power consumption

per connection request staying in the network, which can be formally defined as:

$$\begin{aligned}\frac{1}{z}\Bigg\{ & \underbrace{\sum_{i\in\boldsymbol{V}}\frac{\varepsilon_E^i}{C}(1-\alpha)P_E}_{\text{Electrical Switching Power}} + \underbrace{\sum_{i\in\boldsymbol{V}}\frac{\varepsilon_O^i}{C}(1-\alpha)P_O}_{\text{Optical Switching Power}} \\ & + \underbrace{\sum_{i\in\boldsymbol{V}}\sum_{k=0}^{\phi_T^i} P_T\left[\delta_{i,k}\alpha+(1-\alpha)\frac{\varepsilon_{i,k}}{C}\right]}_{\text{Transmitters Power}} \\ & + \underbrace{\sum_{i\in\boldsymbol{V}}\sum_{l=0}^{\phi_R^i} P_R\left[\delta_{i,l}\alpha+(1-\alpha)\frac{\varepsilon_{i,l}}{C}\right]}_{\text{Receivers Power}} \\ & + \Bigg(\underbrace{\sum_{m\in\boldsymbol{V}}\sum_{n\in\boldsymbol{V}:n\neq m}\sum_{\omega=0}^{W-1}\frac{\varepsilon_{m,n,\omega}}{C}P_A(1-\alpha)\eta_{m,n}}_{\text{Amplifiers Power}}\Bigg) + P_y\Bigg\},\end{aligned} \tag{4.1}$$

where z is the number of connection requests staying in the network when the network snapshot is being taken; $\boldsymbol{V}$ is the set of network nodes; i indexes the nodes in the IP layer; m, n index the nodes in the optical layer; k indexes the transmitters of a IP router; l indexes the receivers of a IP router; ω indexes the wavelengths on a fiber link; W is the number of wavelengths on a fiber link; ε_E^i is the amount of traffic being electrically switched by node i; ε_O^i is the amount of traffic being optically switched by node i; $\varepsilon_{i,k}$ is the amount of traffic going through the kth transmitter of node i; $\varepsilon_{i,l}$ is the amount of traffic going through the lth receiver of node i; $\delta_{i,k}$ indicates whether the kth transmitter of node i is turned on or not; $\delta_{i,l}$ indicates whether the lth receiver of node i is turned on or not; ϕ_T^i denotes the number of transmitters of node i; ϕ_R^i denotes the number of receivers of node i; $\varepsilon_{m,n,\omega}$ is the amount of traffic going through physical link (m,n) using wavelength ω; $\eta^{m,n}$ is the number of amplifiers on physical link (m,n); C is the bandwidth capacity of a wavelength; α is the fixed overhead proportion of a component as already defined in Section 2.3; P_E, P_O, P_T, P_R, P_A have the same meanings as shown in Table 3.1; P_y is the fixed power overhead to run the network infrastructure (including the IP

routers, OXCs, and amplifiers).

We observe that the average power consumption per connection request staying the network for B-PIR is higher than that of PIR but lower than that of HIR under all network loads (in Erlangs). This is because B-PIR tries to delay the exhaustion of critical links by assigning higher weights to them. Therefore, the path selected might not be the most power efficient, meaning the power efficiency of B-PIR is not as good as that of PIR. HIR is not power-aware, so it is no surprise that it has the worst power efficiency. The power efficiency of B-PIR is only about 6% worse than that of PIR. This value is calculated by taking the average of the power efficiency differences between B-PIR and PIR for all the network loads ranging from 100 to 600.

We also observe that when the network load is relatively low, the average power consumption per connection request in the network decreases as the network load increases; however, when the network load is higher than a certain point, the average power consumption per connection request in the network remains relatively stable with the raise of the network load. This is because when the traffic load is relatively low, incoming connection requests have more and more chances to use traffic grooming as traffic load increases, i.e., multiplexing on existing lightpaths to avoid creating new lightpaths, thus without paying for the fixed overhead incurred. However, when the traffic load is high, the advantage of traffic grooming in saving power diminishes because a connection request may have to detour along a long route (which most likely means more power consumed) in order to be accepted by the network.

Blocking Probability Vs. Network Load

We plot the blocking probability of B-PIR, PIR, and HIR under various network loads, as shown in Figs. 4.2(a) and 4.2(b). We observe that the blocking probability

for B-PIR is lower than that of PIR but higher than that of HIR under all network loads (in Erlangs). This demonstrates that by trying to prevent critical links from being exhausted too early, B-PIR does improve the blocking performance compared to PIR. The reason why B-PIR is not as good as HIR in terms of blocking performance is that HIR uses the least network resources by minimizing the number of fiber links traversed by a connection request. The blocking performance of B-PIR is about 12% better than that of PIR. Note that by sacrificing around 6% of power efficiency, B-PIR gains about 12% of blocking performance improvement with respect to PIR, which is worthwhile since high blocking probability is unacceptable in practice.

Virtual Hops Vs. Network Load

The average number of virtual hops per connection request staying in the network for B-PIR, PIR, and HIR under various network loads is as shown in Fig. 4.3. We observe that HIR always consumes the highest number of virtual hops because it does not care about the number of virtual hops so long as the number of physical hops (fiber links) is minimized. PIR, however, tends to reduce the number of virtual hops because higher number of virtual hops means more power is consumed by intermediate transmitters and routers, which is of low power efficiency. As for B-PIR, its performance lies between PIR and HIR, mainly because it puts constraints on the use of links that are critical, meaning it is not as effective as PIR in terms of controlling the number of virtual hops. We notice that B-PIR strikes a balance between PIR and HIR in terms of average number of virtual hops per connection request staying in the network.

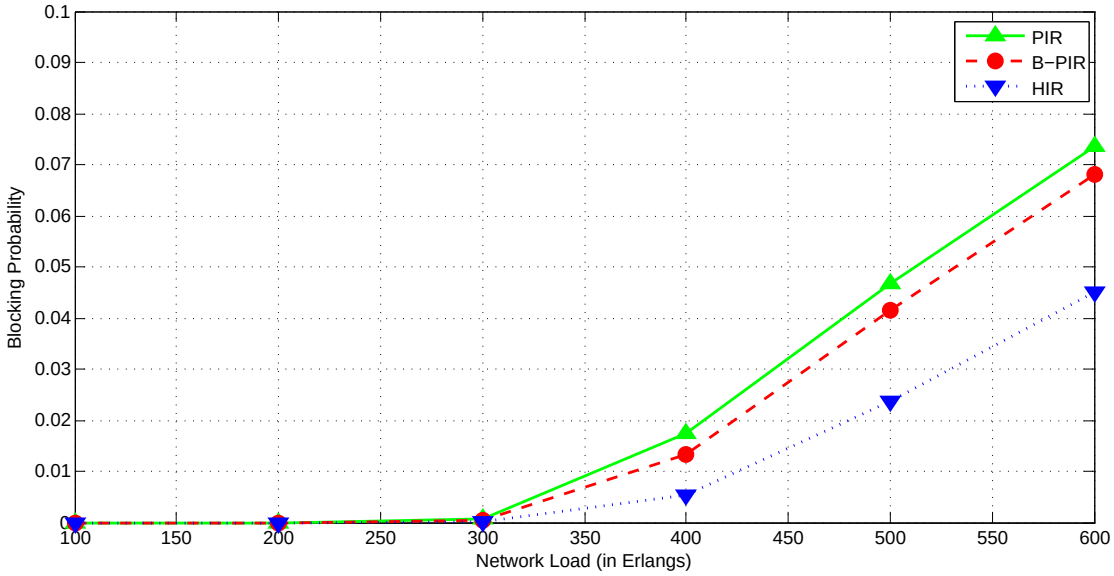

(a) Linear scale plot

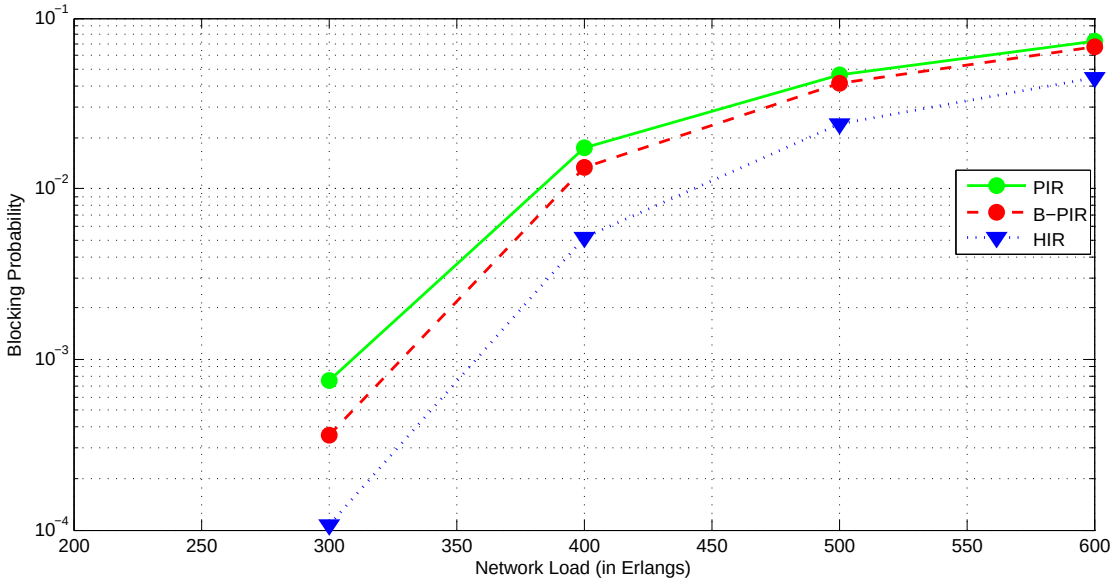

(b) Logarithmic scale plot for y-axis

Figure 4.2: Blocking probability for different network loads (16 wavelengths)

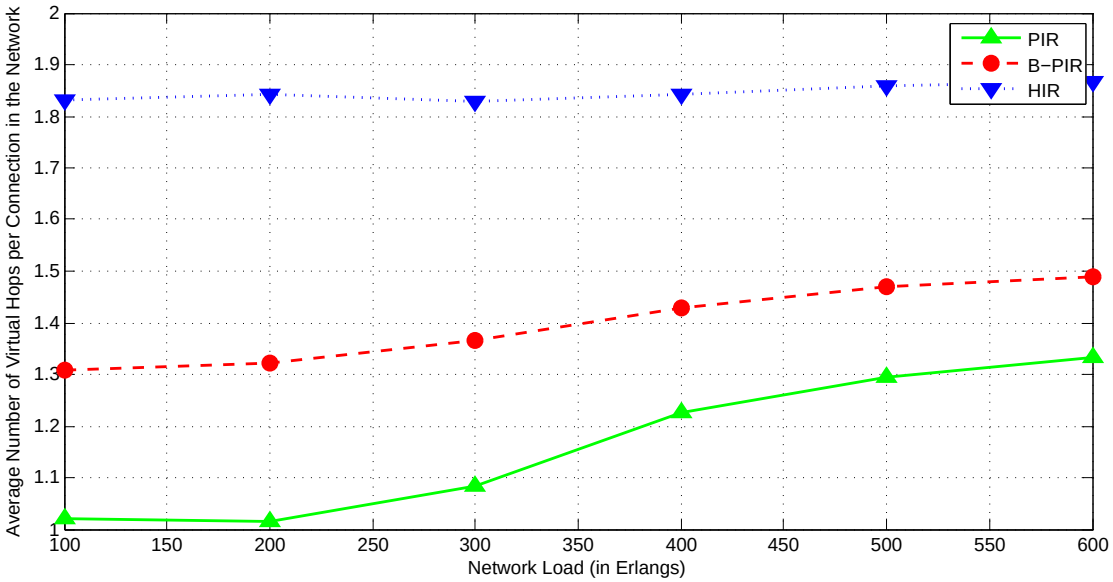

Figure 4.3: Average number of virtual hops per connection request staying in the network (16 wavelengths)

Physical Hops Vs. Network Load

We plot the average number of physical hops per connection request staying in the network for B-PIR, PIR, and HIR under various network loads in Fig. 4.4. We notice that HIR always consumes the lowest amount of physical hops, which is obvious because its only focus is to minimize the number of physical hops. Initially the curve for PIR is lower than that for B-PIR, but the former surpasses the latter when the network load is greater than about 300. The reason for there being a intersection between the curve of B-PIR and that of PIR is as follows. When the network load is low (no blocking ocurs), PIR can select physical links based on their power costs only, regardless of the criticality of each physical link. Therefore the average number of physical hops is lower than that of B-PIR. However, as the network load continues to increase to the level that blocking occurs, the advantage of trying to avoid using physical hops with high criticality has shown up. PIR tends to use longer route (and thus higher number of physical hops) than that of B-

PIR to provision connection requests because of resource scarcity of critical physical links. We observe that B-PIR also strikes a balance between PIR and HIR in terms of average number of physical hops per connection request staying in the network when the network load is greater than a point that blocking starts to happen in the network.

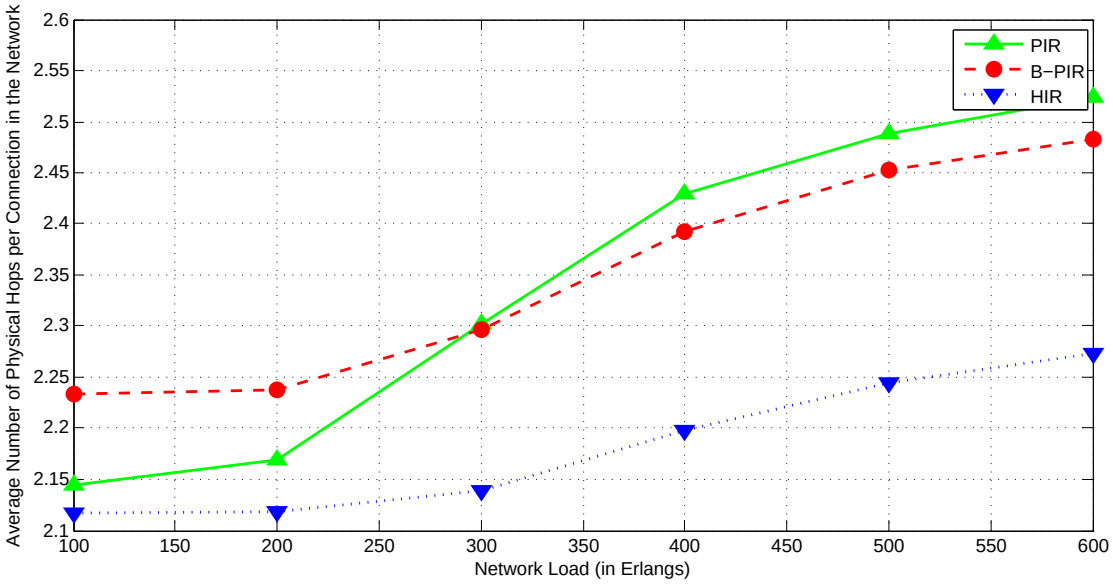

Figure 4.4: Average number of physical hops per connection request staying in the network (16 wavelengths)

4.4.3 Simulation Results for 8 wavelengths

In this section we set the number of wavelengths per fiber link to be 8, and we repeat the simulations in Section 4.4.2. We plot Figs. 4.5, 4.6(a), 4.6(b), 4.7, and 4.8 corresponding to Figs. 4.1, 4.2(a), 4.2(b), 4.3, and 4.4, respectively. Similar curve trends are observed for the two sets of figures. We also notice that for the case of 8 wavelengths, B-PIR reduces the blocking probability by about 30% at the cost of about 9% degradation of power efficiency, which is better than the case of 16 wavelengths (which gains 12% blocking probability improvement at the cost

of 6% degradation of power efficiency) and suggests that B-PIR is more effective for networks with less network bandwidth resources and thus more sensitive to bandwidth allocation schemes.

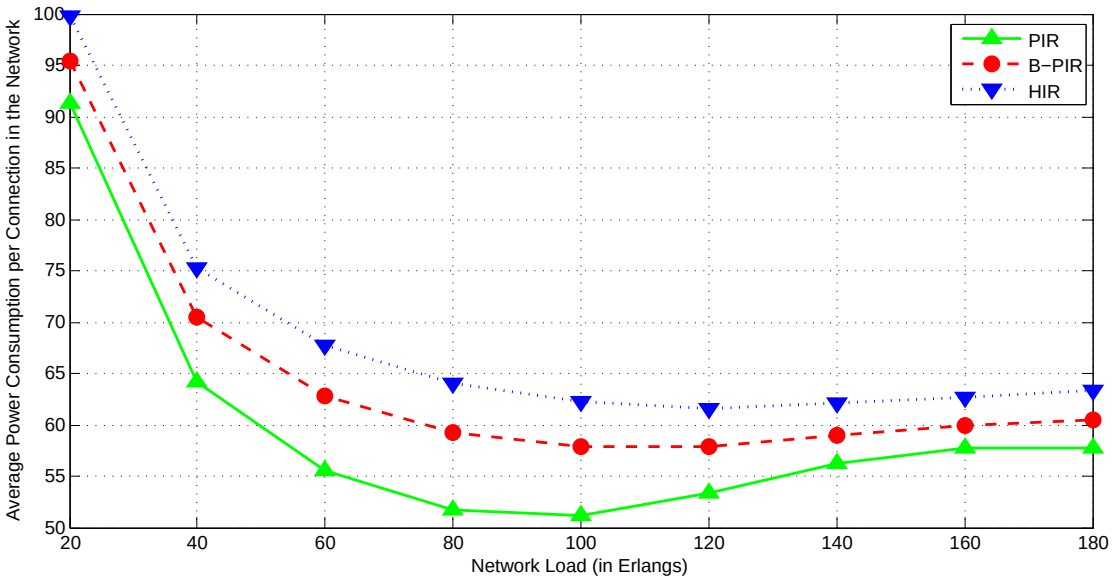

Figure 4.5: Average power consumption per connection request staying in the network (8 wavelengths)

4.4.4 Simulation Results for α=0.3

In this section we increase α the fixed power overhead proportion of a component to 0.3. We have chosen other values for α as well and similar simulation results are obtained. The number of wavelengths per fiber link remains to be 16. We repeat the simulations in Section 4.4.2. We plot Figs. 4.9, 4.10, 4.11, and 4.12 corresponding to Figs. 4.1, 4.2(a), 4.3, and 4.4, respectively. Similar curve trends are also observed for the two sets of figures. We notice that the routing (regarding to blocking probability, average virtual and physical hops per connection request staying in the network) of HIR is not affected by α, which is obvious because HIR is power-unaware. We observe that the average power consumption per connection request staying in the

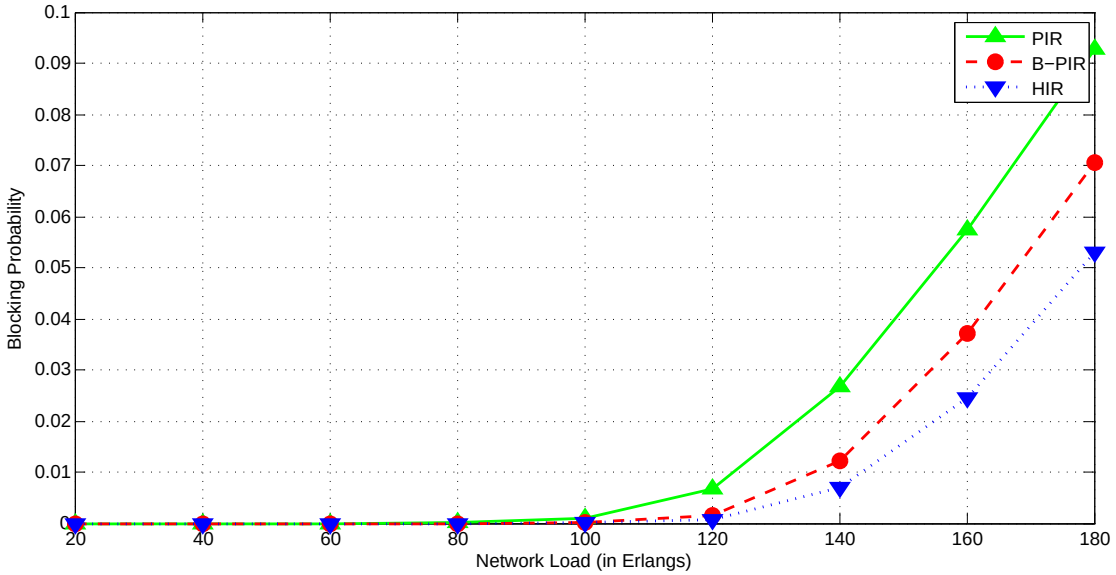

(a) Linear scale plot

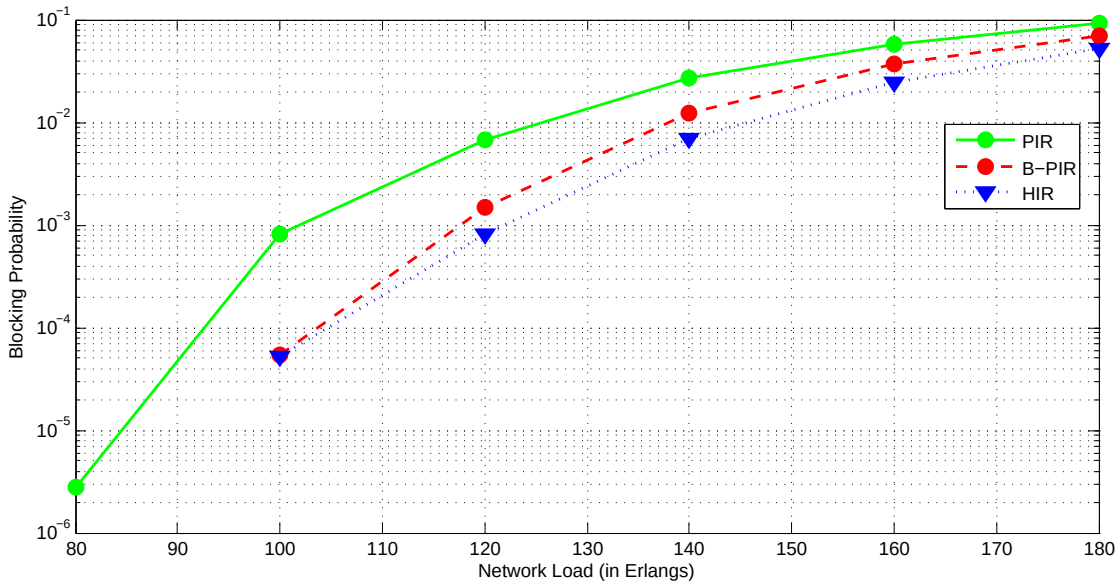

(b) Logarithmic scale plot for y-axis

Figure 4.6: Blocking probability for different network loads (8 wavelengths)

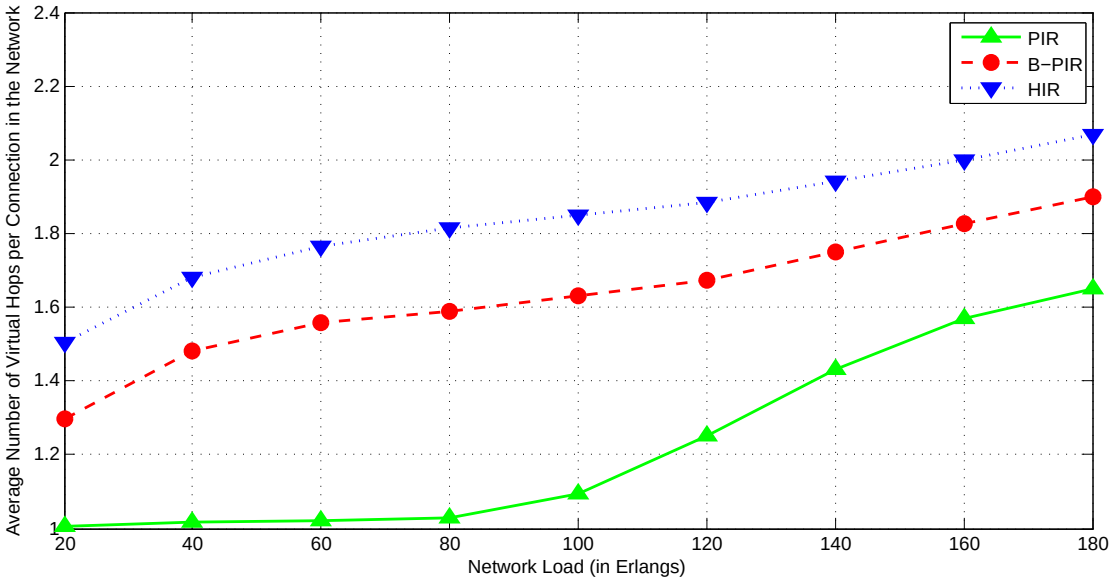

Figure 4.7: Average number of virtual hops per connection request staying in the network (8 wavelengths)

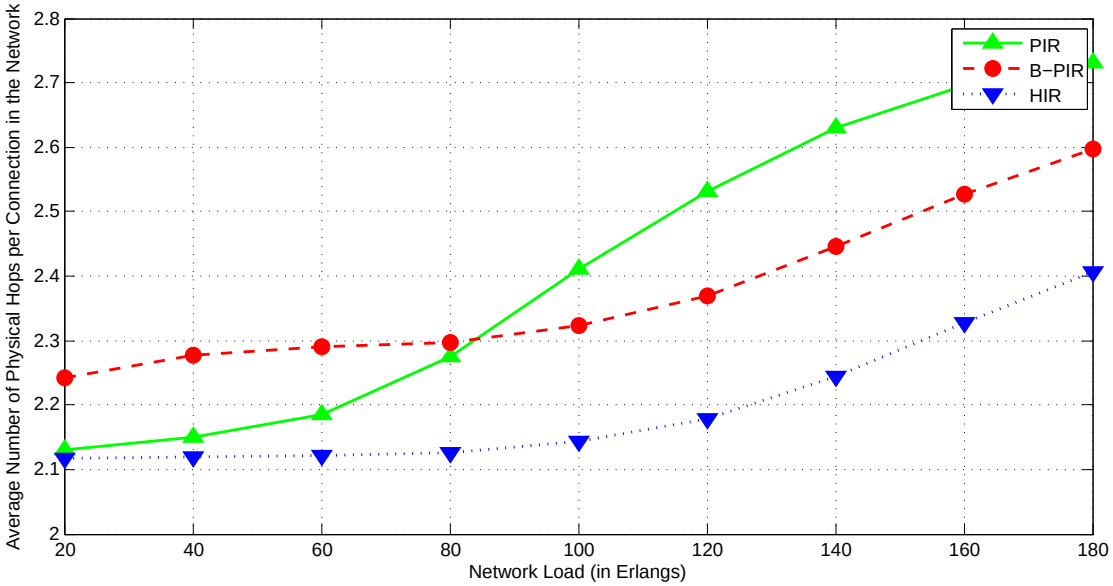

Figure 4.8: Average number of physical hops per connection request staying in the network (8 wavelengths)

network increases with the rise of α because P_y the fixed power overhead to run the network infrastructure also increases with the rise of α, which is shared by every connection request staying in the network. We also observe that there are slight increases of the average number of virtual (physical) hops per connection request staying in the network for PIR and B-PIR, reason being that with the increase of the fixed overhead proportion α both PIR and B-PIR tend to multiplex new connection requests onto existing lightpaths so as to avoid creating new lightpaths (which incur fixed power overhead), leading to longer route and therefore higher number of virtual (physical) hops.

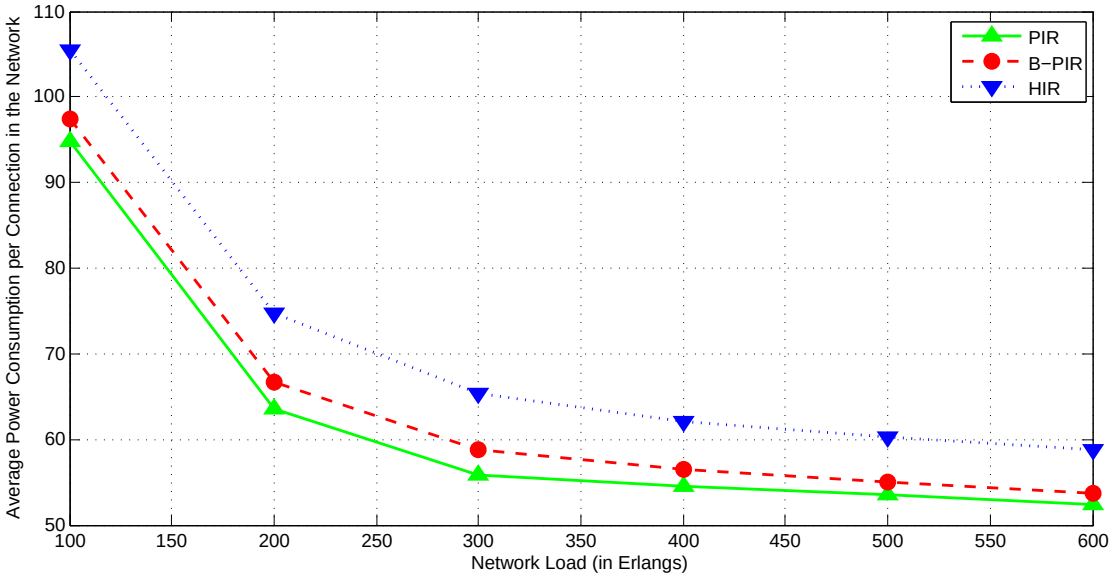

Figure 4.9: Average power consumption per connection request staying in the network (α=0.3)

4.5 Summary

Improving energy efficiency of communication networks is essential considering the ever-increasing traffic volume transported by current networks. However, they should not significantly affect other metrics. In this chapter, we struck a balance

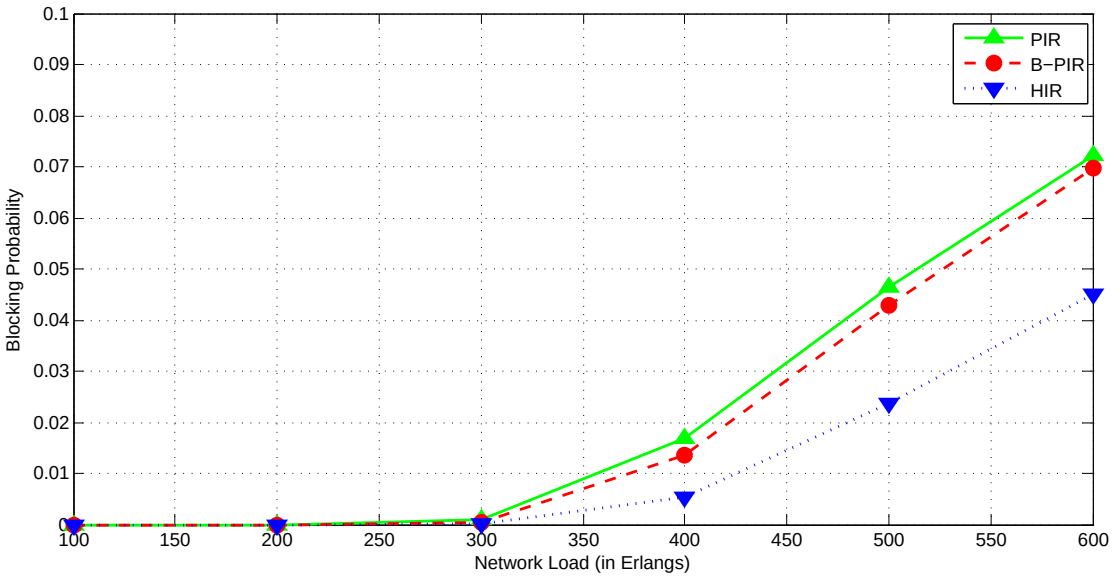

Figure 4.10: Blocking probability for different network load (α=0.3)

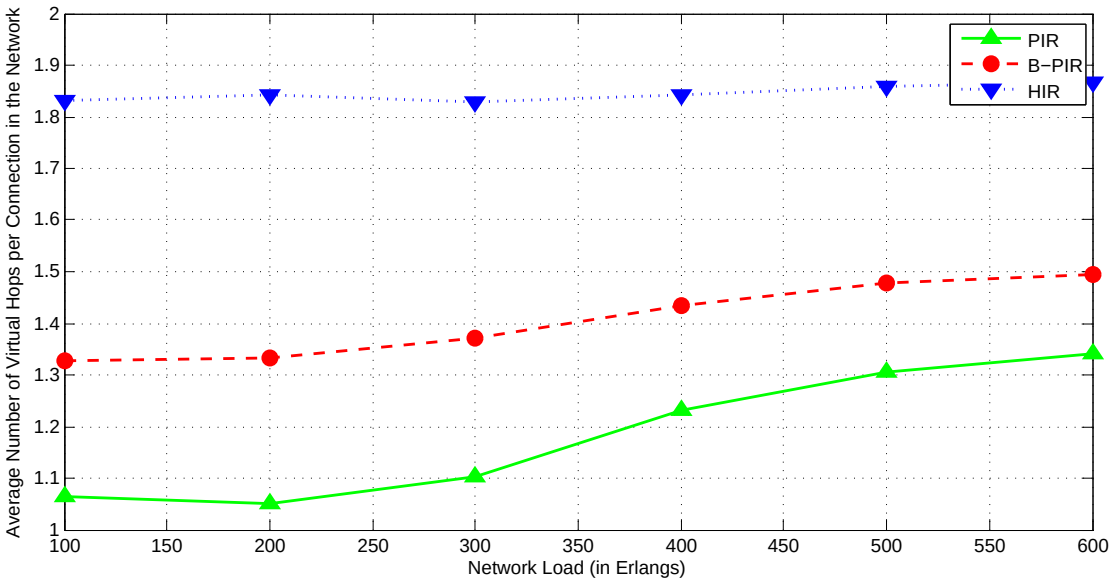

Figure 4.11: Average number of virtual hops per connection request staying in the network (α=0.3)

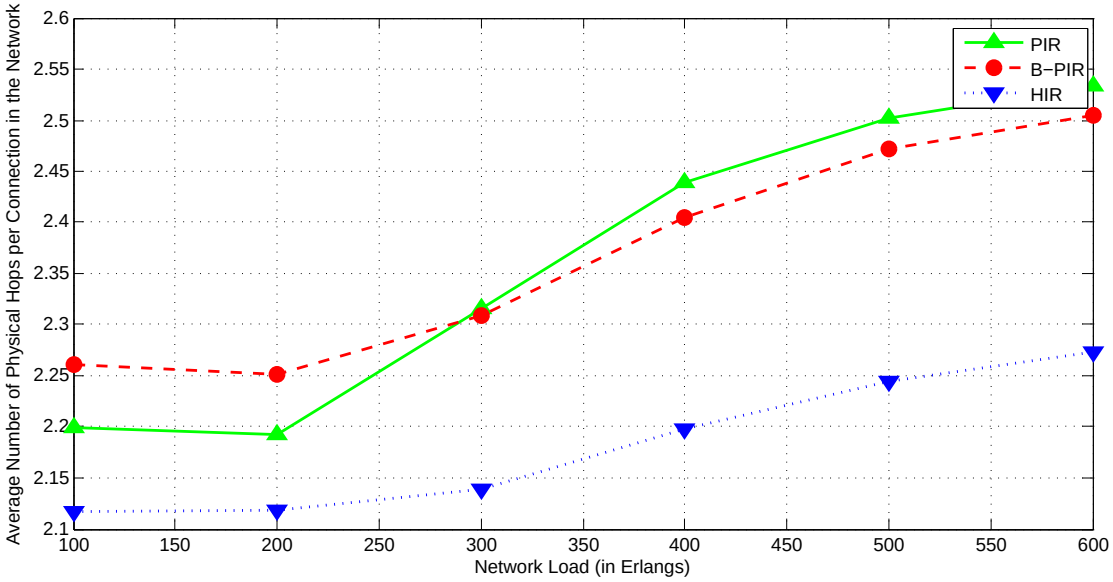

Figure 4.12: Average number of physical hops per connection request staying in the network (α=0.3)

between power efficiency and blocking performance by using the idea of the criticality of a link while considering the power cost of a link. The criticality of a link is defined as the number of times a link belongs to the minimum cut sets of *s-d* pairs in the network. The rationale for the definition of link criticality is that if a link belongs to the minimum cut set of an *s-d* pair then the reduction of its residual bandwidth capacity will lead to the decrease of the maximum flow value between that *s-d* pair, making it worthwhile to protect the link from being exhausted too fast. We proposed B-PIR algorithm based on the idea of protecting critical links. We also presented an auxiliary graph that considers both power consumption and link criticality at weight assignment stage. We conducted extensive simulations with metrics like average power consumption per connection request staying in the network, blocking probability for different network load, average number of virtual hops per connection request staying in the network, and average number of physical hops per connection request staying in the network, for different numbers of wavelength

and varying fixed power overhead α. Performance study shows that B-PIR significantly reduces the blocking probability compared to PIR at the cost of relatively little degradation of power efficiency. The simulations suggest that B-PIR is more effective for networks with less network bandwidth resources. We observe that the average power consumption per connection request staying in the network increases with the rise of α, as the fixed power overhead to run the network infrastructure becomes higher and higher with the rise of α. We also observe that when α increases there would be slight increases of the average number of virtual (physical) hops per connection request staying in the network for PIR and B-PIR. The reason is that with the increase of α both PIR and B-PIR tend to multiplex new connection requests onto existing lightpaths so as to avoid creating new lightpaths (which incur fixed power overhead), leading to longer route and therefore higher number of virtual (physical) hops.

Chapter 5

Bandwidth-varying Connection Provisioning

5.1 Introduction

In this chapter, we investigate energy efficient provisioning of bandwidth-varying scheduled connection requests. The problem is to decide the routing, time and bandwidth allocation schemes for the set of scheduled connection requests such that their energy consumption is minimized while meeting their data transmission deadline. For bandwidth-varying scheduled connection requests, continuous and fixed-bandwidth data transmission are not mandatory, therefore the network can exploit this bandwidth allocation flexibility to schedule the bandwidth of a connection request at each time slot so that fewer data transmission time slots might be needed and thus transmitters and receivers can remain on for a shorter time, leading to energy savings. We first give the problem definition. We then give an illustrative example to show that bandwidth-varying scheduled traffic model leads to energy savings compared to fixed-window scheduled traffic model. We present an ILP formulation to minimize the energy consumption of a set of static bandwidth-varying

scheduled connection requests. Based on the ILP formulation, we then propose a simple and efficient heuristic that sorts the set of connection requests according to sort criterion and provisions the sorted connection requests one by one such that the incremental energy consumption due to the newly provisioned connection request is minimized. We next conduct performance study to demonstrate the effectiveness of our proposed ILP formulation and heuristic algorithm for bandwidth-varying scheduled traffic model in saving energy compared to that for fixed-window scheduled traffic model.

5.2 Problem Definition

We define the problem of minimizing the energy consumption of scheduled connection requests as follows:

We are given a network graph $\boldsymbol{G}$ representing the physical topology of an IP over WDM network. We are also given a set of scheduled connection requests (be it fixed-window or bandwidth-varying). A scheduled connection request is specified by the source node, the destination node, the data volume, the earliest possible start time, the preferred start time, the preferred end time, and the latest possible end time. The goal is to decide the routing, time and bandwidth allocation schemes for the set of scheduled connection requests such that their energy consumption is minimized while meeting their data transmission deadline.

5.3 Is Bandwidth-varying More Energy Efficient than Fixed-window?

We illustrate the advantages of bandwidth-varying scheduled traffic model in improving energy efficiency compared to fixed-window scheduled traffic model by a simple

example. We consider the network in Fig. 5.1, which shows the logical topology of a small network with three nodes and two lightpaths (or logical links) represented by circles and solid lines (with an arrow showing the direction of a lightpath), respectively. We denote a connection request as a triple $< s, d, \beta >$, where s, d, and β represent the source node, the destination node, and the required bandwidth (which is normalize to be in the range of $(0, 1]$)), respectively. We have three connection requests: $r_{[\text{req}],1} :< 0, 1, 0.2 >$, $r_{[\text{req}],2} :< 1, 2, 0.2 >$, $r_{[\text{req}],3} :< 0, 2, 0.2 >$. The holding time for each connection request is shown in Fig. 5.2. We assume time is slotted and each time slot denotes one unit of time. Slotted time allocation is a common practice in networking field and is known to have better resource utilization compared to unslotted scheduling. A famous example is that slotted ALOHA is better than unslotted ALOHA in terms of resource utilization. We also assume that $r_{[\text{req}],1}$ creates the lightpath $l_{[\text{lp}],1}$, $r_{[\text{req}],2}$ creates the lightpath $l_{[\text{lp}],2}$, and $r_{[\text{req}],3}$ multiplexes on lightpaths $l_{[\text{lp}],1}$ and $l_{[\text{lp}],2}$. Suppose the power consumption of a lightpath can be formulated as:

$$p(t_{[\text{ld}]}) = \alpha + (1 - \alpha)t_{[\text{ld}]}, \tag{5.1}$$

where α is the fixed overhead proportion and $\alpha \in (0, 1]$); $t_{[\text{ld}]}$ is the traffic load going through the lightpath and is normalize to be in the range of $(0, 1]$); $p(t_{[\text{ld}]})$ is the power consumption of the lightpath in which the traffic load is $t_{[\text{ld}]}$, and $p(t_{[\text{ld}]}) \in (0, 1])$. We assume a lightpath can be switched off when there is no traffic going through it.

The energy consumption $E_{[\text{fxd}]}$ for the three connection requests under fixed-window scheduled traffic model as shown in Fig. 5.2 can be calculated as follows. The energy consumption of $l_{[\text{lp}],1}$ is:

$$\underbrace{\alpha \times 2 + (1-\alpha) \times 0.2 \times 2}_{\text{Energy consumption of } l_{[\text{lp}],1} \text{ in } [0,t_2]} + \underbrace{\alpha \times 2 + (1-\alpha) \times 0.4 \times 2}_{\text{Energy consumption of } l_{[\text{lp}],1} \text{ in } [t_2,t_4]} + \underbrace{\alpha \times 4 + (1-\alpha) \times 0.2 \times 4}_{\text{Energy consumption of } l_{[\text{lp}],1} \text{ in } [t_4,t_8]} = 6\alpha + 2. \tag{5.2}$$

The energy consumption of $l_{[\text{lp}],2}$ is:

$$\underbrace{\alpha \times 1 + (1-\alpha) \times 0.2 \times 1}_{\text{Energy consumption of } l_{[\text{lp}],2} \text{ in } [t_1,t_2]} + \underbrace{\alpha \times 4 + (1-\alpha) \times 0.4 \times 4}_{\text{Energy consumption of } l_{[\text{lp}],2} \text{ in } [t_2,t_6]} + \underbrace{\alpha \times 2 + (1-\alpha) \times 0.2 \times 2}_{\text{Energy consumption of } l_{[\text{lp}],1} \text{ in } [t_6,t_8]} = 4.8\alpha + 2.2. \tag{5.3}$$

$E_{[\text{fxd}]}$ equals the sum of the energy consumption of both $l_{[\text{lp}],1}$ and $l_{[\text{lp}],2}$. Therefore, we have

$$E_{[\text{fxd}]} = (6\alpha + 2) + (4.8\alpha + 2.2) = 10.8\alpha + 4.2 \tag{5.4}$$

When bandwidth-varying scheduled traffic model is used, a connection request does not need continuous and fixed-bandwidth transmission. For simplicity consideration, we assume only $r_{[\text{req}],3}$ has this flexibility, as shown in Fig. 5.3. We notice that the transmission time of $r_{[\text{req}],3}$ is reduced from 6 time slots (shown in Fig. 5.2) to 2 time slots because of larger bandwidth provisioning (shown in Fig. 5.3 with a thicker line). The energy consumption $E_{[\text{bv}]}$ for the three connection requests under bandwidth-varying scheduled traffic model as shown in Fig. 5.3 can be calculated as follows. The energy consumption of $l_{[\text{lp}],1}$ is:

$$\underbrace{\alpha \times 2 + (1-\alpha) \times 0.2 \times 2}_{\text{Energy consumption of } l_{[\text{lp}],1} \text{ in } [0,t_2]} + \underbrace{\alpha \times 2 + (1-\alpha) \times 0.8 \times 2}_{\text{Energy consumption of } l_{[\text{lp}],1} \text{ in } [t_2,t_4]} = 2\alpha + 2. \tag{5.5}$$

The energy consumption of $l_{[\text{lp}],2}$ is:

$$\underbrace{\alpha \times 1 + (1-\alpha) \times 0.2 \times 1}_{\text{Energy consumption of } l_{[\text{lp}],2} \text{ in } [t_1,t_2]} + \underbrace{\alpha \times 2 + (1-\alpha) \times 0.8 \times 2}_{\text{Energy consumption of } l_{[\text{lp}],2} \text{ in } [t_2,t_4]} + \underbrace{\alpha \times 2 + (1-\alpha) \times 0.2 \times 2}_{\text{Energy consumption of } l_{[\text{lp}],2} \text{ in } [t_4,t_6]} = 2.8\alpha + 2.2. \tag{5.6}$$

$E_{[\text{bv}]}$ equals the sum of the energy consumption of both $l_{[\text{lp}],1}$ and $l_{[\text{lp}],2}$. Therefore, we have

$$E_{[\text{bv}]} = (2\alpha + 2) + (2.8\alpha + 2.2) = 4.8\alpha + 4.2 \tag{5.7}$$

Since $\alpha \in (0, 1]$, we have

$$E_{[\text{bv}]} < E_{[\text{fxd}]}, \tag{5.8}$$

meaning bandwidth-varying scheduled traffic model leads to better energy efficiency. The larger α is, the more energy savings can be gained. In fact, there is no energy saving for bandwidth-varying scheduled traffic model at all if α is zero for this example.

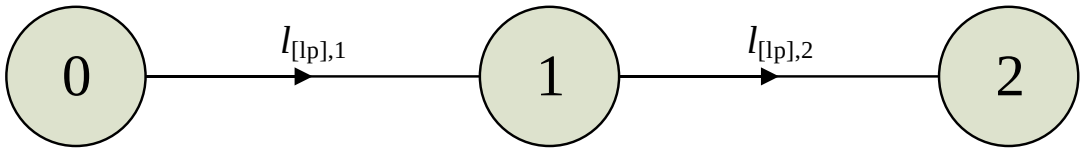

Figure 5.1: Example of a virtual topology

5.4 ILP formulation

In this section we present the ILP formulation for minimizing the network energy consumption under static bandwidth-varying scheduled traffic model (ILP-BV). We also formulate an ILP for minimizing energy consumption under static fixed-window scheduled traffic model (ILP-FW), for comparison purpose.

5.4.1 ILP for Static Bandwidth-varying Scheduled Traffic Model (ILP-BV)

We are given the following inputs to the problem:

1. $\boldsymbol{G} = (\boldsymbol{V}, \boldsymbol{F})$, which represents the network topology. $\boldsymbol{V}$ is the set of network nodes and $\boldsymbol{F}$ is the set of undirected fiber links. An entry $F_{m,n}$ of $\boldsymbol{F}$ is a Boolean

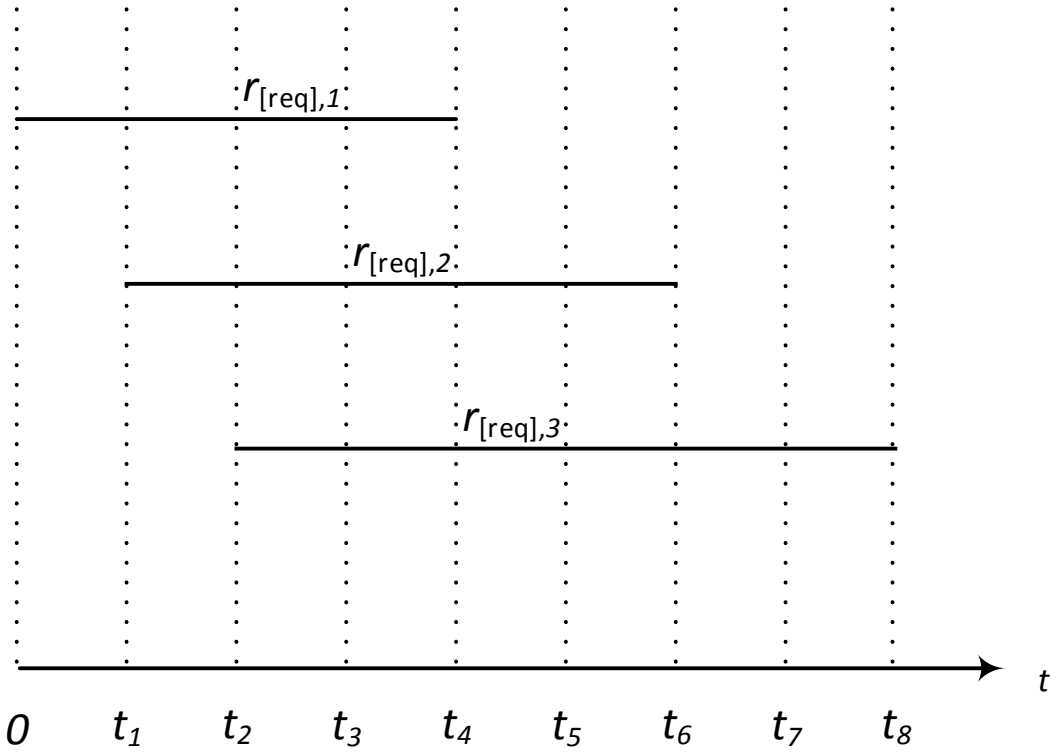

Figure 5.2: Connection requests under fixed-window scheduled traffic model

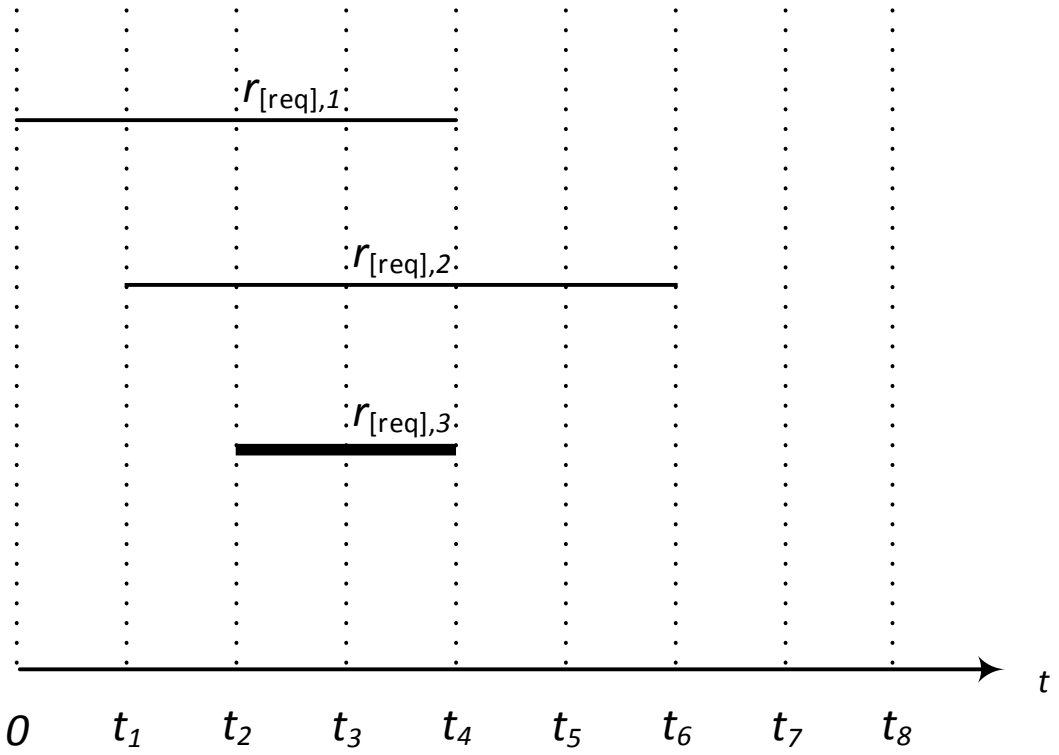

Figure 5.3: Connection requests under bandwidth-varying scheduled traffic model

variable that represents whether the fiber link from node m to node n exists or not. Each fiber link can support W wavelengths and the bandwidth capacity of each wavelength is C, which is in multiple of the minimal granularity. The number of nodes in $\boldsymbol{V}$ is denoted as $N = |\boldsymbol{V}|$.

2. $\boldsymbol{\lambda}$, which is the data volume matrix of a set of connection requests. $\boldsymbol{\lambda}$ is a two-dimensional matrix of $N \times N$. An entry $\lambda^{s,d}$ in $\boldsymbol{\lambda}$ denotes a connection request from node s to node d with $\lambda^{s,d}$ volume of data to be transmitted.

3. $\boldsymbol{N}_{[t]}$, which is the set of time-slots. We have $\boldsymbol{N}_{[t]} = \{0, 1, \cdots, |\boldsymbol{N}_{[t]}| - 1\}$, where $|\boldsymbol{N}_{[t]}|$ is the number of time-slots in total.

4. $\tilde{t}_h$, which is the duration of time-slot h, and is set as 1 in this work.

5. $t^{s,d}_{[\text{so}]}, t^{s,d}_{[\text{si}]}, t^{s,d}_{[\text{ei}]}, t^{s,d}_{[\text{eo}]}$: which specify the earliest possible start time, preferred start time, preferred end time, and latest possible end time of a connection request sourced at node s and destined to node d.

6. P_E, P_O, P_T, P_R, P_A, which are the power consumption for processing a full wavelength bandwidth amount of traffic, in terms of electrical switching, optical switching, transmitting, receiving, and amplifying, respectively. We denote α as the fixed overhead proportion of a power consumption component, as aforementioned.

7. P_y, which is the fixed overhead for maintaining the presence of IP routers, OXCs, and amplifiers.

8. $\boldsymbol{\phi_T}, \boldsymbol{\phi_R}$, which represent the numbers of transmitters and receivers of network nodes, respectively. An entry ϕ^i_T of $\boldsymbol{\phi_T}$ denotes the number of transmitters of node i. Similarly, an entry ϕ^i_R of $\boldsymbol{\phi_R}$ denotes the number of receivers of node i.

9. $\boldsymbol{\eta}$, which is a two-dimensional matrix of $N \times N$ with each entry $\eta^{m,n}$ representing the number of amplifiers on physical link (m, n).

10. W, which is the number of wavelengths on a physical link.

We apply the following general indexing rules to the formulation:

1. m, n: index the nodes in the optical layer.

2. i, j: index the nodes in the IP layer.

3. s, d: index the source node and the destination node of a connection request, respectively.

4. h: index the time-slots.

5. k: index the transmitters.

6. l: index the receivers.

7. ω: index the wavelengths on physical links (fiber links).

8. a connection request is specified by a set of parameters: $< s, d, \lambda^{s,d}, t^{s,d}_{[\text{so}]}, t^{s,d}_{[\text{si}]}, t^{s,d}_{[\text{ei}]}, t^{s,d}_{[\text{eo}]} >$, where $s, d, \lambda^{s,d}, t^{s,d}_{[\text{so}]}, t^{s,d}_{[\text{si}]}, t^{s,d}_{[\text{ei}]}, t^{s,d}_{[\text{eo}]}$ have the same meanings as defined before.

9. a lightpath is indexed as $< i, j, k, l, \omega >$, where i, j, k, l, ω have the same meanings as defined before. Note that a lightpath cannot be denoted just as $< i, j, \omega >$ because there may be more than one lightpath sourced at node i, destined to node j, and allocated with wavelength ω, so long as they follow link-disjoint routes.

The following variables are defined:

1. $\varepsilon_E^{i,h}$: the bandwidth being electrically switched by node i at time-slot h; we have $\varepsilon_E^{i,h} \geq 0$.

2. $\varepsilon_O^{i,h}$: the bandwidth being optically switched by node i at time-slot h; we have $\varepsilon_O^{i,h} \geq 0$.

3. $\delta_{i,k}^h$: 1 if the kth transmitter of node i is turned on at time-slot h, 0 otherwise.

4. $\delta_{i,l}^h$: 1 if the lth receiver of node i is turned on at time-slot h, 0 otherwise.

5. $\varepsilon_{i,k}^h$: the bandwidth going through the kth transmitter of node i at time-slot h; we have $0 \leq \varepsilon_{i,k}^h \leq C$.

6. $\varepsilon_{i,l}^h$: the bandwidth going through the lth receiver of node i at time-slot h; we have $0 \leq \varepsilon_{i,l}^h \leq C$.

7. $\varepsilon_{m,n,\omega}^h$: the bandwidth going through physical link (m,n) using wavelength ω at time-slot h; we have $0 \leq \varepsilon_{m,n,\omega}^h \leq C$.

8. $\lambda^{s,d,h}$: the bandwidth sourced from s destined to d at time-slot h; we have $\lambda^{s,d,h} \geq 0$.

9. $\delta^{s,d,h}$: 1 if the connection sourced from s destined to d is active at time-slot h.

10. $\mu_{i,j,k,l,\omega}^{s,d,h}$: 1 if connection sourced from s destined to d is routed through lightpath $< i,j,k,l,\omega >$ at time-slot h, 0 otherwise.

11. $\nu_{i,j,k,l,\omega}^{s,d,h}$: the bandwidth of connection source from s destined to d that traverses lightpath $< i,j,k,l,\omega >$ at time-slot h; we have $0 \leq \nu_{i,j,k,l,\omega}^{s,d,h} \leq C$.

12. $\rho_{m,n,h}^{i,j,k,l,\omega}$: 1 if lightpath $< i,j,k,l,\omega >$ goes through physical link (m,n) at time-slot h, 0 otherwise.

13. $\theta_{m,n,h}^{i,j,k,l,\omega}$: the amount of traffic from lightpath $< i,j,k,l,\omega >$ that traverses physical link (m,n) at time-slot h; we have $0 \leq \theta_{m,n,h}^{i,j,k,l,\omega} \leq C$.

14. $\rho_h^{i,j,k,l,\omega}$: 1 if lightpath $< i,j,k,l,\omega >$ exists at time-slot h, 0 otherwise.

15. $\theta_h^{i,j,k,l,\omega}$: the bandwidth traverses lightpath $< i, j, k, l, \omega >$ at time-slot h; we have $0 \leq \theta_h^{i,j,k,l,\omega} \leq C$.

16. $\rho_{x,h}^{i,j,k,l,\omega}$: 1 if the lightpath $< i, j, k, l, \omega >$ uses the xth physical route at time-slot h.

The ILP model for energy efficient provisioning of connection requests under static bandwidth-varying scheduled traffic model (ILP-BV) is defined as follows:

Objective: Minimize

$$\begin{aligned}
\sum_{h \in \boldsymbol{N}_{[t]}} \tilde{t}_h \cdot \Bigg\{ & \underbrace{\sum_{i \in \boldsymbol{V}} \frac{\varepsilon_E^{i,h}}{C}(1-\alpha)P_E}_{\text{Electrical Switching Power}} + \underbrace{\sum_{i \in \boldsymbol{V}} \frac{\varepsilon_O^{i,h}}{C}(1-\alpha)P_O}_{\text{Optical Switching Power}} \\
& + \underbrace{\sum_{i \in \boldsymbol{V}} \sum_{k=0}^{\phi_T^i} P_T \left[\delta_{i,k}^h \alpha + (1-\alpha)\frac{\varepsilon_{i,k}^h}{C} \right]}_{\text{Transmitters Power}} \\
& + \underbrace{\sum_{i \in \boldsymbol{V}} \sum_{l=0}^{\phi_R^i} P_R \left[\delta_{i,l}^h \alpha + (1-\alpha)\frac{\varepsilon_{i,l}^h}{C} \right]}_{\text{Receivers Power}} \\
& + \underbrace{\sum_{m \in \boldsymbol{V}} \sum_{n \in \boldsymbol{V}: n \neq m} \sum_{\omega=0}^{W-1} \frac{\varepsilon_{m,n,\omega}^h}{C} P_A (1-\alpha)\eta_{m,n} + P_y}_{\text{Amplifiers Power}} \Bigg\}
\end{aligned} \tag{5.9}$$

Subject to:

1. *Power Component Bandwidth Equalities*

$$\begin{aligned}
& \sum_{j \in \boldsymbol{V}: j \neq i} \sum_{k=0}^{\phi_T^i} \sum_{l=0}^{\phi_R^j} \sum_{\omega=0}^{W-1} \theta_h^{i,j,k,l,\omega} + \sum_{j \in \boldsymbol{V}: j \neq i} \sum_{k=0}^{\phi_T^j} \sum_{l=0}^{\phi_R^i} \sum_{\omega=0}^{W-1} \theta_h^{j,i,k,l,\omega} \\
& = \varepsilon_E^{i,h} \quad \forall i \in \boldsymbol{V}, h \in \boldsymbol{N}_{[t]}.
\end{aligned} \tag{5.10}$$

Constraint (5.10) says that the amount of traffic being electrically switched by node i is composed of two parts:

- The traffic amount of the lightpaths with node i as the source node.

- The traffic amount of the lightpaths with node i as the destination node.

$$\begin{aligned}&\sum_{j\in\boldsymbol{V}:j\neq i}\sum_{k=0}^{\phi_T^i}\sum_{l=0}^{\phi_R^j}\sum_{\omega=0}^{W-1}\theta_h^{i,j,k,l,\omega}+\sum_{j\in\boldsymbol{V}:j\neq i}\sum_{k=0}^{\phi_T^j}\sum_{l=0}^{\phi_R^i}\sum_{\omega=0}^{W-1}\theta_h^{j,i,k,l,\omega}\\&+\sum_{s\in\boldsymbol{V}:s\neq i}\sum_{j\in\boldsymbol{V}:j\neq s,i}\sum_{n\in\boldsymbol{V}:n\neq i}\sum_{k=0}^{\phi_T^s}\sum_{l=0}^{\phi_R^j}\sum_{\omega=0}^{W-1}\theta_{i,n,h}^{s,j,k,l,\omega}\\&=\varepsilon_O^{i,h}\quad\forall i\in\boldsymbol{V},h\in\boldsymbol{N}_{[\boldsymbol{t}]}.\end{aligned}\tag{5.11}$$

Constraint (5.11) says that the amount of traffic being optically switched by node i is composed of three parts:

- The traffic amount of the lightpaths with node i as the source node.
- The traffic amount of the lightpaths with node i as the destination node.
- The traffic amount of the lightpaths with node i as the intermediate node.

$$\sum_{j\in\boldsymbol{V}:j\neq i}\sum_{l=0}^{\phi_R^j}\sum_{\omega=0}^{W-1}\theta_h^{i,j,k,l,\omega}=\varepsilon_{i,k}^h\quad\forall i\in\boldsymbol{V},k\in[0,\phi_T^i],h\in\boldsymbol{N}_{[\boldsymbol{t}]}.\tag{5.12}$$

Constraint (5.12) says that the amount of traffic going through the kth transmitter of node i is equal to the traffic amount of the lightpath using that transmitter.

$$\sum_{j\in\boldsymbol{V}:j\neq i}\sum_{k=0}^{\phi_T^j}\sum_{\omega=0}^{W-1}\theta_h^{j,i,k,l,\omega}=\varepsilon_{i,l}^h\quad\forall i\in\boldsymbol{V},l\in[0,\phi_R^i],h\in\boldsymbol{N}_{[\boldsymbol{t}]}.\tag{5.13}$$

Constraint (5.13) says that the amount of traffic going through the lth receiver of node i equals the traffic amount of the lightpath using that receiver.

$$\sum_{j\in\boldsymbol{V}:j\neq i}\sum_{l=0}^{\phi_R^j}\sum_{\omega=0}^{W-1}\rho_h^{i,j,k,l,\omega}=\delta_{i,k}^h\quad\forall i\in\boldsymbol{V},k\in[0,\phi_T^i],h\in\boldsymbol{N}_{[\boldsymbol{t}]}.\tag{5.14}$$

$$\sum_{j\in \boldsymbol{V}:j\neq i}\sum_{k=0}^{\phi_T^j}\sum_{\omega=0}^{W-1}\rho_h^{j,i,k,l,\omega}=\delta_{i,l}^h \quad \forall i\in \boldsymbol{V}, l\in[0,\phi_R^i], h\in \boldsymbol{N}_{[t]}. \tag{5.15}$$

Constraint (5.14) and (5.15) say that a transmitter/receiver is turned on if there is a lightpath using it.

$$\sum_{i\in \boldsymbol{V}}\sum_{j\in \boldsymbol{V}:j\neq i}\sum_{k=0}^{\phi_T^i}\sum_{l=0}^{\phi_R^j}\theta_{m,n,h}^{i,j,k,l,\omega}=\varepsilon_{m,n,\omega}^h \tag{5.16}$$
$$\forall m,n\in \boldsymbol{V}: m\neq n, \omega\in[0,W-1], h\in \boldsymbol{N}_{[t]}.$$

Constraint (5.16) says that the amount of traffic going through physical link (m,n) using wavelength ω is equal to the traffic amount of the lightpath using the wavelength ω of physical link (m,n).

2. *Flow conservation constraints in the IP layer*

$$\sum_{j\in \boldsymbol{V}:j\neq i}\sum_{k=0}^{\phi_T^i}\sum_{l=0}^{\phi_R^j}\sum_{\omega=0}^{W-1}\nu_{i,j,k,l,\omega}^{s,d,h}-\sum_{j\in \boldsymbol{V}:j\neq i}\sum_{k=0}^{\phi_T^j}\sum_{l=0}^{\phi_R^i}\sum_{\omega=0}^{W-1}\nu_{j,i,k,l,\omega}^{s,d,h}$$
$$=\begin{cases}\lambda^{s,d,h}, & \text{if } i=s\\ -\lambda^{s,d,h}, & \text{if } i=d\\ 0, & \text{otherwise}\end{cases} \tag{5.17}$$
$$\forall s,d,i\in \boldsymbol{V}: s\neq d; \forall h\in \boldsymbol{N}_{[t]}.$$

Constraint (5.17) represents the flow conservation constraints in the IP layer. It ensures that in all nodes, excluding the source and the destination nodes, the total amount of incoming traffic equals the total amount of outgoing traffic.

3. *Virtual link capacity constraints*

$$\begin{aligned} &\sum_{s\in\boldsymbol{V}}\sum_{d\in\boldsymbol{V}:d\neq s}\nu_{i,j,k,l,\omega}^{s,d,h}=\theta_h^{i,j,k,l,\omega}\\ &\forall i,j\in\boldsymbol{V}:i\neq j;\forall h\in\boldsymbol{N}_{[t]}\\ &\forall k\in[0,\phi_T^i],l\in[0,\phi_R^j],\omega\in[0,W-1]. \end{aligned} \tag{5.18}$$

Constraint (5.18) says that the traffic amount of a lightpath equals the sum of the traffic amount of each connection request using that lightpath.

$$\begin{aligned} &\theta_h^{i,j,k,l,\omega}\leq C\\ &\forall i,j\in\boldsymbol{V}:i\neq j;\forall h\in\boldsymbol{N}_{[t]}\\ &\forall k\in[0,\phi_T^i],l\in[0,\phi_R^j],\omega\in[0,W-1]. \end{aligned} \tag{5.19}$$

Constraint (5.19) ensures that the traffic amount of a lightpath does not exceed its capacity.

4. *Finish-data-transmission constraints*

$$\sum_{h\in\boldsymbol{N}_{[t]}}\tilde{t}_h\lambda^{s,d,h}=\lambda^{s,d}\quad\forall s,d\in\boldsymbol{V}:s\neq d. \tag{5.20}$$

Constraint (5.20) says that for each *s*-*d* pair, the sum of the volume of data being transmitted in each time-slot should be equal to the specified volume of data when the connection request was accepted into the network.

$$0\leq\lambda^{s,d,h}\leq\frac{\lambda^{s,d}}{\tilde{t}_h}\quad\forall s,d\in\boldsymbol{V}:s\neq d;\forall h\in\boldsymbol{N}_{[t]}. \tag{5.21}$$

Constraint (5.21) sets the lower and upper bounds of $\lambda^{s,d,h}$.

$$\sum_{h\notin[t_{[\mathrm{so}]}^{s,d},t_{[\mathrm{eo}]}^{s,d}]}\lambda^{s,d,h}=0\quad\forall s,d\in\boldsymbol{V}:s\neq d. \tag{5.22}$$

Constraint (5.22) ensures that a connection request is only transmitted within its specified time-slots.

5. *Flow conservation constraints in the optical layer*

$$\begin{aligned}
&\sum_{n\in\boldsymbol{V}:n\neq m}\theta_{m,n,h}^{i,j,k,l,\omega}-\sum_{n\in\boldsymbol{V}:n\neq m}\theta_{n,m,h}^{i,j,k,l,\omega}\\
&=\begin{cases}\theta_h^{i,j,k,l,\omega}, & \text{if } m=i\\ -\theta_h^{i,j,k,l,\omega}, & \text{if } m=j\\ 0, & \text{otherwise}\end{cases}\\
&\forall m,i,j\in\boldsymbol{V}:i\neq j;\forall h\in\boldsymbol{N}_{[t]}\\
&\forall k\in[0,\phi_T^i],l\in[0,\phi_R^j],\omega\in[0,W-1].
\end{aligned}\tag{5.23}$$

Constraint (5.23) represents the flow conservation constraints in the optical layer. It ensures that in all nodes, excluding the source and the destination nodes, the total amount of incoming traffic equals the total amount of outgoing traffic.

6. *Wavelength constraints*

$$\begin{aligned}
&\sum_{i\in\boldsymbol{V}}\sum_{j\in\boldsymbol{V}:j\neq i}\sum_{k=0}^{\phi_T^i}\sum_{l=0}^{\phi_R^j}\sum_{\omega=0}^{W-1}\rho_{m,n,h}^{i,j,k,l,\omega}\leq F_{m,n}\\
&\forall m,n\in\boldsymbol{V}:m\neq n\\
&\forall\omega\in[0,W-1];\forall h\in\boldsymbol{N}_{[t]}.
\end{aligned}\tag{5.24}$$

Constraint (5.24) says that a wavelength on a fiber link can be used by at most one lightpath traversing this fiber link, provided that the fiber link exists.

7. *Physical link capacity constraints*

$$\begin{aligned}
&\sum_{i\in\boldsymbol{V}}\sum_{j\in\boldsymbol{V}:j\neq i}\sum_{k=0}^{\phi_T^i}\sum_{l=0}^{\phi_R^j}\sum_{\omega=0}^{W-1}\theta_{m,n,h}^{i,j,k,l,\omega}\leq WCF_{m,n}\\
&\forall m,n\in\boldsymbol{V}:m\neq n;\forall h\in\boldsymbol{N}_{[t]}.
\end{aligned}\tag{5.25}$$

Constraint (5.25) says that the total amount of traffic going through a fiber link should not exceed its capacity.

8. *Variable value constraints*

$$\begin{aligned}
&\mu^{s,d,h}_{i,j,k,l,\omega} \leq \nu^{s,d,h}_{i,j,k,l,\omega} \leq C\mu^{s,d,h}_{i,j,k,l,\omega} \\
&\forall s,d,i,j \in \boldsymbol{V} : s \neq d, i \neq j; \forall h \in \boldsymbol{N}_{[t]}; \\
&\forall k \in [0,\phi^i_T], l \in [0,\phi^j_R], \omega \in [0, W-1].
\end{aligned} \tag{5.26a}$$

$$\begin{aligned}
&0 \leq \lambda^{s,d,h} - \nu^{s,d,h}_{i,j,k,l,\omega} \leq C(1-\mu^{s,d,h}_{i,j,k,l,\omega}) \\
&\forall s,d,i,j \in \boldsymbol{V} : s \neq d, i \neq j; \forall h \in \boldsymbol{N}_{[t]}; \\
&\forall k \in [0,\phi^i_T], l \in [0,\phi^j_R], \omega \in [0, W-1].
\end{aligned} \tag{5.26b}$$

Constraints (5.26a) and (5.26b) ensure that if $\mu^{s,d,h}_{i,j,k,l,\omega} = 0$, we have $\nu^{s,d,h}_{i,j,k,l,\omega} = 0$; if $\mu^{s,d,h}_{i,j,k,l,\omega} = 1$, we have $\nu^{s,d,h}_{i,j,k,l,\omega} = \lambda^{s,d,h} > 0$. In other words, splitting the traffic of a connection request onto multiple lightpaths is not allowed.

$$\begin{aligned}
&\rho^{i,j,k,l,\omega}_{m,n,h} \leq \theta^{i,j,k,l,\omega}_{m,n,h} \leq C\rho^{i,j,k,l,\omega}_{m,n,h} \\
&\forall i,j,m,n \in \boldsymbol{V} : i \neq j, m \neq n; \forall h \in \boldsymbol{N}_{[t]} \\
&\forall k \in [0,\phi^i_T], l \in [0,\phi^j_R], \omega \in [0, W-1].
\end{aligned} \tag{5.27a}$$

$$\begin{aligned}
&0 \leq \theta^{i,j,k,l,\omega}_{h} - \theta^{i,j,k,l,\omega}_{m,n,h} \leq C(1-\rho^{i,j,k,l,\omega}_{m,n,h}) \\
&\forall i,j,m,n \in \boldsymbol{V} : i \neq j, m \neq n; \forall h \in \boldsymbol{N}_{[t]} \\
&\forall k \in [0,\phi^i_T], l \in [0,\phi^j_R], \omega \in [0, W-1].
\end{aligned} \tag{5.27b}$$

Constraints (5.27a) and (5.27b) ensure that if $\rho^{i,j,k,l,\omega}_{m,n,h} = 0$, we have $\theta^{i,j,k,l,\omega}_{m,n,h} = 0$; if $\rho^{i,j,k,l,\omega}_{m,n,h} = 1$, we have $\theta^{i,j,k,l,\omega}_{m,n,h} = \theta^{i,j,k,l,\omega}_{h} > 0$. In other words, bifurcated routing of a lightpath is prohibited.

$$\rho_h^{i,j,k,l,\omega} \leq \theta_h^{i,j,k,l,\omega} \leq C\rho_h^{i,j,k,l,\omega}$$
$$\forall i,j \in \boldsymbol{V} : i \neq j; \forall h \in \boldsymbol{N}_{[t]} \tag{5.28}$$
$$\forall k \in [0, \phi_T^i], l \in [0, \phi_R^j], \omega \in [0, W-1].$$

Constraint (5.28) ensures that if $\theta_h^{i,j,k,l,\omega} = 0$, we have $\rho_h^{i,j,k,l,\omega} = 0$; if $\theta_h^{i,j,k,l,\omega} > 0$, we have $\rho_h^{i,j,k,l,\omega} = 1$. In other words, if a lightpath exists, then its traffic amount shall not be zero.

$$\delta_{i,k}^h \leq \varepsilon_{i,k}^h \leq C\delta_{i,k}^h \forall i \in \boldsymbol{V}, k \in [0, \phi_T^i], h \in \boldsymbol{N}_{[t]}. \tag{5.29}$$

Constraint (5.29) ensures that if $\varepsilon_{i,k}^h = 0$, we have $\delta_{i,k}^h = 0$; if $\varepsilon_{i,k}^h > 0$, we have $\delta_{i,k}^h = 1$. In other words, a transmitter is switched on only if it is needed to transmit data.

$$\delta_{i,l}^h \leq \varepsilon_{i,l}^h \leq C\delta_{i,l}^h \forall i \in \boldsymbol{V}, l \in [0, \phi_R^i], h \in \boldsymbol{N}_{[t]}. \tag{5.30}$$

Constraint (5.30) ensures that if $\varepsilon_{i,l}^h = 0$, we have $\delta_{i,l}^h = 0$; if $\varepsilon_{i,l}^h > 0$, we have $\delta_{i,l}^h = 1$. In other words, a receiver is switched on only if it is needed to receive data.

9. *Additional constraints for confining the physical route of a lightpath*

One additional input is $\rho_{m,n}^{i,j,x}$ which specifies the xth physical route of all lightpaths sourced at i destined at j. We assume there are X candidate physical routes for each source-destination pair, ,meaning $x = 0, 1, \cdots, X-1$. If the xth physical route of the lightpath sourced at i destined at j uses physical link

(m, n), we have $\rho_{m,n}^{i,j,x} = 1$, otherwise $\rho_{m,n}^{i,j,x} = 0$.

$$\begin{aligned} &\sum_{x=0}^{X-1} \left(\rho_{x,h}^{i,j,k,l,\omega} \cdot \rho_{m,n}^{i,j,x} \right) = \rho_{m,n,h}^{i,j,k,l,\omega} \\ &\forall i, j, m, n \in \boldsymbol{V} : i \neq j, m \neq n; \forall h \in \boldsymbol{N}_{[t]} \\ &\forall k \in [0, \phi_T^i], l \in [0, \phi_R^j], \omega \in [0, W-1]. \end{aligned} \tag{5.31a}$$

$$\begin{aligned} &\sum_{x=0}^{X-1} \rho_{x,h}^{i,j,k,l,\omega} = \rho_h^{i,j,k,l,\omega} \\ &\forall i, j \in \boldsymbol{V} : i \neq j; \forall h \in \boldsymbol{N}_{[t]} \\ &\forall k \in [0, \phi_T^i], l \in [0, \phi_R^j], \omega \in [0, W-1]. \end{aligned} \tag{5.31b}$$

Constraints (5.31a) and (5.31b) ensure that a lightpath can only select a physical route among the X candidate physical routes.

5.4.2 ILP for Satic Fixed-window Scheduled Traffic Model (ILP-FW)

For comparison purpose, we also formulate an ILP for minimizing energy consumption under static fixed-window scheduled traffic model (ILP-FW). In this case, we should let $t_{[\text{si}]}^{s,d} = t_{[\text{so}]}^{s,d}$ and $t_{[\text{ei}]}^{s,d} = t_{[\text{eo}]}^{s,d}$. What is more, we should add one additional constraint besides the objective function and all the constraints aforementioned.

$$\lambda^{s,d,h} = \frac{\lambda^{s,d}}{t_{[\text{ei}]}^{s,d} - t_{[\text{si}]}^{s,d} + 1} \quad \forall s, d \in \boldsymbol{V} : s \neq d; \forall h \in [t_{[\text{si}]}^{s,d}, t_{[\text{ei}]}^{s,d}]. \tag{5.32}$$

Constraint (5.32) sets the bandwidth value within the data transmission time-slots of a connection request.

5.4.3 Complexity Analysis

It is well known that traffic grooming problem is NP-complete [33]. Traffic grooming problem is a subproblem of the aforementioned ILP formulations, therefore they

are also NP-complete. In terms of computational complexity, the aforementioned formulations have a total of $O(N^4 \cdot \max\{\boldsymbol{\phi_T}\} \cdot \max\{\boldsymbol{\phi_R}\} \cdot W \cdot |\boldsymbol{N_{[t]}}|)$ variables and constraints. There are a huge number of variables and constraints if N is very large, making the problem more complex to get optimal results at a reasonable time for real (large) networks and heavy loads.

5.4.4 Numerical Results

We illustrate the correctness of our ILP formulations by reconsidering the illustrative example as shown in Section 5.3, similar to [66]. We can now model the three connection requests as $r_{[\text{req}],1} :< 0, 1, 0.8, 0, 0, 3, 3 >$, $r_{[\text{req}],2} :< 1, 2, 1.0, 1, 1, 5, 5 >$, $r_{[\text{req}],3} :< 0, 2, 1.2, 2, 2, 7, 7 >$. We adopt the power consumption value (in unit) of each component as listed in Table 3.1 [80] and we set the fixed overhead α to be 50%. For fixed-window scheduled traffic model, after solving the ILP-FW, we get the provisioning scheme as listed in Table 5.1. The total energy consumption for ILP-FW is 330.9. We list the numerical results of ILP-BV (for bandwidth-varying scheduled traffic model) in Table 5.2. The total energy consumption for ILP-BV is 231.3. ILP-BV gains 30% energy savings compared to ILP-FW.

5.5 Heuristic for Energy Efficient Scheduled Connection Provisioning

In this section, we present a Heuristic for energy efficient Provisioning of Bandwidth-Varying scheduled connection requests (HPBV). For comparison purpose, we also propose a Heuristic for energy efficient Provisioning of Fixed-Window scheduled connection requests (HPFW), which is similar to HPBV.

HPBV is depicted in Algorithm 3. The proposed HPBV attempts to minimize

Table 5.1: ILP-FW numerical results

Time-slot	Lightpath(s)	Connection	Data volume
0	0→1	0→1	0.2
1	0→1	0→1	0.2
	1→2	1→2	0.2
2	0→1	0→1	0.2
	0→1, 1→2	0→2	0.2
3	0→1	0→1	0.2
	0→1, 1→2	0→2	0.2
4	0→1, 1→2	0→2	0.2
	1→2	1→2	0.2
5	0→1, 1→2	0→2	0.2
	1→2	1→2	0.2
6	0→ 1 →2	0→2	0.2
7	0→ 1 →2	0→2	0.2

Table 5.2: ILP-BV numerical results

Time-slot	Lightpath(s)	Connection	Data volume
0			
1	1→2	1→2	1.0
2	0→1	0→1	0.8
3			
4			
5	0→1, 1→2	0→2	0.2
6	0→1, 1→2	0→2	1.0
7			

Algorithm 3 HPBV

Input: The set of bandwidth-varying scheduled connections Q_{unsorted}

Output: The provisioning scheme for Q_{unsorted}

1: Sort Q_{unsorted} in descending order of their data volume, to get Q_{sorted}
2: **for** Each connection request q_c in Q_{sorted} **do**
3: **if** q_c is the first connection request, denoted as q_{c1} **then**
4: Use ILP-BV (with all decision variables undetermined) to find optimal provisioning scheme (that is, to determine the decision variables) for q_{c1}
5: **else**
6: Update ILP-BV with the non-zero decision variables, which are determined by solving ILP-BV for previous connection requests), as additional constraints
7: Use the updated ILP-BV to find optimal provisioning scheme (determine the decision variables) for q_c
8: **end if**
9: **end for**

the incremental energy consumption consumed by the network due to the admission of a new connection request. It first sorts the set of bandwidth-varying scheduled connection requests Q_{unsorted} in descending order of their data volume, to get Q_{sorted}. This is similar to the incremental traffic model. It then provisions the connection requests in Q_{sorted} one at a time. The first connection request in Q_{sorted} will be provisioned first, followed by the second one, etc. If current connection request under consideration is the first element of Q_{sorted}, denoted as q_{c1}, then the ILP-BV with all decision variables undetermined will be used to find optimal provisioning scheme (that is, to determine the decision variables) for q_{c1}. If current connection request is not the first element of Q_{sorted}, then we will first update the ILP-BV with all the non-zero decision variables, which are determined by provisioning previous connection requests, as additional constraints. This is to ensure the provisioning of current connection request is based on the residual network resources of the previous provisioned connection requests. We next provision the connection request by solving the updated ILP-BV. HPBV reduces computing resources consumption compared to ILP-BV because it provisions one connection request at a time, instead

of treating the set connection requests as a whole (which is exactly what ILP-BV does).

HPFW is the same as HPBV, except that "the set of bandwidth-varying scheduled connection requests" in line 1 of Algorithm 3 should be replaced by "the set of fixed-window scheduled connection requests", and all "ILP-BV" in Algorithm 3 should be replaced by "ILP-FW".

5.6 Performance Study

In this section we present the energy efficiency of HPBV and HPFW under different fixed overhead proportion α and network topologies. The simulation settings are similar to Section 4.4.1. The 11-node COST239 shown in Fig. 5.4 and 14-node NSFNET shown in Fig. 3.3(b) are used. The number of time-slots $|\boldsymbol{N}_{[t]}|$ is set as 24. The connection requests are generated as below: the source node s and the destination node d are randomly selected among all nodes such that $s \neq d$; the preferred start time $t^{s,d}_{[\text{si}]}$ is selected randomly among all time-slots, the preferred end time $t^{s,d}_{[\text{ei}]}$ is selected such that $t^{s,d}_{[\text{ei}]} - t^{s,d}_{[\text{si}]}$ is uniformly distributed between 2 time-slots and 4 time-slots. The earliest start time $t^{s,d}_{[\text{so}]}$ and the latest end time $t^{s,d}_{[\text{eo}]}$ are selected such that $(t^{s,d}_{[\text{eo}]} - t^{s,d}_{[\text{so}]}) - (t^{s,d}_{[\text{ei}]} - t^{s,d}_{[\text{si}]}) = 4$. The data volume $\lambda^{s,d}$ is set as $b_w \cdot (t^{s,d}_{[\text{ei}]} - t^{s,d}_{[\text{si}]})$, where b_w is a random variable following uniform distribution in range $(0, 1]$. Note that we force b_w to be an integral multiple of 0.01 in our simulations. Also note that for a set of connection requests (e.g., a network load with its value as 70 means a set of 70 connection requests), each connection request in the set should have distinct source-destination pair. For fixed-window scheduled connection requests, we let $t^{s,d}_{[\text{si}]} = t^{s,d}_{[\text{so}]}$, $t^{s,d}_{[\text{ei}]} = t^{s,d}_{[\text{eo}]}$.

The energy consumption of HPBV (for bandwidth-varying scheduled connection requests) and HPFW (for fixed-window scheduled connection requests) under dif-

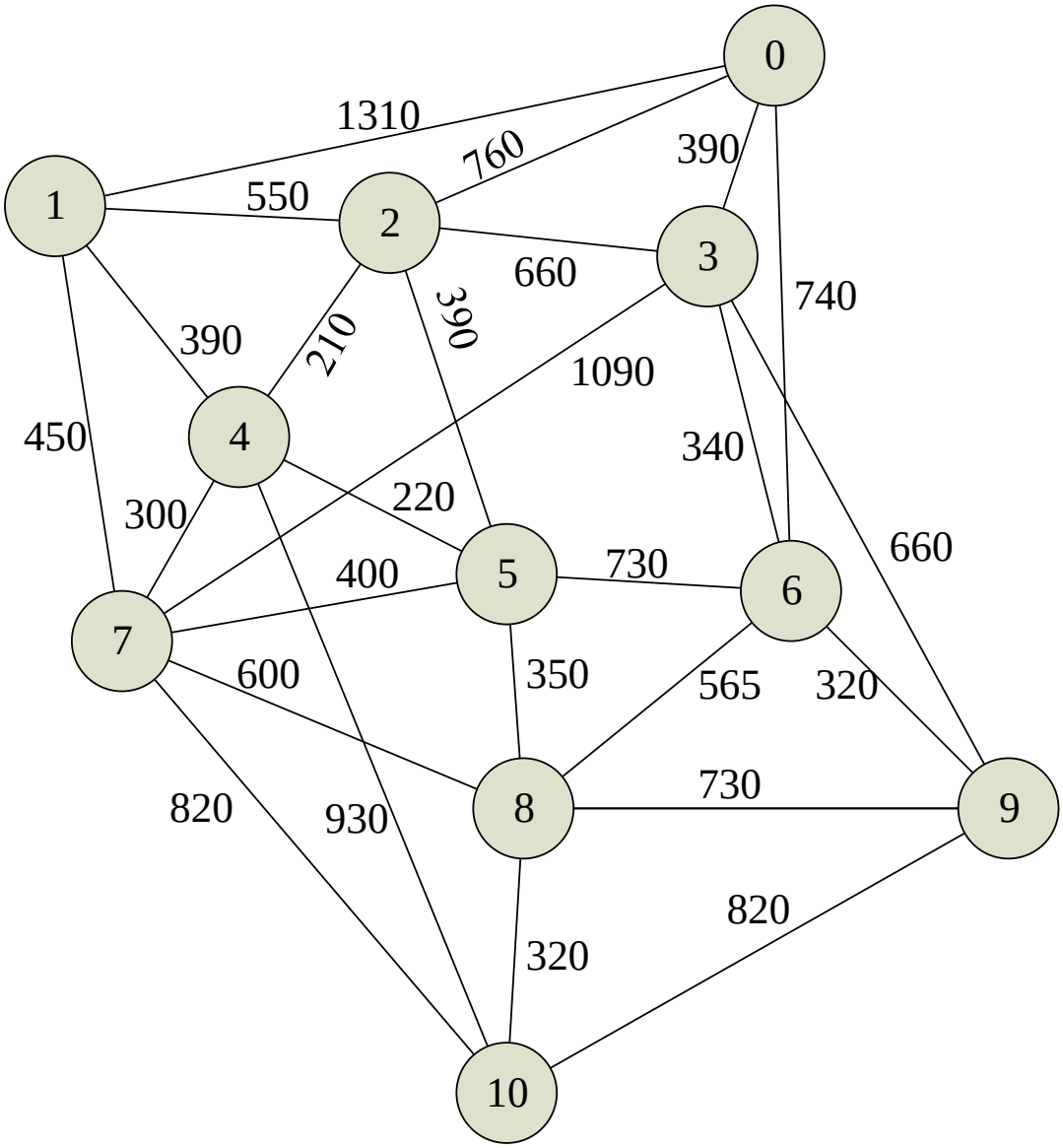

Figure 5.4: 11-node COST239 with fiber link lengths (in km) marked on each link

ferent fixed overhead proportion α and various network loads, in 11-node network is shown in Fig. 5.5. We let α take values 0, 50%, and 100%. We observe that HPBV always consumes less energy compared to HPFW for a given α, which demonstrates the effectiveness of HPBV in saving energy compared to HPFW. We also obverve that as α decreases, the energy consumption of both HPBV and HPFW decreases. Meanwhile, the gap between HPBV and HPFW also reduces. This is because the decrease of α means the energy consumption of the network is more commensurate with the network load. When $\alpha = 0$, the energy consumption is fully proportional to the network load, leading to the vanish of the gap between HPBV and HPFW in terms of energy consumption. We note that the energy consumption of both HPBV and HPFW increases with the increase of the network load, which is obvious because larger number of connections leads to more energy consumption. The energy savings (in percentage) of HPBV compared to HPFW under different fixed overhead proportion α and various network loads, in 11-node network are shown in Fig. 5.6. We observe that the energy savings are quite stable with the network load, with an average of about 10% for $\alpha = 100\%$ and about 6% for $\alpha = 50\%$. As the network load increases, the absolute energy savings also increases. In fact, even 1% energy saving percentage would lead to significant absolute energy savings for larger number of connection requests.

The impact of network topology is studied in Fig. 5.7, which shows the energy consumption for both HPBV and HPFW in 11-node and 14-node networks under various network loads, when $\alpha = 50\%$. We observe that the curves for 14-node network follow similar trend with that for 11-node network, except that 14-node network generally consumes more energy that 11-node network. This is because 14-node network has larger number of network nodes, and thus more energy is consumed to maintain network presence for routers, OXCs and amplifiers. We further plot Fig. 5.8, which shows the average energy consumption per connection for both HPBV

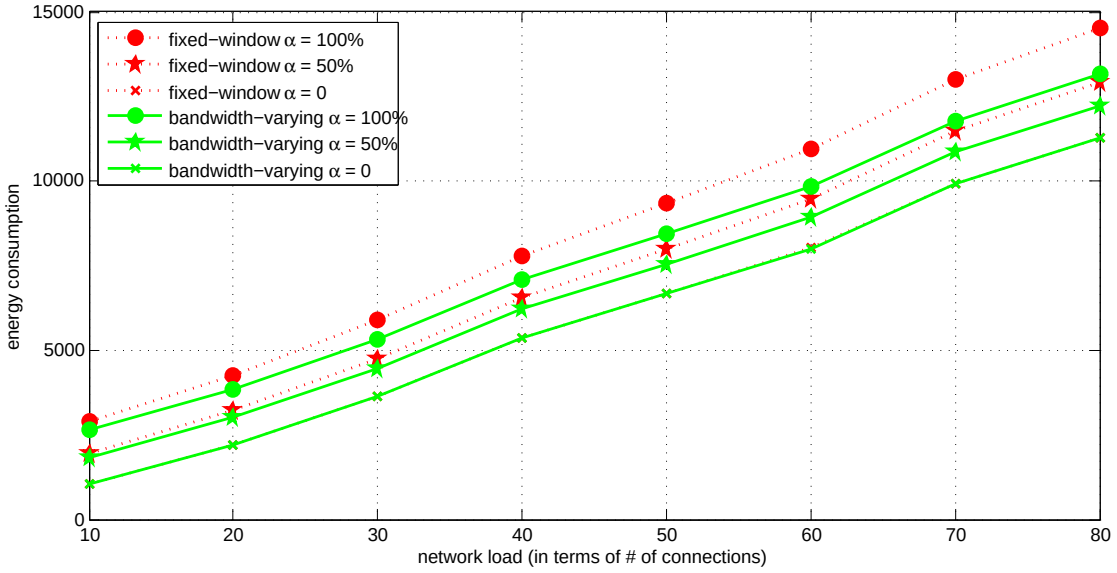

Figure 5.5: Energy consumption for both fixed-window and bandwidth-varying scheduled traffic models under different α

and HPFW in 11-node and 14-node networks under various network loads, when $\alpha = 50\%$. The curves for both networks initially decrease with the increase of the network load, and then become almost flat as the network load continues to increase. The reason for the former is because initially the fixed energy overhead to run the network is shared by larger and larger number of connection requests with the increase of the network load, and thus the average energy consumption per connection reduces. The reason for the latter is because as the network becomes more and more congested, the energy consumed to provision a connection request might increase due to longer route and longer data transmission time, thereby offsetting the impact of the fixed energy overhead to run the network.

5.7 Summary

This chapter studied energy efficient provisioning of static bandwidth-varying scheduled connection requests in IP over WDM networks, which to our knowledge has not

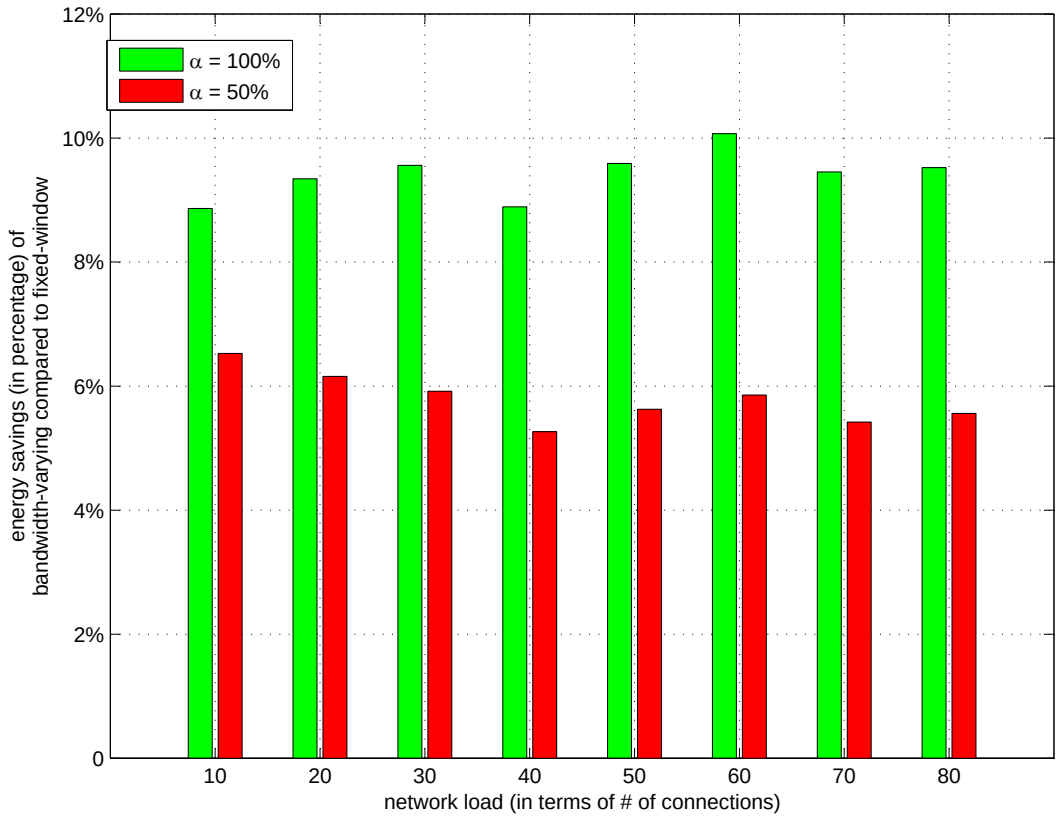

Figure 5.6: Energy savings (in percentage) of bandwidth-varying scheduled traffic model compared to fixed-window scheduled traffic model under different α

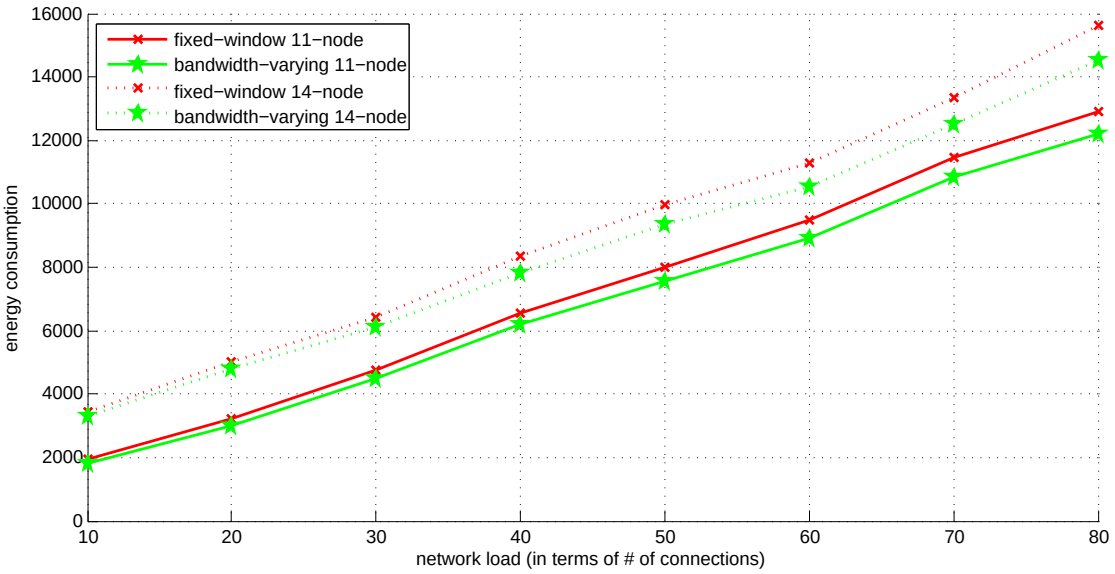

Figure 5.7: Energy consumption for both fixed-window and bandwidth-varying scheduled traffic models, in 11-node and 14-node networks, $\alpha = 50\%$

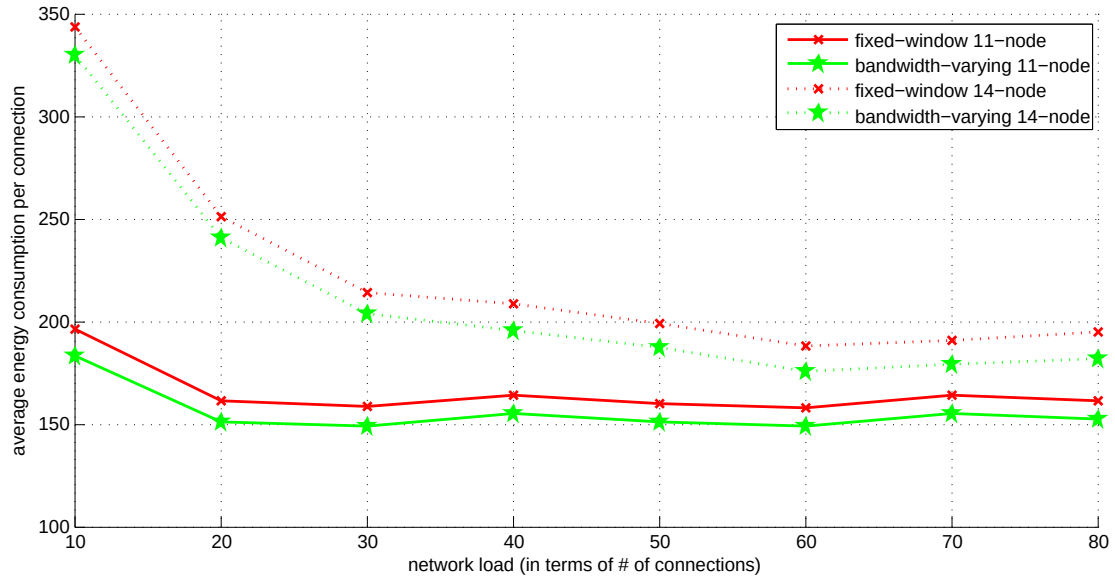

Figure 5.8: Average energy consumption per connection for both fixed-window and bandwidth-varying traffic model, in 11-node and 14-node networks, $\alpha = 50\%$

been considered before. We first presented an ILP formulation (ILP-BV) for scheduling and allocating resources such that the total energy consumption of the network is minimized. We then proposed a computationally simple and efficient heuristic that sorts connections in order and then provisions one connection at a time such that the incremental energy consumption of the network due to the admission of a new connection request is minimized. Performance study shows the advantage of bandwidth-varying scheduled traffic model in gain energy savings compared to fixed-window scheduled traffic model. Specifically, we observe an average energy saving percentage of about 10% if $\alpha = 100\%$ and about 6% if $\alpha = 50\%$, in a 11-node network. The exploitation of bandwidth-varying feature does lead to improved network energy efficiency. A larger network generally leads to more network-wide energy consumption and more average energy consumption per connection, because a larger network means more fixed energy overhead to run the network.

Chapter 6

Power Efficient Integrated Routing with Reliability Constraints

6.1 Introduction

In this chapter, we investigate the problem of improving power efficiency as well as satisfying reliability requirements. We propose a Power Efficient Integrated Routing algorithm with Reliability constraints (PEIRR). PEIRR is used for energy efficient routing of dynamic connection requests with differentiated reliability requirements. PEIRR basically searches for the first k most power efficient paths and then tries to find the first path that meets reliability constraints. The reliability model is presented first, followed by the problem definition. We then present the algorithm description of PEIRR. We next evaluate the performance of PEIRR together with a benchmark algorithm in terms of various metrics. Finally, a summary is given.

6.2 Reliability Model

The reliability of a path is the product of the reliability of its individual fiber links with the same fiber link being calculated only once, as in (6.1):

$$r(p) = \prod_{i=1}^{N} r(l_i) \tag{6.1}$$

where p represents a path; $r(\cdot)$ is the reliability function; l_i is a fiber link of the path p and differs from other fiber links in the path; N is the total number of different fiber links of the path. A path may traverse a fiber link more than once because different lightpaths may use common fiber links. Suppose a path p_1 goes through fiber links $l_1 \rightarrow l_2 \rightarrow l_3 \rightarrow l_2 \rightarrow l_4$ in sequence, then the reliability of p_1 is $r(l_1) \cdot r(l_2) \cdot r(l_3) \cdot r(l_4)$, not $r(l_1) \cdot r(l_2) \cdot r(l_3) \cdot r(l_2) \cdot r(l_4)$.

6.3 Problem Definition

We define the problem of minimizing the power consumption of an IP over WDM network for dynamic routing of sub-lambda connections as follows:

We are given an undirected network graph $\boldsymbol{G} = (\boldsymbol{V}, \boldsymbol{F})$ representing the physical topology of an IP over WDM network, where $\boldsymbol{V}$ is the set of network nodes and $\boldsymbol{F}$ is the set of fiber links. The reliability of each fiber link is assumed to be known in advance. The power consumption value of each component is also given as an input. Connections arrive to the network one by one in a random manner. A connection is specified as a quadruple $< s, d, b, r >$, where s is the source node of the connection; d is the destination node of the connection; b is the required bandwidth of the connection; r is the reliability demand of the connection. The goal is to find the most power efficient route for a connection while satisfying reliability constraints.

6.4 Algorithm Description

Based on the auxiliary graph constructed in Section 3.4.2, we develop PEIRR algorithm. For a connection request, PEIRR determines the first k most power efficient paths by using a standard k-shortest path algorithm, such as Yen's algorithm [81]. It then verifies the reliability of these paths one by one in order. The algorithm completes provisioning a connection if it finds one such path that satisfies reliability constraints among these k paths. However, if it cannot find a satisfactory path, it will instead find the most reliable path and will accept the path if it meets the reliability requirement, otherwise it will reject the connection. If a connection is provisioned successfully, its corresponding power consumption, the number of virtual hops and physical hops will be recorded in some predefined arrays. The algorithm description of PEIRR is shown in Algorithm 4.

Algorithm 4 PEIRR

Input: A connection request c

Output: The provisioning scheme for c

```
Run Yen's algorithm in auxiliary graph G to find the first k most power efficient paths
Choose the first path p_eff that satisfies the reliability requirement of c
if there exists such a path p_eff then
    Record the provisioning information of c
else
    Run Dijkstra's algorithm in auxiliary graph G to find the most reliable path p_rel
    if there exists such a path p_eff and it meet the reliability requirement of c then
        Record the provisioning information of c
    else
        Reject c
    end if
end if
```

In order to compare the effectiveness of PEIRR, an algorithm called Minimum physical Hops Integrated Routing with Reliability constraints (MHIRR) is also implemented. MHIRR uses almost the same auxiliary graph as that of PEIRR. How-

ever, MHIRR assigns a cost value of 1 to fiber edges and a much smaller cost value (e.g., 0.0001) to transmission edges and receiver edges. This kind of edge cost assignment ensures that MHIRR always finds the route with the minimum number of physical hops. For each connection, MHIRR finds out the first k-shortest paths and selects the first one that meets reliability constraints. If there exists such a path, then this connection is provisioned successfully and its corresponding power consumption, the number of virtual hops and physical hops will be recorded in arrays. However, if no such path exists, the connection will be rejected.

6.5 Complexity Analysis

The computational complexity of the proposed PEIRR routing algorithm is the same as Yen's algorithm, i.e., $O(kV_n^3)$, where V_n is the total number of nodes in the auxiliary graph. We hence conclude that the worst-case complexity of the proposed PEIRR routing algorithm is $O(kV_n^3)$. Similarly, the computational complexity of MHIRR is also $O(kV_n^3)$.

6.6 Performance Study

In this section, we compare the performance of PEIRR and MHIRR in terms of power efficiency, the number of connections rejected and the average number of physical hops and virtual hops per (accepted) connection goes through, under various network loads. Power efficiency is in terms of the average power consumption of all the accepted connections. The network load is defined as the number of arriving connection requests.

6.6.1 Simulation Settings

We adopt an incremental dynamic traffic model wherein randomly generated connections arrive one by one but do not leave the network. A 24-node USNET with 43 fiber links is employed for the simulations, as shown in Fig. 3.3(b). A link that connects two OXCs is comprised of a bidirectional fiber link with 16 wavelengths. Amplifiers are deployed along fiber links one for every 80 km. The reliability values of the fiber links are uniformly distributed in range $[0.995, 1)$. The bandwidth capacity of a wavelength is normalized to 1. connections are generated with source-destination node pairs chosen randomly among all the node pairs. The bandwidth of a connection is generated randomly between 0.01 and 0.20. Note that the minimum bandwidth interval is 0.01, meaning the bandwidth of a connection should be an integral multiple of 0.01. The reliability demand of a connection is selected stochastically from the set $\{0.97, 0.98, 0.99\}$. The value of k is set to 4. The relative power consumption of each network component is as listed in Table 3.1. We assume these components all follow affine power profile which is defined in Section 2.3, and we set the fixed overhead proportion α of a component to be 10% by default. The results plotted are the average of several dozen repeated simulations. Similar results are obtained for different parameter settings.

6.6.2 Power Consumption Vs. Network Load

Fig. 6.1 shows the average power consumption per accepted connection of the two algorithms under various network loads. We observe that PEIRR always requires less power than MHIRR. This is because PEIRR tends to find a power efficient route while MHIRR is power-unaware. As the network load increases, the average power consumption per accepted connection tends to decrease for both schemes. This is because more lightpaths are created when the network load increases, leading to

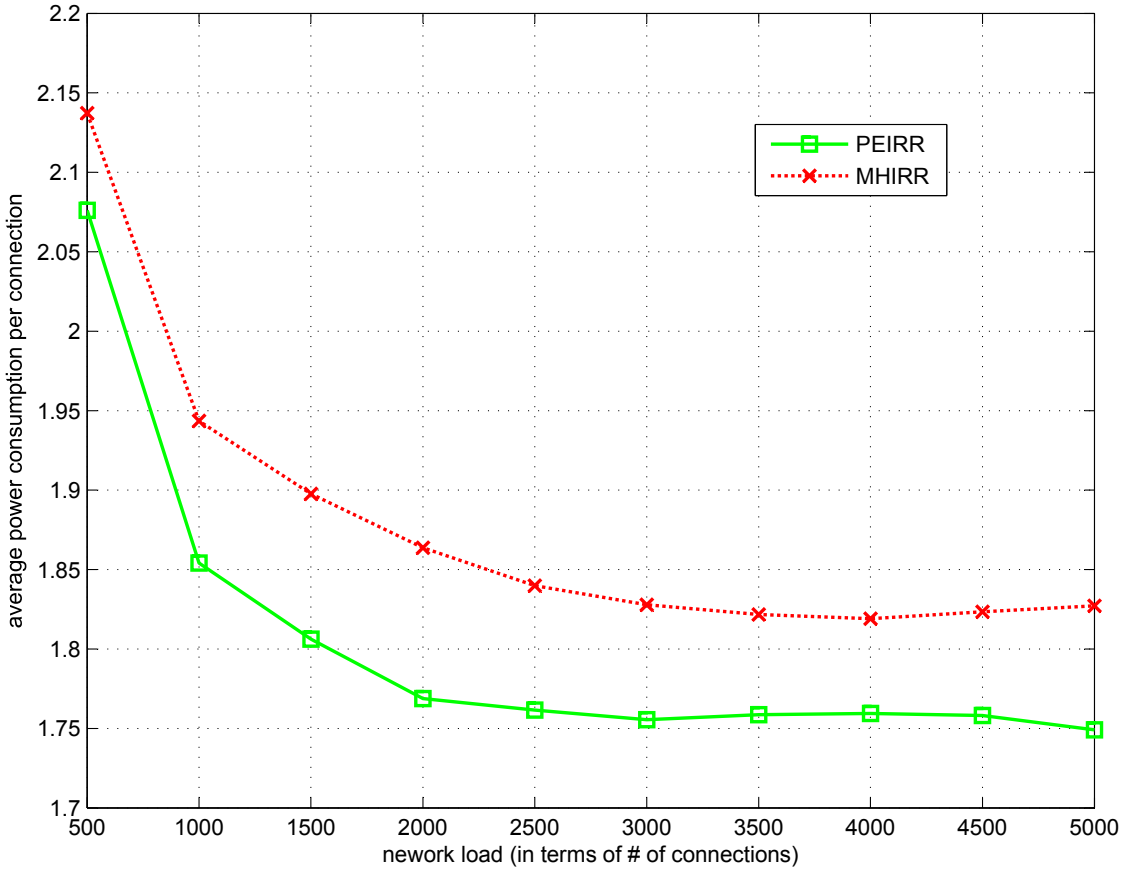

Figure 6.1: Average power consumption per accepted connection

lower growth rate of the number of new transmitters and receivers turned on.

6.6.3 Blocking Performance Vs. Network Load

We compare the number of blocked connections of the two algorithms, as shown in Fig. 6.2. We observe that the number of blocked connections of PEIRR is always lower than that of MHIRR when the network load is less than around 3800. However, after the network load has been greater than around 3800, the number of blocked connections of PEIRR exceeds that of MHIRR. The reason why PEIRR has a smaller blocking when the network load is relatively low is due to the fact that when PEIRR cannot find a viable route in a power efficient way, it will instead find the most reliable route, thereby trying to prevent a connection from being rejected.

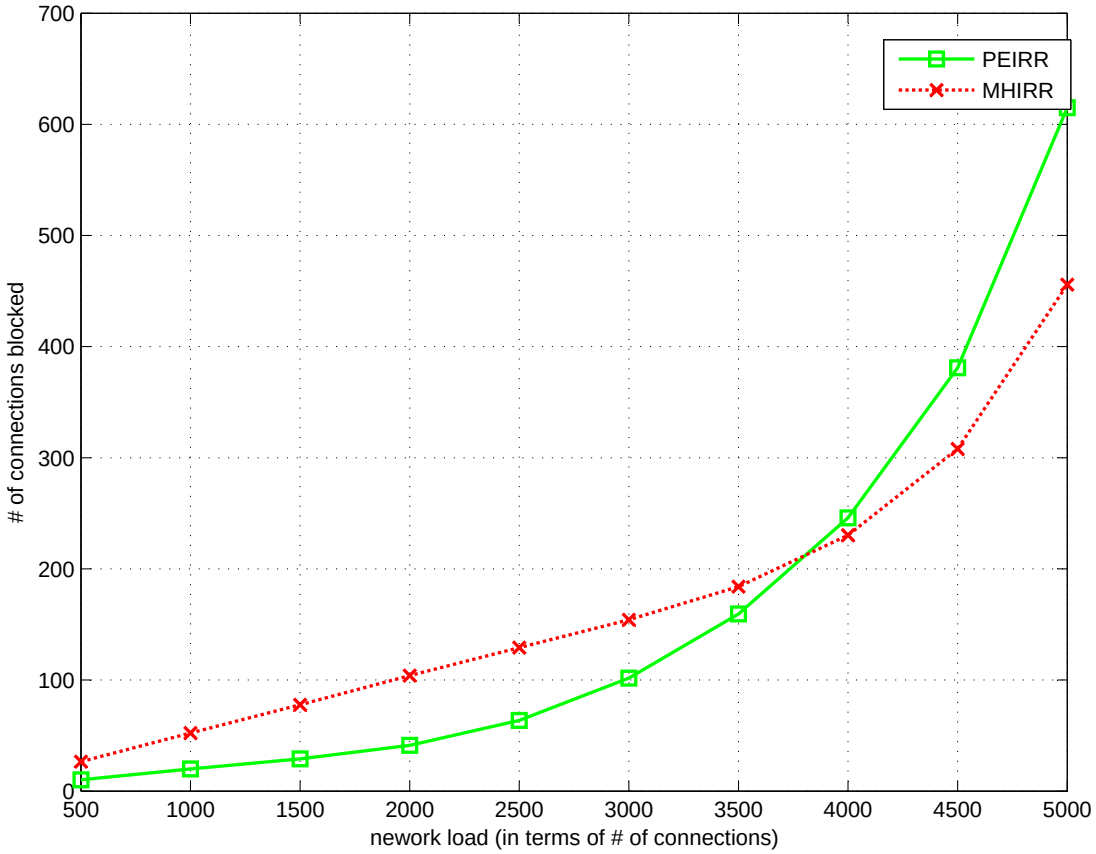

Figure 6.2: The number of blocked connections

The reason for there being a turning point for PEIRR is that basically PEIRR requires more physical hops to honor a connection than MHIRR does, and thus is less resource efficient.

6.6.4 Physcial and Virtual Hops Vs. Network Load

We plot the average number of physical and virtual hops per accepted connection for PEIRR and MHIRR under various network loads in Fig. 6.3. we observe that PEIRR always requires less average number virtual hops than MHIRR does, which is due to the fact that PEIRR is relatively more likely to create a direct lightpath compared to MHIRR in order to decrease the use of power-consuming E components. We also observe that the average number of physical hops per accepted connection

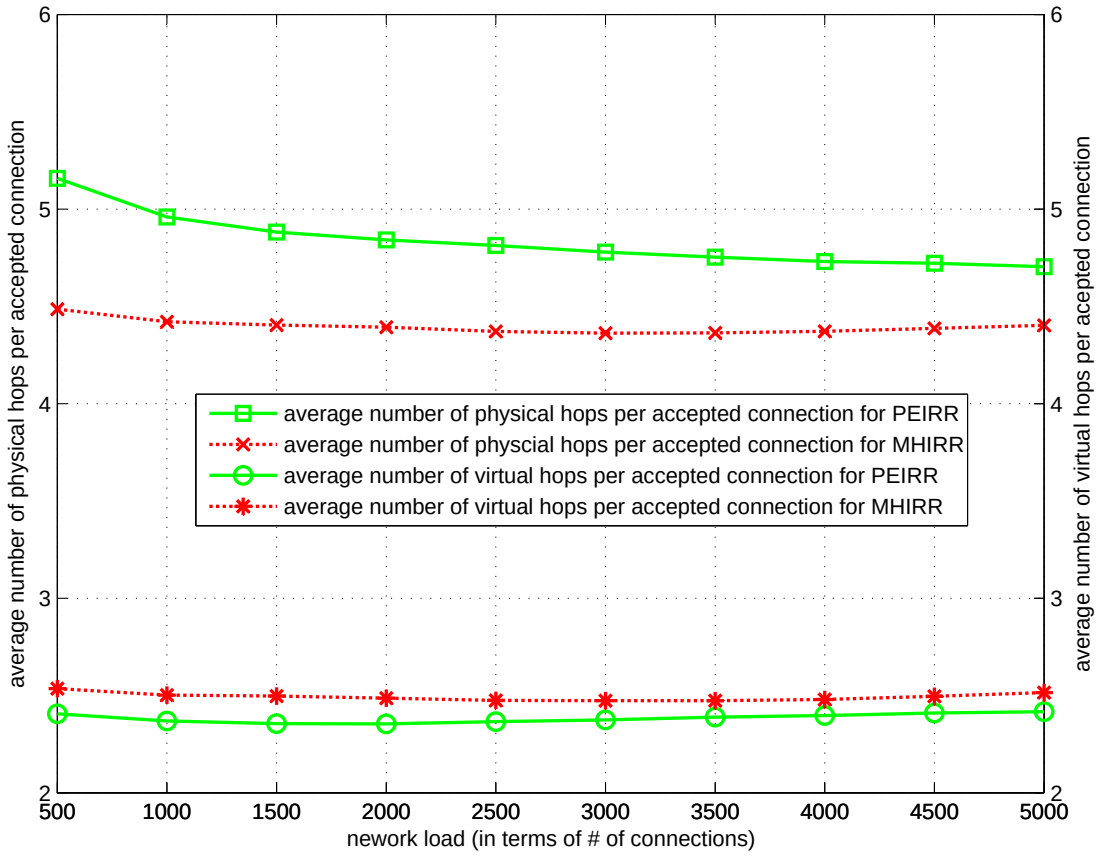

Figure 6.3: Average physical hops and virtual hops per accepted connection goes through

for MHIRR is always lower than that for PEIRR, of which the reason is because the main objective of MHIRR is to minimize the number of physical hops for an accepted connection.

6.7 Summary

In this chapter, we developed PEIRR algorithm to address the ever-increasing power consumption concerns as well as the differentiated reliability requirements of current backbone networks. Based on the auxiliary graph proposed, PEIRR can be implemented by using the k-shortest path algorithm. Performance study demonstrates

the effectiveness of the proposed algorithm in saving power in comparison with a power-unaware algorithm. We also compared the two algorithms in terms of number of connections blocked, average number of physical/virtual hops per accepted connection goes through.

Chapter 7

Conclusion and Future Work

7.1 Conclusion

Green networking has become more and more critical over the last decade due to the steep rising curve of the energy consumption of the ICT sector. This thesis carried out four research works to improve the energy efficiency of IP over WDM optical backbone networks.

We first studied power efficient integrated routing with traffic splitting considering different power profiles, motivated by the fact that the power needed to route an amount of traffic on a path might be reduced if the traffic is bifurcated on multiple paths. We investigated both static and dynamic traffic models. As we have the information of the connection requests in advance for the static traffic model, we formulated integer programming models to minimize the network power consumption. With respect to the dynamic traffic model, we build an auxiliary graph and assign link weight in accordance with its power cost, thereby a standard shortest-path routing algorithm can be used.

We then tried to strike a balance between power efficiency and blocking performance. We proposed B-PIR algorithm, which uses the idea of link criticality to

prevent critical resources from being exhausted too fast. B-PIR deals with dynamic traffic, and therefore the previous type of auxiliary graph can be adapted to facilitate the use of a standard shortest-path routing algorithm.

We next explored energy efficient integrated routing of bandwidth-varying scheduled connection requests. Scheduled traffic models generally benefit the network resource allocation because the transmission start times and end times of connection requests are known in advance. Bandwidth-varying scheduled traffic model is flexible in both data transmission time and instant bandwidth, yielding advantages from the perspective of energy efficiency. We explored its energy saving prospect by formulating ILP models and designing efficient heuristics.

Finally, we considered the reliability requirements of connection requests while providing power efficient paths. We realized this by sorting the possible paths for a connection request in ascend oder of the power cost of a path, followed by selecting the first one that meets the reliability requirements.

We demonstrated the effectiveness of our proposed energy efficient schemes through numerical results obtained from solving integer programming models or simulation results acquired based on various network topologies and scenarios.

It is possible to combine some algorithms together, e.g. using traffic splitting and considering reliability together. However, that does not necessarily mean the computational complexity of the combined algorithm will be asymptotically more complex than the individual algorithms. For example, if the combined algorithm needs $3n$ basic operations to complete and the individual algorithms need $2n$ basic operations to complete, the combined algorithm and the individual algorithms are essentially of the same asymptotic computational complexity.

7.2 Future Work

It is desirable to consider impairments while routing, or the so called impairment-aware routing. As an optical signal traverses a lightpath towards its destination, the signal's quality degrades (which means increase of the BER of the signal) since there is no conversion to the electrical domain and therefore no signal regeneration is achievable [82]. It is unacceptable if the BER is higher than a threshold, for example, 10^{-3} before Forward Error Correction (FEC). It is also not acceptable if the setup of a new lightpath leads to increase of the BER of other lightpaths above the threshold, which is possible due to crosstalk or cross-saturation effect. A increase of the BER means higher number of retransmissions and thus lower throughout. Therefore, it is more practical to consider impairment while improving energy efficiency. Most of existing work focuses on impairment-aware routing only [83–86], few work takes joint energy efficiency and impairment-aware into consideration.

Survivability is of paramount importance to optical backbone networks due to the huge amount of data being handled and the unavoidable link failures. Chapter 6 partially achieved survivability by proposing an algorithm with link failure probability awareness. By partially we mean on the one hand the algorithm satisfies the reliability requirements of an accepted connection request; on the other hand, the algorithm does not have the capability of automatically recovering from link failures. It would be better if proactive protection techniques are used. Survivability schemes usually achieve their goal by reserving extra resources to honor connection requests, whereas energy efficiency mechanisms tend to reduce network redundancy to achieve better energy commensuration with network load. How to elegantly coordinate energy efficiency with survivability remains an open problem which deserves more research efforts.

Our proposed energy efficiency schemes require a centralized manager that is

aware of all the necessary network and connection information. On the one hand, this centralized control leads to better performance than distributed control. On the other hand, the failure of the centralized manager is disastrous. What is more, centralized control results in scalability and complexity problems especially under dynamic traffic models. Therefore it would be necessary to study distributed energy efficiency schemes as well.

Fairness is another interesting research direction but is not considered in our proposed energy efficiency schemes. Fairness means that the acceptance probabilities among connection requests from different source-destination pairs should be equal [68, 87, 88]. Without fairness consideration, connection requests that require longer path (and thus more network resources) might have higher chance of being blocked. Therefore, schemes with joint energy efficiency and fairness consideration would be more practical and attractive.

List of Publications

Journal Papers

1. G. Wu and G. Mohan, "Power-efficient integrated routing of sublambda connection requests with traffic splitting in IP over WDM networks," *Comput. Networks*, vol. 70, pp. 16-29, 2014.

2. G. Wu and G. Mohan, "A Tradeoff between power efficiency and blocking performance in IP over WDM networks," *Comput. Commun.*, revised paper under review.

3. G. Wu and G. Mohan, "Energy efficiency in IP over WDM networks with bandwidth-varying scheduled connections," *Optical Communications and Networking, IEEE/OSA Journal of*, under review.

Conference Papers

1. G. Wu and G. Mohan, "Power-efficient connection provisioning with traffic splitting in IP over WDM networks," in *Proc. HPSR*, 2013.

2. G. Wu and G. Mohan, "Power Efcient Integrated Routing with Reliability Constraints in IP over WDM Networks," in *Proc. ICCS*, 2012.

Bibliography

[1] J. C. C. Restrepo, C. G. Gruber, and C. M. Machuca, "Energy Profile Aware Routing," in *Proc. ICC WKSHPS*, 2009.

[2] Y. Zhang, P. Chowdhury, M. Tornatore, and B. Mukherjee, "Energy Efficiency in Telecom Optical Networks," *Communications Surveys & Tutorials, IEEE*, vol. 12, no. 4, pp. 441–458, 2010.

[3] M. Gupta and S. Singh, "Greening of the Internet," in *Proc. SIGCOMM*, 2003.

[4] Miniwatts Marketing Group, "INTERNET GROWTH STATISTICS," 2014. [Online]. Available: http://www.internetworldstats.com/emarketing.htm

[5] Cisco White Paper, "The Zettabyte Era: Trends and Analysis," 2014. [Online]. Available: http://www.cisco.com/

[6] ——, "Cisco IP over DWDM Solution: Transport for the Approaching Zettabyte Era," 2012. [Online]. Available: http://www.cisco.com/

[7] J. Baliga, R. Ayre, K. Hinton, W. V. Sorin, and R. S. Tucker, "Energy Consumption in Optical IP Networks," *Lightwave Technology, IEEE/OSA Journal of*, vol. 27, no. 13, pp. 2391–2403, 2009.

[8] J. Chabarek, J. Sommers, P. Barford, C. Estan, D. Tsiang, and S. Wright, "Power Awareness in Network Design and Routing," in *Proc. INFOCOM*, Apr. 2008.

[9] E. Bonetto, L. Chiaraviglio, F. Idzikowski, and E. Le Rouzic, "Algorithms for the Multi-Period Power-Aware Logical Topology Design With Reconfiguration Costs," *Journal of Optical Communications and Networking*, vol. 5, no. 5, p. 394, Apr. 2013.

[10] C. Lange, D. Kosiankowski, C. Gerlach, F. Westphal, and A. Gladisch, "Energy consumption of telecommunication networks," in *Proc. ECOC*, 2009.

[11] C. Lange, D. Kosiankowski, R. Weidmann, and A. Gladisch, "Energy Consumption of Telecommunication Networks and Related Improvement Options," *Selected Topics in Quantum Electronics, IEEE Journal of*, vol. 17, no. 2, pp. 285–295, 2011.

[12] A. Elwalid, S. Low, B. Labs, M. Hill, A. Arbor, and A. Motivation, "MATE : MPLS Adaptive Traffic Engineering," in *Proc. INFOCOM*, 2001.

[13] D. Wischik, M. Handley, and M. B. Braun, "The resource pooling principle," *Computer Communication Review, SIGCOMM*, vol. 38, no. 5, pp. 47–52, Sep. 2008.

[14] W. Hou, L. Guo, and X. Wei, "Robust and Integrated Grooming for Power- and Port-Cost-Efficient Design in IP Over WDM Networks," *Lightwave Technology, IEEE/OSA Journal of*, vol. 29, no. 20, pp. 3035–3047, 2011.

[15] P. Wiatr, P. Monti, and L. Wosinska, "Power savings versus network performance in dynamically provisioned WDM networks," *Communications Magazine, IEEE*, vol. 50, no. 5, pp. 48–55, 2012.

[16] N. Charbonneau and V. M. Vokkarane, "A Survey of Advance Reservation Routing and Wavelength Assignment in Wavelength-Routed WDM Networks," *Communications Surveys & Tutorials, IEEE*, vol. 14, no. 4, pp. 1037–1064, 2012.

[17] J. Roberts and K. Liao, "Traffic models for telecommunication services with advance capacity reservation," *Computer Networks and ISDN Systems*, vol. 10, no. 34, pp. 221–229, 1985.

[18] R. A. Gdrin, A. Urda, and A. Motivarions, "Networks with advance reservations: the routing perspective," in *Proc. INFOCOM*, 2000.

[19] J. Zheng and H. T. Mouftah, "Supporting advance reservations in wavelength-routed WDM networks," in *Proc. ICCCN*, 2001.

[20] M. To and P. Neusy, "Unavailability analysis of long-haul networks," *Selected Areas in Communications, IEEE Journal on*, vol. 12, no. 1, pp. 100–109, 1994.

[21] C. V. Saradhi, G. Mohan, and L. Zhou, "Distributed network control for establishing reliability-constrained least-cost lightpaths in WDM Mesh networks," *Computer Communications*, vol. 30, no. 7, pp. 1546–1561, 2007.

[22] Wikipedia, "Internet," 2014. [Online]. Available: http://en.wikipedia.org/wiki/Internet

[23] R. He, "Survivability schemes for dynamic traffic in optical networks," Ph.D. dissertation, National University of Singapore, 2010.

[24] J. F. Kurose and K. W. Ross, *Computer Networking: A Top-Down Approach*, 6th ed. Pearson, 2012.

[25] Pulak Chowdhury, "Energy-Efficient Next-Generation Networks (E2NGN)," Ph.D. dissertation, University of California, Davis, 2011.

[26] J. Qiu, "Survivability schemes for metro Ethernet networks," Ph.D. dissertation, National University of Singapore, 2010.

[27] Wikipedia, "Core network," 2014. [Online]. Available: http://en.wikipedia.org/wiki/Core_network

[28] C. S. R. Murthy and G. Mohan, *WDM Optical Networks: Concepts, Design, and Algorithms*. Prentice Hall, 2001.

[29] Wikipedia, "Smoke signal," 2014. [Online]. Available: http://en.wikipedia.org/wiki/Smoke_signal

[30] K. C. Kao and G. A. Hockham, "Dielectric-fibre surface waveguides for optical frequencies," in *Proceedings of the Institution of Electrical Engineers*, vol. 113, no. 7. IET, 1966, pp. 1151–1158.

[31] R. Ramaswami and K. N. Sivarajan, *Optical Networks: A Practical Persepective*, 3rd ed. San Francisco, CA: Morgan Kaufmann, 2002.

[32] G. Mohan and C. S. R. Murthy, "Lightpath Restoration in WDM Optical Networks," *Network, IEEE*, vol. 14, no. 6, pp. 24–32, 2000.

[33] K. Zhu and B. Mukherjee, "Traffic grooming in an optical WDM mesh network," *Selected Areas in Communications, IEEE Journal on*, vol. 20, no. 1, pp. 122–133, 2002.

[34] Wikipedia, "NP-complete," 2014. [Online]. Available: http://en.wikipedia.org/wiki/NP-complete

[35] ——, "Multiprotocol Label Switching," 2014. [Online]. Available: http://en.wikipedia.org/wiki/Multiprotocol_Label_Switching

[36] M. Kodialam and T. V. Lakshman, "Integrated dynamic IP and wavelength routing in IP over WDM networks," in *Proc. INFOCOM*, 2001.

[37] D. Zhou and S. Subramaniam, "Survivability in Optical Networks," *Network, IEEE*, vol. 14, no. 6, pp. 16–23, 2000.

[38] P. Cholda, A. Mykkeltveit, B. E. Helvik, O. J. Wittner, and A. Jajszczyk, "A survey of resilience differentiation frameworks in communication networks," *Communications Surveys & Tutorials, IEEE*, vol. 9, no. 4, pp. 32–55, 2007.

[39] J. Kuri, N. Puech, M. Gagnaire, E. Dotaro, and R. Douville, "Routing and wavelength assignment of scheduled lightpath demands," *Selected Areas in Communications, IEEE Journal on*, vol. 21, no. 8, pp. 1231–1240, 2003.

[40] B. Wang, T. Li, X. Luo, Y. Fan, and C. Xin, "On service provisioning under a scheduled traffic model in reconfigurable WDM optical networks," in *Proc. BROADNETS*, 2005.

[41] Y. Chen, A. Jaekel, and A. Bari, "A new model for allocating resources to scheduled lightpath demands," *Computer Networks*, vol. 55, no. 13, pp. 2821–2837, 2011.

[42] D. Andrei, H.-H. Yen, M. Tornatore, C. U. Martel, and B. Mukherjee, "Integrated Provisioning of Sliding Scheduled Services Over WDM Optical Networks [Invited]," *Optical Communications and Networking, IEEE/OSA Journal of*, vol. 1, no. 2, pp. A94–A105, 2009.

[43] B. Zhai, D. Blaauw, D. Sylvester, and K. Flautner, "Theoretical and Practical Limits of Dynamic Voltage Scaling," in *Proc. DAC*, 2004.

[44] P. Reviriego, K. Christensen, J. Rabanillo, and J. A. Maestro, "An Initial Evaluation of Energy Efficient Ethernet," *Communications Letters, IEEE*, vol. 15, no. 5, pp. 578–580, May 2011.

[45] K. Christensen, P. Reviriego, B. Nordman, M. Bennett, M. Mostowfi, and J. A. Maestro, "IEEE 802.3az: the road to energy efficient ethernet," *Communications Magazine, IEEE*, vol. 48, no. 11, pp. 50–56, 2010.

[46] C. E. Jones, K. M. Sivalingam, P. Agrawal, and J. C. Chen, "A Survey of Energy Efficient Network Protocols for Wireless Networks," *Wireless Networks*, vol. 7, no. 4, pp. 343–358, 2001.

[47] M. Gupta, S. Grover, and S. Singh, "A feasibility study for power management in LAN switches," in *Proc. ICNP*, 2004.

[48] M. Gupta and S. Singh, "Using Low-Power Modes for Energy Conservation in Ethernet LANs," in *Proc. INFOCOM*, 2007.

[49] ——, "Dynamic Ethernet Link Shutdown for Energy Conservation on Ethernet Links," in *Proc. ICC*, 2007.

[50] C. Gunaratne, S. Member, K. Christensen, S. Member, B. Nordman, and S. Suen, "Reducing the Energy Consumption of Ethernet with Adaptive Link Rate (ALR)," *Computers, IEEE Transactions on*, vol. 57, no. 4, pp. 448–461, 2008.

[51] C. Gunaratne, K. Christensen, and B. Nordman, "Managing energy consumption costs in desktop PCs and LAN switches with proxying, split TCP connections, and scaling of link speed," *International Journal of Network Management*, vol. 15, no. 5, pp. 297–310, 2005.

[52] H. Zhu, H. Zang, K. Zhu, and B. Mukherjee, "Dynamic traffic grooming in WDM mesh networks using a novel graph model," in *Proc. GLOBECOM*, vol. 3, 2002, pp. 2681—-2685 vol.3.

[53] K. Zhu, H. Zhu, and B. Mukherjee, "Traffic engineering in multigranularity heterogeneous optical WDM mesh networks through dynamic traffic grooming," *Network, IEEE*, vol. 17, no. 2, pp. 8–15, 2003.

[54] H. Zhu, H. Zang, K. Zhu, and B. Mukherjee, "A novel generic graph model for traffic grooming in heterogeneous WDM mesh networks," *Networking, IEEE/ACM Transactions on*, vol. 11, no. 2, pp. 285–299, 2003.

[55] X. Wan, Y. Li, H. Zhang, and X. Zheng, "Dynamic Traffic Grooming in Flexible Multi-Layer IP/Optical Networks," *Communications Letters, IEEE*, vol. 16, no. 12, pp. 2079–2082, 2012.

[56] H. Wang and G. N. Rouskas, "Traffic grooming in optical networks: Decomposition and partial linear programming (LP) relaxation," *Optical Communications and Networking, IEEE/OSA Journal of*, vol. 5, no. 8, pp. 535–825, 2013.

[57] ——, "Hierarchical traffic grooming: A tutorial," *Computer Networks*, vol. 69, pp. 147–156, May 2014.

[58] S. Huang, D. Seshadri, and R. Dutta, "Traffic Grooming: A Changing Role in Green Optical Networks," in *Proc. GLOBECOM*, 2009.

[59] E. Yetginer and G. N. Rouskas, "Power Efficient Traffic Grooming in Optical WDM Networks," in *Proc. GLOBECOM*, 2009.

[60] M. Xia, M. Tornatore, Y. Zhang, P. Chowdhury, C. Martel, and B. Mukherjee, "Greening the Optical Backbone Network: A Traffic Engineering Approach," in *Proc. ICC*, 2010.

[61] M. Xia, M. Tornatore, Y. Zhang, P. Chowdhury, C. U. Martel, and B. Mukherjee, "Green Provisioning for Optical WDM Networks," *Selected Topics in Quantum Electronics, IEEE Journal of*, vol. 17, no. 2, pp. 437–445, 2011.

[62] M. M. Hasan, F. Farahmand, a. N. Patel, and J. P. Jue, "Traffic Grooming in Green Optical Networks," in *Proc. ICC*, 2010.

[63] M. M. Hasan, F. Farahmand, and J. P. Jue, "Energy-Awareness in Dynamic Traffic Grooming," in *Proc. OFC/NFOEC*, 2010.

[64] F. Farahmand, M. M. Hasan, I. Cerutti, J. P. Jue, and J. J. P. C. Rodrigues, "Differentiated Energy Savings in Optical Networks with Grooming Capabilities," in *Proc. GLOBECOM*, 2010.

[65] S. Zhang, D. Shen, and C. K. Chan, "Energy Efficient Time-Aware Traffic Grooming in Wavelength Routing Networks," in *Proc. GLOBECOM*, 2010.

[66] ——, "Energy-Efficient Traffic Grooming in WDM Networks With Scheduled Time Traffic," *Lightwave Technology, IEEE/OSA Journal of*, vol. 29, no. 17, pp. 2577–2584, 2011.

[67] Y. Chen and A. Jaekel, "Energy-Aware Scheduling and Resource Allocation for Periodic Traffic Demands," *Optical Communications and Networking, IEEE/OSA Journal of*, vol. 5, no. 4, p. 261, 2013.

[68] G. Mohan and C. S. R. Murthy, "Routing dependable connections in WDM optical networks," *Computer Communications*, vol. 24, no. 13, pp. 1225–1241, 2001.

[69] G. Mohan, C. S. R. Murthy, and A. K. Somani, "Efficient algorithms for routing dependable connections in WDM optical networks," *Networking, IEEE/ACM Transactions on*, vol. 9, no. 5, pp. 553–566, 2001.

[70] C. V. Saradhi and C. Siva Ram Murthy, "Dynamic establishment of segmented protection paths in single and multi-fiber WDM mesh networks," in *Proc. OptiComm*, 2002.

[71] Z. Qin and G. Mohan, "LSP partial spatial-protection in MPLS over WDM optical networks," *Communications, IEEE Transactions on*, vol. 57, no. 4, pp. 1109–1118, 2009.

[72] A. Muhammad, P. Monti, I. Cerutti, L. Wosinska, P. Castoldi, and A. Tzanakaki, "Energy-Efficient WDM Network Planning with Dedicated Protection Resources in Sleep Mode," in *Proc. GLOBECOM*. Ieee, Dec. 2010.

[73] C. Cavdar, F. Buzluca, and L. Wosinska, "Energy-Efficient Design of Survivable WDM Networks with Shared Backup," in *Proc. GLOBECOM*, 2010.

[74] R. Bolla, R. Bruschi, F. Davoli, and F. Cucchietti, "Energy Efficiency in the Future Internet: A Survey of Existing Approaches and Trends in Energy-Aware Fixed Network Infrastructures," *Communications Surveys & Tutorials, IEEE*, vol. 13, no. 2, pp. 223–244, 2011.

[75] F. Idzikowski, S. Orlowski, C. Raack, H. Woesner, and A. Wolisz, "Saving energy in IP-over-WDM networks by switching off line cards in low-demand scenarios," in *Proc. ONDM*, 2010.

[76] L. Chiaraviglio, M. Mellia, and F. Neri, "Minimizing ISP Network Energy Cost : Formulation and Solutions," *Networking, IEEE/ACM Transactions on*, vol. 20, no. 2, pp. 463–476, 2012.

[77] R. S. Tucker, "The Role of Optics and Electronics in High-Capacity Routers," *Lightwave Technology, IEEE/OSA Journal of*, vol. 24, no. 12, pp. 4655–4673, 2006.

[78] G. Shen and R. S. Tucker, "Energy-Minimized Design for IP Over WDM Networks," *Optical Communications and Networking, IEEE/OSA Journal of*, vol. 1, no. 1, pp. 176–186, 2009.

[79] T. H. Cormen, C. E. Leiserson, R. L. Rivest, and C. Stein, *Introduction to Algorithms*, 3rd ed. The MIT Press, 2009.

[80] G. Wu and G. Mohan, "Power-efficient integrated routing of sublambda connection requests with traffic splitting in IP over WDM networks," *Computer Networks*, vol. 70, pp. 16–29, 2014.

[81] J. Y. Yen, "Finding the K Shortest Loopless Paths in a Network," *Management Science*, vol. 17, no. 11, pp. 712–716, 1971.

[82] A. G. Rahbar, "Review of Dynamic Impairment-Aware Routing and Wavelength Assignment Techniques in All-Optical Wavelength-Routed Networks," *Communications Surveys & Tutorials, IEEE*, vol. 14, no. 4, pp. 1065–1089, 2012.

[83] Y. Huang, J. P. Heritage, and B. Mukherjee, "Connection provisioning with transmission impairment consideration in optical WDM networks with high-speed channels," *Lightwave Technology, Journal of*, vol. 23, no. 3, pp. 982–993, 2005.

[84] R. Martinez, C. Pinart, F. Cugini, N. Andriolli, L. Valcarenghi, P. Castoldi, L. Wosinska, J. Comellas, and G. Junyent, "Challenges and requirements for introducing impairment-awareness into the management and control planes of ASON/GMPLS WDM networks," *Communications Magazine, IEEE*, vol. 44, no. 12, pp. 76–85, 2006.

[85] C. V. Saradhi and S. S. Subramaniam, "Physical layer impairment aware routing (PLIAR) in WDM optical networks: issues and challenges," *Communications Surveys & Tutorials, IEEE*, vol. 11, no. 4, pp. 109–130, 2009.

[86] K. Christodoulopoulos, K. Manousakis, and E. Varvarigos, "Offline Routing and Wavelength Assignment in Transparent WDM Networks," *Networking, IEEE/ACM Transactions on*, vol. 18, no. 5, pp. 1557–1570, 2010.

[87] K. Ratnam, M. Gurusamy, and L. Zhou, "Differentiated survivability with improved fairness in IP/MPLS-over-WDM optical networks," *Computer Networks*, vol. 53, no. 5, pp. 634–649, 2009.

[88] J. de Santi, A. C. Drummond, N. L. S. da Fonseca, and A. Jukan, "Load Balancing for Holding-Time-Aware Dynamic Traffic Grooming," in *Proc. GLOBECOM*, 2010.